Fisheries New Zealand
Tini a Tangaroa

Investigating length-based management procedures for *Trachurus novaezelandiae* in the Bay of Plenty purse-seine fishery

New Zealand Fisheries Assessment Report 2025/49

P. Neubauer,
K. Kim,
D.A.J. Middleton,
D. Cook,
T. A'mar

ISSN 1179-5352 (online)
ISBN 978-1-991407-40-5 (online)

November 2025

Te Kāwanatanga o Aotearoa
New Zealand Government

Disclaimer

Requests for further copies should be directed to:

Fisheries Science Editor
Fisheries New Zealand
Ministry for Primary Industries
PO Box 2526
Wellington 6140
NEW ZEALAND

Email: Fisheries-Science.Editor@mpi.govt.nz
Telephone: 0800 00 83 33

This publication is also available on the Ministry for Primary Industries websites at:
http://www.mpi.govt.nz/news-and-resources/publications
http://fs.fish.govt.nz go to Document library/Research reports

Please cite this report as:

Neubauer, P.; Kim, K.; Middleton, D.A.J.; Cook, D.; A'mar, T. (2025). Investigating length-based management procedures for *Trachurus novaezelandiae* in the Bay of Plenty purse-seine fishery. *New Zealand Fisheries Assessment Report 2025/49*. 78 p.

TABLE OF CONTENTS

PLAIN LANGUAGE SUMMARY

This study evaluated using fish length to adjust catch limits for a jack mackerel species in New Zealand waters, with a view to developing simple length metrics to help manage this species. The effectiveness of length-based management depended greatly on biological factors like recruitment, growth, and natural mortality. Current uncertainties about these factors make length-based rules less reliable than expected. Alternative approaches using age data might provide a better way to support sustainable management of this species.

EXECUTIVE SUMMARY

Neubauer, P.[1]; Kim, K.[1]; Middleton, D.A.J.[2]; Cook, D.[3]; A'mar, T.[1] (2025). Investigating length-based management procedures for *Trachurus novaezelandiae* in the Bay of Plenty purse-seine fishery.

***New Zealand Fisheries Assessment Report 2025/49*. 78 p.**

The jack mackerel stock in JMA 1 is a three-species complex made up of *Trachurus novaezelandiae* (JMN), *T. declivis* (JMD), and *T. murphyi* (JMM). It is targeted by a fleet of purse seine vessels that, in recent years, has primarily operated in the Bay of Plenty, although the extent of the fishery was wider before operation of the fishery was consolidated in 2018. The total allowable commercial catch (TACC) for the complex has been unchanged since 1996, when it was increased following the influx of Chilean jack mackerel (JMM). However, despite the presence of JMM being highly variable, there is currently no management strategy in place which would allow for TACC adjustments over time to reflect abundance changes in the different species present in the management complex.

Monitoring studies have been conducted to assess catch composition, including species mix, length, and age data. JMN has been the dominant species in the catch in most years since the mid-1990s. While low estimates of JMN fishing mortality from recent studies suggest less urgency for immediate catch adjustments, developing cost-effective methods to adjust catches based on population trends is essential for long-term sustainability. Currently, there is no suitable abundance index for any of the jack mackerel species in JMA 1, making it challenging to assess stock status. Composition data (length and age frequency data) have been used as performance indicators for fisheries and, especially in the case of length compositions, are relatively easy to collect.

This study investigates the evaluation of a length-based control rule as an option for adjusting JMN catch in the JMA 1 fishery. This evaluation is based on a simple metric of fishing impacts on length compositions (mean length of catch) in the context of uncertain stock dynamics and biological information. Although mean length is a basic measure, it is commonly used in stock assessment to check if models can replicate relevant composition changes and, at least in deterministic cases, can indicate changes in fishing mortality. However, the appropriateness of length-based control rules depends on various factors, including recruitment variability, fishery selectivity, and life-history assumptions. To account for uncertainties in life history and stock demography, this study fitted a flexible length- and age-based model to available data and evaluated mean-length-based harvest control rules to determine their potential impact on yield and risk when compared to a constant catch strategy.

The results indicate that the performance of these rules depends on the life-history characteristics considered. In cases with higher natural mortality, some rules provided additional yield at equivalent risk levels, but this advantage did not hold for scenarios with lower natural mortality. This dependency on life history suggests that these rules are less adequate in scenarios with high relative fishing mortality (F/Fmsy), possibly due to the high overlap of length-at-age distributions among ages selected by the fishery. This complexity in size composition makes it difficult to infer fishing mortality levels solely from mean size.

The study also highlighted uncertainties regarding the appropriateness of life-history parameters and stock structure representations in the models used. Current evidence suggests JMN exhibit fast growth and low natural mortality, characteristics that contrast with expected values for similar pelagic species. These discrepancies in parameters pose challenges for developing effective length-based control rules. Additionally, the assumption of logistic selectivity and the absence of any refuge from fishing pressure in the model led to potentially overly conservative assumptions about stock vulnerability. The lack of a

[1]Dragonfly Data Science, Wellington, New Zealand
[2]Pisces Research, Wellington, New Zealand
[3]Faber R&D Limited, Tauranga, Bay of Plenty, New Zealand

mechanism for mean-size-based control rules to account for environmental variability further compromises the performance of such rules.

The findings of this evaluation contrast with previous studies that used length-based monitoring to determine catch levels. In those studies, rules based on length-based spawning potential ratio (LB-SPR) allowed for rebuilding of the population to desired levels. However, the differences between these evaluations and the present one lie in the life-history assumptions and operating models used, which strongly influence the appropriateness of management reference points and procedures. Given the unresolved nature of life-history assumptions for JMN, the study opted for a relative evaluation approach but found that sensitivity to these assumptions still impacts performance. It suggests the need for further exploration of alternative metrics and the need for a more comprehensive management strategy, based on age composition, to address the uncertainties and challenges associated with JMN management.

1. INTRODUCTION

Jack mackerel (JMA) stocks in New Zealand comprise a three-species complex made up of *Trachurus novaezelandiae* (JMN), *T. declivis* (JMD), and *T. murphyi* (JMM). In the JMA 1 quota management area, off north-eastern Aotearoa/New Zealand, these species are mainly fished by a purse seine fleet operating out of Tauranga. Although effort has largely been limited to the Bay of Plenty in recent years, the fleet previously operated in East Northland and occasionally further afield (Hill-Moana et al. 2025).

Jack mackerels entered the Quota Management System in 1986, with the JMA 1 TACC set near 6000 t initially. The TACC was reviewed in the mid-1990s and increased to 10 000 t after an influx of *T. murphyi* led the fishery to considerably over-catch the allocated TACC (by up to 50%). The TACC has remained stable since 1996 and, with only sporadic abundance of JMM, the largest proportion the catch has comprised JMN in recent years (Fisheries New Zealand 2022). During the 1990s, catches of JMN were typically less than 5000 t per annum, but catches increased in the 2000s, exceeding 7500 t (and reaching up to 9500 t) for much of the 2010s. Catch of JMN has declined in recent years, largely due to operational constraints in the fishery during a period of adjustment after the consolidation of the two main purse seine businesses in 2018. Catch of JMN in recent years has been more consistent with catches in the 1990s.

A number of monitoring studies have been conducted to evaluate the catch-composition in terms of species mix, length, and age (e.g., Langley et al. 2016, Hartill et al. 2022). Length-compositions have been sampled routinely in the Tauranga-based Licensed Fish Receivers since 2005, and a number of age-compositions have been sampled in recent years to estimate total and fishing mortality. However, to date, these data have not been used to adjust catch levels. While low estimates of fishing mortality from recent ageing studies may point to less urgency for immediate monitoring and catch adjustments, developing a cost-effective method to adjust catches to take account of trends in JMN populations is desirable to ensure the long-term sustainability of the fishery and the services it provides.

Although composition data are available for the fishery, there is currently no suitable abundance index to fit in stock assessment models. Catch-per-unit-effort is notoriously difficult to obtain from purse-seine fleets (see Hill-Moana et al. 2025, for an in depth review of the issue in the context of this fishery), and has therefore not been used to track abundance. Available fisheries independent surveys in the Bay of Plenty use trawl gear, and focus on snapper. These tend to catch juvenile JMN, and estimate biomass with a high CV (Parsons & Bian 2022). There is little understanding of the proportion of the stock that is covered by the survey. Composition data are, therefore, the only immediately available data that may provide a basis for cost-effective monitoring.

Composition data, including length compositions, have been used for a long time to measure fishing impacts (Beverton & Holt 1957, Gulland & Rosenberg 1992): they are often relatively easy and cheap to collect, and provide an easily communicated performance indicator for fisheries (e.g., Froese 2004, Cope & Punt 2009). In recent years, a number of length-based methods have been proposed as possible candidates for monitoring stocks (Froese 2004, Cope & Punt 2009, Hordyk et al. 2015a, Rudd & Thorson 2018, Ault et al. 2019) that are "data poor" – the latter being characterised by the lack of an abundance index or even catch data (Chong et al. 2020). Given a set of life history characteristics and ranges of plausible fishing mortality, these methods compare observed and predicted compositions given a particular demographic model and summary metric. Ultimately, these methods rely on compositions to reflect the impacts of fishing over other influences, such as recruitment variation. Chong et al. (2020) showed that some of these methods can perform well under certain circumstances. In addition, some methods, such as length-based spawning-potential-ratio and mean length, have been shown to be effective monitoring strategies for harvest strategies under some settings (Klaer et al. 2012, Hordyk et al. 2015b). However, the review by Chong et al. (2020) also emphasised that the performance of length-based monitoring methods is subject to noise from recruitment variability and other factors. As a result, length-based methods would ideally be thoroughly tested before being employed in particular circumstances.

Here, we test a length-based control rule as an option for adjusting catches of JMN in the JMA 1 fishery. Our evaluation was based on using a simple metric of fishing impacts on length compositions (mean length of catch), in a context of highly uncertain stock dynamics and biological information. Although mean length appears a crude measure of a composition, it is often used in stock assessment to check if assessment models can reproduce relevant changes in compositions, and can be a reasonable indicator of deterministic changes in biomass (Punt et al. 2001, Rochet & Trenkel 2003, Froese 2004). In addition, mean-length based control rules have been shown to be effective for a range of Australian stocks with varying life histories (Klaer et al. 2012). Nevertheless, previous evaluations of the appropriateness of length-based control-rules have also pointed out the dependence of a rule's performance on the operating model and life history assumptions (Punt et al. 2001, Klaer et al. 2012). To adequately reflect uncertainties about life history and stock demography, our study first fitted a flexible length- and age-based model to available length and age composition data for JMN in JMA 1, using a range of biological, demographic, and depletion assumptions. We then evaluated mean-length based harvest control rules, and assessed whether applying such rules would lead to increased yield over constant catches at equivalent risk (or, conversely, lower risk at equivalent yield).

2. METHODS

A management procedure for JMN in JMA 1, based on mean fish length and termed Length-Moving-Average-Range (LMAR), was developed and presented to the Northern Inshore Working Group over a series of presentations between 2019 and 2021 (Bentley & Middleton, unpublished data; provided here as Appendix D). Although the evaluation of the rule showed promise, the Working Group requested that additional biological assumptions be tested. The Working Group also questioned the use of an age-based model with age-based selectivity for a length-based process, in addition to some aspects of the conditioning method which may have led to evaluation over a range of high stock status assumptions only, with no evaluation of the rule at lower stock sizes, where risk is likely to be higher.

The present study attempted to address these queries, and to provide a more complete evaluation of the LMAR rules, based on a length-and age structured model that can resolve length-based processes and represent alternative biological assumptions.

2.1 Length- and age-structured model

We built a length- and age-structured model (LASM), which extended models developed over time by Parma & Deriso (1990), Deriso & Parma (1988), Quinn et al. (1998), and Kim (2022). Mathematical details for the model are described in Appendix A; we therefore only provide a brief overview of the model here. Age-structure forms the core of the model, but the survivorship that determines transitions between age classes in the model is based on the length of individual fish. The key advantage of this model is that it accounts for changes in length-at-age distributions over time; these distributions are often assumed to be constant in age-structured models, an assumption that is likely to be violated at high harvest rates (Figure 1).

The model is based on the following structure and key assumptions:

1. The stock is categorised into 19 age classes (ages 2 to 20) and 24 length classes (ranging from 19 to 42 cm).
2. The length-at-age distributions are normally distributed with a mean length and standard deviation that varies by age class.
3. The length-at-age distribution is cohort-specific and changes over time due to growth variation (due to density dependence) and selective fishing pressure.
4. The mean length-at-age distribution follows a von Bertalanffy growth curve, the parameters of which were obtained from the literature (see Appendix A).
5. The standard deviation of the length-at-age distribution is a function of age and size, increasing asymptotically with age.
6. Selectivity of the fishery is length-dependent, and the selectivity curve is logistic and fixed over time.
7. Natural mortality is constant over time and age.

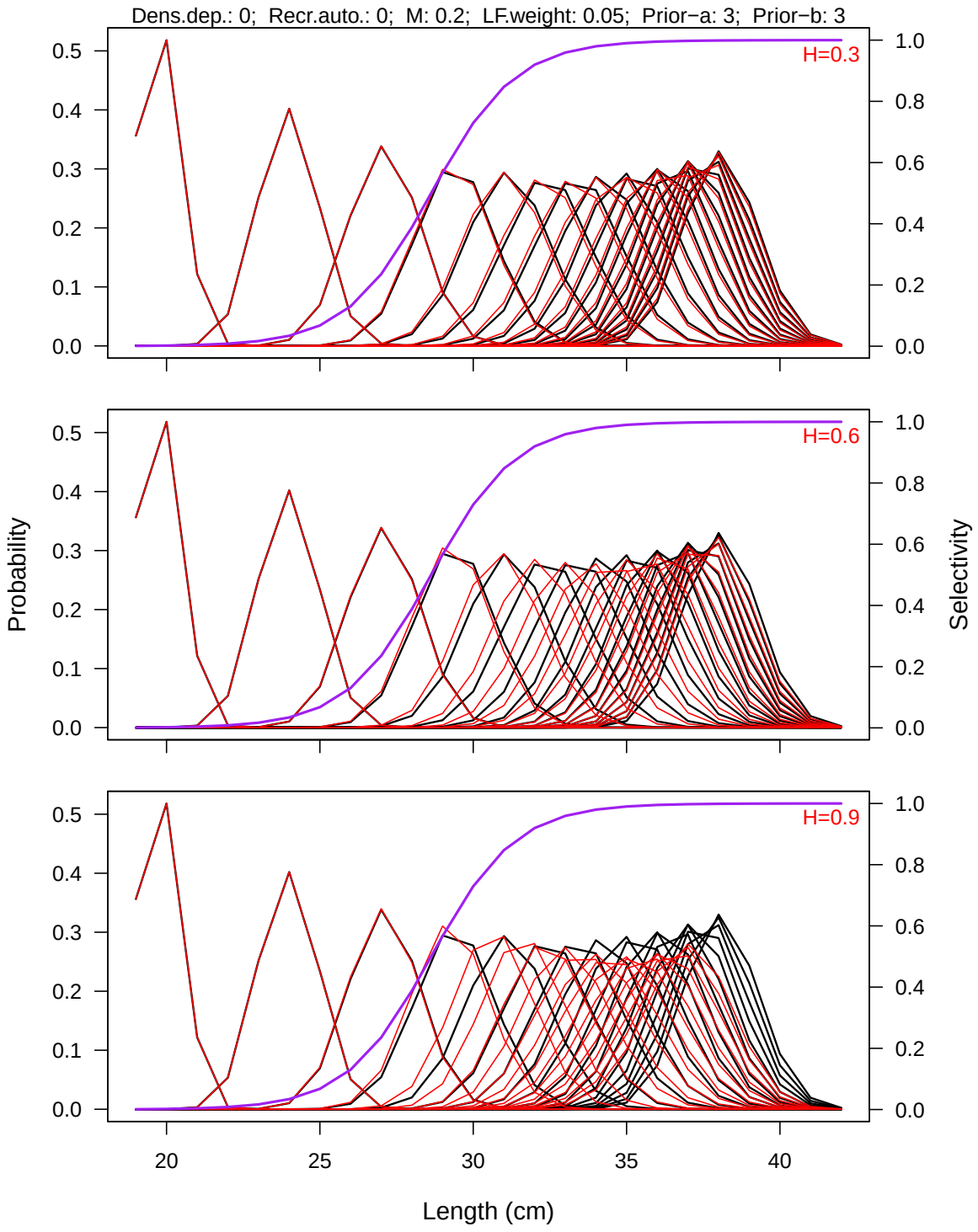

Figure 1: Illustration of probability densities for length at age at equilibrium for different harvest rates (H) for a standard age-structured model (black) and the length- and age-structured model developed for the present project (red). The assumed length-based selectivity is shown in purple. At high harvest rates, the length-at-age diverges between the models because length-based removals affect the length distribution of individual year classes in the length- and age-structured model.

2.2 Prior conditioning

Setting a wide prior on scale parameters (e.g., recruitment at unexploited equilibrium) can drive stock status close to 100% B_0 in a model with limited information on population scale (e.g., lacking a biomass index with contrast; see Thorson & Cope 2017). This is because prior distributions of the parameters are typically interpreted as the range of possible values in the input-space, rather than as possible values of outcomes in the output-space, such as stock status. To avoid this issue, we performed a prior conditioning procedure, which tuned the input-space prior distributions to produce a desired range of outcomes in the output-space. The procedure was based on the following steps:

1. The model was run using 10 000 sets of parameter values drawn from their initial prior distributions (hereafter, referred to as the input-space prior) as the input values, without fitting to the data.
2. The prior predictive distribution of the final-year stock status was conditioned on a beta distribution (hereafter, referred to as the output-space prior), which was used to represent the plausible range of the stock level in the final year.
3. To have consistent prior distributions between the input and output spaces, the input-space prior was iteratively updated using the sampling importance resampling (SIR) algorithm until the prior predictive distribution of the final year stock status closely matched the output-space prior. The details of the use of the SIR algorithm for prior conditioning are further explored in Kim & Neubauer (2025).

We allowed the conditioning procedure to incorporate correlations between the parameters into an updated joint prior distribution. To do this, we assumed that a joint prior distribution of the log- or logit-transformed parameters ($\boldsymbol{\theta}$) in the input space was multivariate normal (MVN) with the mean vector $\mathbf{X}$ and the covariance matrix $\Sigma^{\boldsymbol{\theta}}$:

$$\boldsymbol{\theta} \sim MVN(\mathbf{X}, \Sigma^{\boldsymbol{\theta}}).$$

A list of input-space parameters and their hyper-parameter values for the joint prior that serves as the basis for this conditioning approach is given in Table 1.

Table 1: Parameters estimated within the model and their hyper-parameter values for the joint MVN prior. The final column indicates the transformation applied to each parameter; i.e., let x be the transformed form of parameter θ. Then, for the bounded logit transformation, $x \sim N\left(\mathbf{mean}, \mathbf{SD}^2\right)$, **where** $x = \mathbf{logit}[(\theta - \mathbf{low})/(\mathbf{up} - \mathbf{low})]$ **and for the log transformation,** $x \sim N\left(\mathbf{mean}, \mathbf{SD}^2\right)$, **where** $x = \log(\theta)$**.**

Description (notation)	mean, or (lower and upper bounds)	SD	transform
unfished biomass at equilibrium (B_0)	12.9	5	log
SD of length-at-recruitment age ($\sigma_{L,1}$)	$(0.5, 1.5)$	1.6	logit
SD for length distributions of between age groups ($\sigma_{L,2}$)	$(0.8, 1.8)$	1.6	logit
Length at 95% selectivity (γ_{95})	$(27, 35)$	1.6	logit
Length at 5% selectivity (γ_5)	$(21, 27)$	1.6	logit

2.3 Model fitting

Most of the model parameters utilised in this study were obtained from previous studies (Horn 1991); fixed parameters are listed in Table 2. To estimate the remaining parameters, the model was fitted to the data using Bayesian inference (details about likelihood components are given in Appendix A). After carrying out the prior conditioning approach (for three different prior settings; see above), an updated joint MVN prior was assigned to the parameters.

The annual catch data (Figure 2) were treated as known without error and used to derive annual harvest rates within the model. The joint likelihood function of the model was constructed based on the following data sources: (1) length composition data from 2005 to 2014 with missing data in 2007, and (2) age composition data in 2020 and 2021.

The model was fitted using the No-U-Turn Sampler (NUTS) algorithm (Hoffman & Gelman 2014) implemented in `Stan`. The model was run for 8 chains with 800 iterations each, and the first 400 iterations were discarded as warm-up. The convergence of the model was assessed using the Gelman-Rubin statistic (Gelman & Rubin 1992) and the effective sample size (Vehtari et al. 2021). The model was fitted using the `cmdstanr` package in `R` (Gabry et al. 2023).

Table 2: Input parameter values used in the model. The value of the steepness was arbitrarily chosen.

Description (notation)	Value	Reference
Recruitment age bin	2	Age composition data
Maximum age bin (A)	20	Age composition data
Length (cm) at 95% maturity (v_{95})	30	Fisheries New Zealand (2022)
Length (cm) at 50% maturity (v_{50})	26	Fisheries New Zealand (2022)
Asymptotic length (cm; L_∞)	36	Horn (1991)
Growth coefficient (κ)	0.3	Horn (1991)
Theoretical age at length 0 (a_0)	−0.65	Horn (1991)
Steepness (h)	0.8	

2.4 Alternative model configurations

The sensitivity of the model and management procedure to alternative assumptions regarding the model parameters and processes was evaluated by examining models with different configurations (Table 3). While variable length-at-age has the potential to influence the performance of the management procedure, no evidence currently supports the notion that the growth rates of this species are variable. It is plausible that future investigations or environmental changes may identify this phenomenon, but in the absence of strong evidence for growth variability, we only ran a small subset of models for this sensitivity.

Table 3: Alternative models with the values used for their construction. The short notation used for each assumption is given.

Description	Value	Short notation
Weights given to the length composition data	0.05 or 0.5	LF.weight
Beta prior assumptions on stock status	(3,3) or (3,7) or (7,3)	Prior-a and Prior-b
Recruitment autocorrelation	0 or 0.6	Recr.auto.
Existence of density dependent growth in length	0 or 0.2	Dens.dep.
Natural mortality	0.2 or 0.3	M

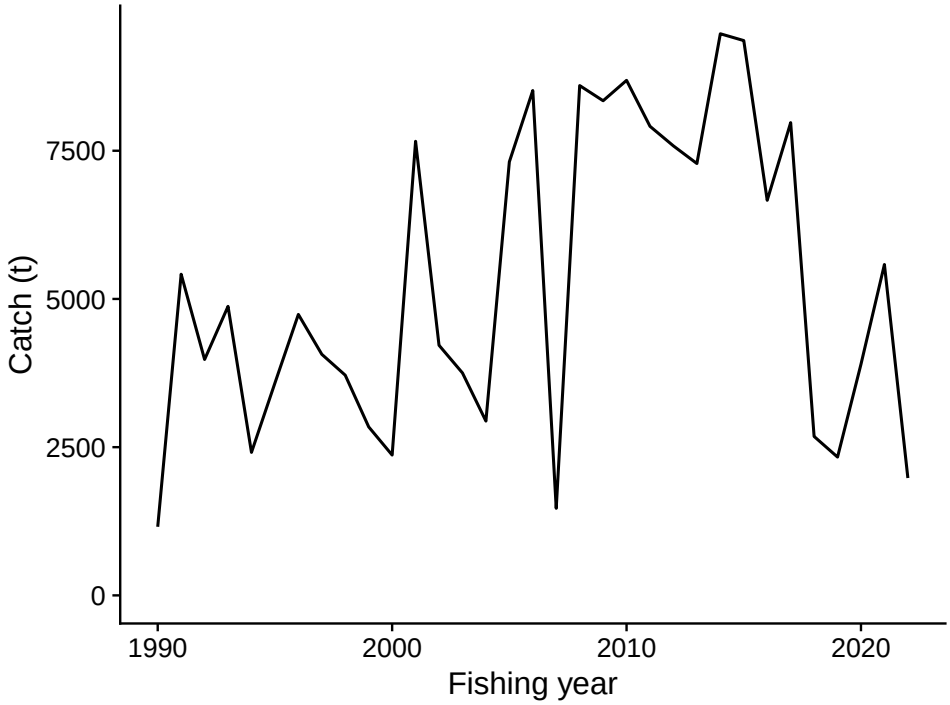

Figure 2: Catch time series for JMN used to fit the operating model used in the management procedure evaluation.

2.5 Management procedure evaluation

2.5.1 The Length-Moving-Average-Range control rule

The Length-Moving-Average-Range (LMAR) class of management procedures (developed by Bentley & Middleton, unpublished data, see Appendix D) for the JMN component of JMA 1 alter the catch limit in response to changes in the mean length of the catch. The approach of the LMAR management procedure is to maintain the mean length, as a proxy for exploitation rates, within a range. All else being equal, when exploitation rates are higher, mean length will be smaller (e.g., Gulland & Rosenberg 1992). If the mean length falls below the lower bound of the range then the catch limit is cut by a fixed percentage. Conversely, if mean length rises above the upper bound of the range, indicating lower exploitation rates, the catch limit is increased by the same fixed percentage.

More precisely, LMAR uses some measure, L_y, of the central tendency of the length distribution of the catch in each year. For simplicity, and because the length distribution of the JMA 1 catch is relatively symmetric, we have used the mean length of the catch (alternatives would include the median and geometric mean). To mitigate the effects of potential observation or process error on variation in the mean length, the measure is smoothed using an exponential moving average,

$$\tilde{L_y} = rL_y + (1-r)\tilde{L}_{y-1}$$

where r is the *Responsiveness* control parameter. A higher value for r will result in $\tilde{L_y}$ being more responsive to changes in mean length in the last year. When $r = 1$, there is no smoothing.

In each year, $\tilde{L_t}$ is compared to a range defined by the two control parameters *Target*, t, and *Buffer*, b (Figure 3). If the value is outside the range defined by those parameters then there is an increase or decrease in the catch limit, the magnitude of which is determined by (i) how far the mean length is below or above target, (ii) the *Reaction* parameter, a. When $\tilde{L_y} > t + b$ or $\tilde{L_y} < t - b$ then the catch limit is multiplied by $(\tilde{L_y}/t)^a$. For example, if $t = 30$ *cm*, $b = 1$ *cm* and $a = 1$, and if $\tilde{L_y} = 28$ (i.e. 93% of

target) then the existing catch limit will be reduced to $(28/30)^1 = 93\%$ of its current value. However, if $a = 3$ then it would be reduced to $(28/30)^3 = 81\%$.

We evaluated the harvest control rule over a period of 100 years from 2022, using a range of control-rule parameters and 96 model combinations. Due to the combinatorial nature of the simulations (each combination of parameters was evaluated for all 96 models, using 500 MCMC draws from the model to implement the MPE), we were limited in the number of options that could be evaluated. We, therefore, focused on a range of parameters that appeared most influential in previous evaluations (Bentley & Middleton, unpublished data; provided here as Appendix D) and initial investigations during the present project (Table 4).

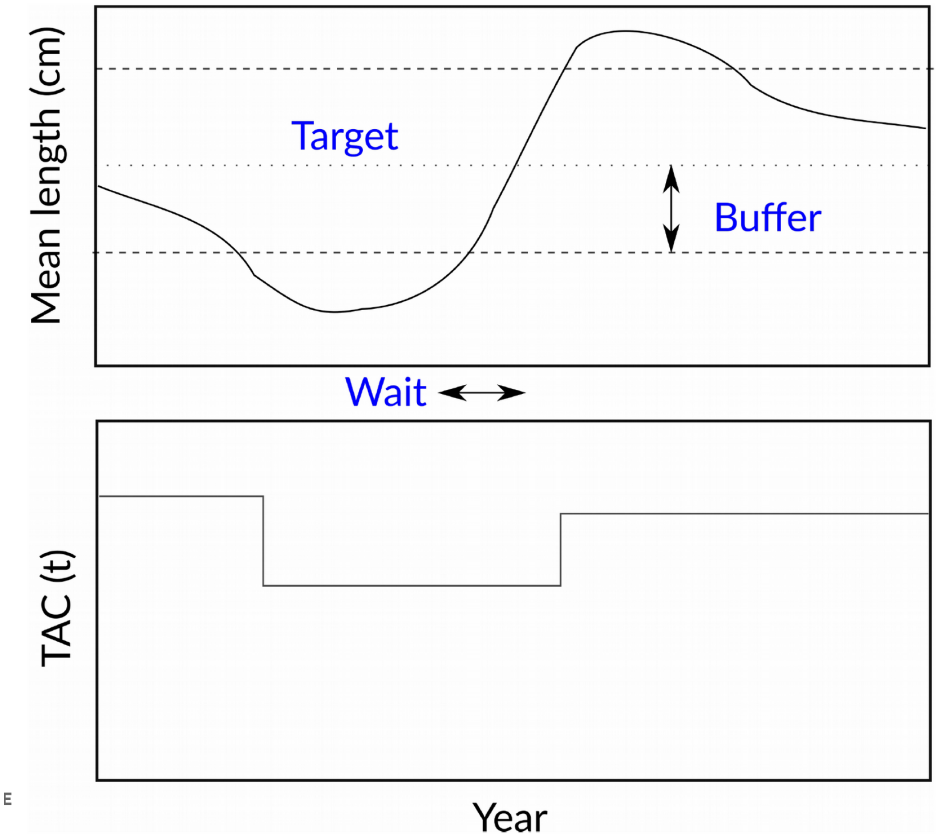

Figure 3: The "Length-Moving-Average-Range" (LMAR) management procedure: if the (potentially smoothed) mean length value is outside the range defined by the target length and buffer, then there is an increase or decrease in the catch limit with magnitude determined by how far the mean length is below or above target, and the "reaction" parameter (i.e., the "wait")(figure from Bentley & Middleton, unpublished data; see Appendix D).

Table 4: Reference and alternative values for control parameters of the LMAR management procedure

Parameter	Value	Alternatives
Smoothing (r)	1	-
Target (t; cm)	31	30, 30.5
Buffer (b; cm)	0.5	0.2
Reaction (a)	1	2
Wait (w; yrs)	2	1
Maximum TACC (t)	7 500	15 000

In particular, the target length appeared highly influential in previous evaluations: effectively, the target length is equivalent to a target harvest rate at equilibrium.We therefore sought to test a range of target lengths that correspond to default target assumptions for species of medium productivity; specifically the harvest rate leading to a default target of 40% of unfished spawning potential ($H_{SPR}40\%$). The correspondence between mean length and harvest rate is further detailed in Appendix B.3. The calculation suggested a target harvest rate of 0.3–0.35 at a mean length of 31 cm for an assumed natural mortality of 0.2, and a harvest rate of around 0.6 at a mean length between 30 and 30.5 cm for $M = 0.3$ (Figure 4).

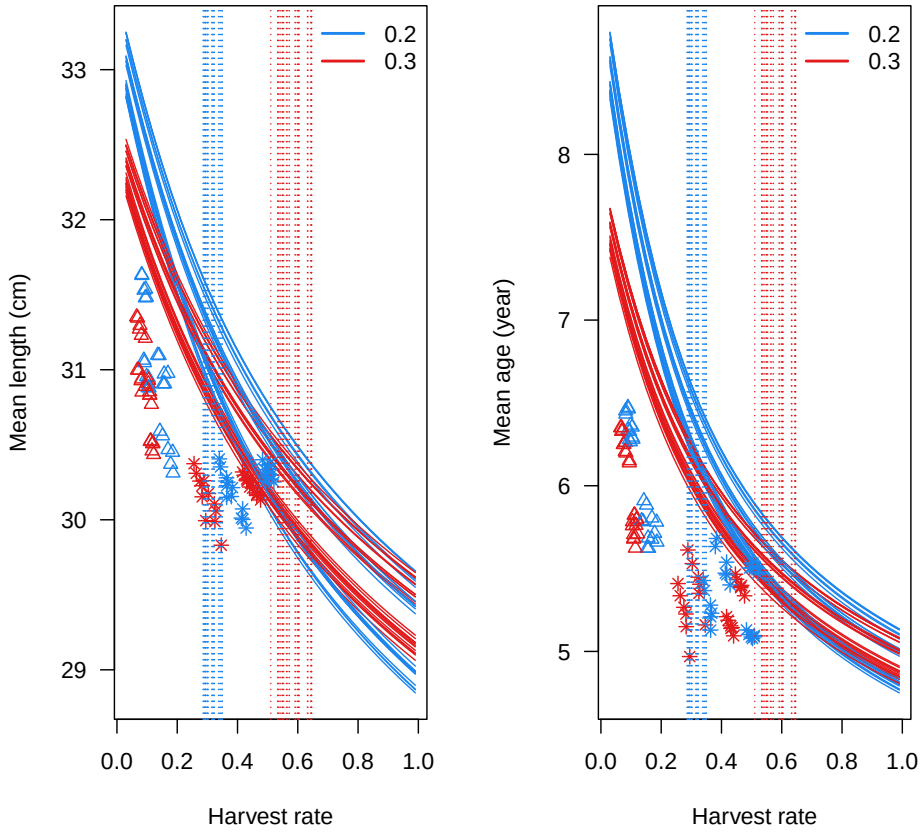

Figure 4: Equilibrium mean length at a given harvest rate for all models, coloured by the assumed natural mortality. Dashed vertical lines show the default target of 40% of unfished spawning potential ($H_{SPR}40\%$) for the range of models fitted to data. Triangles show the harvest rate and mean length for the most recent fishing year (2022; 1979 t catch) as estimated from fitted models, while stars show the harvest rate and mean length in 2015, the peak catch year for the decade with the highest sustained catches (mean 8187.5 t).

2.5.2 Evaluation of the LMAR control rule

The evaluation of control-rules is usually conducted with respect to default or otherwise agreed reference points. However, the validity of reference points, and the performance of management procedures based on status relative to these reference points, is strongly dependent on having sufficiently accurate life-history information. For example, the mean length in models used here and therefore the target length, depends strongly on the assumption about natural mortality and growth (the M/K ratio), as well as selectivity. Basing targets on the wrong value can lead to poor performance of control rules (Punt et al. 2001, Klaer et al. 2012) with respect to keeping the stock at acceptable biomass levels (e.g., within levels of biomass required under risk constraints in the New Zealand Harvest Strategy Standard).

An alternative evaluation is to not consider absolute risk, by comparing against fishing mortality or other reference points, but to evaluate relative risk compared with a strategy of maintaining a constant TACC —which has effectively been the case for JMN since the mid-1990s. Performance can then be measured as the yield achieved under the control rule relative to constant catch at a given level of depletion or risk. This way performance is measured in relative terms, such that the least risky strategy can be used, even if the absolute risk is not known (Figure 5).

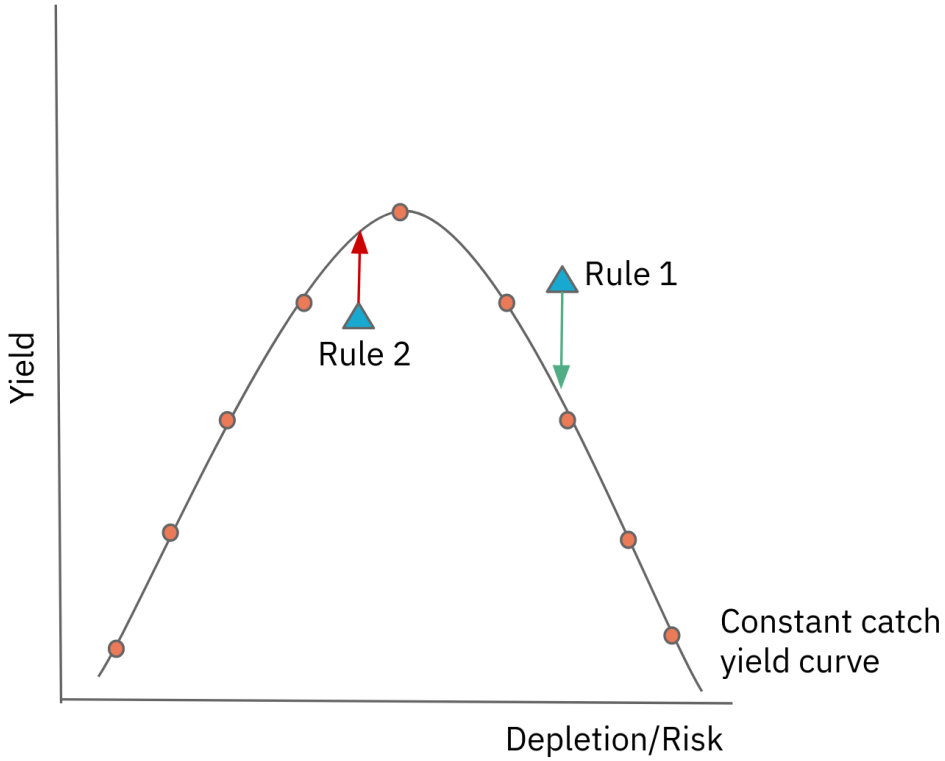

Figure 5: Illustration of comparisons of risk/performance of alternative control rules relative to a fixed catch set at the mean yield of the control rule scenarios. The performance metric is 'yield at equivalent risk', i.e., at a given risk level, does a management procedure based on a given control rule lead to, on average, increased yield over that provided by a constant catch across the time series?

3. RESULTS

3.1 Prior conditioning and model fitting

Prior (catch-only) conditioning led to a range of predicted stock depletion levels in the last year of data (2022) that closely reflected the beta input priors (Figure 6). However, in full model fitting, these priors had relatively limited influence on the estimated stock status (Figure 7). The posterior (estimated) stock status depended on length-frequency weighting and model assumptions (Figures 8, 9); across all models, stock status in recent years tended to increase as a result of relatively low recent catches. Nevertheless, the models displayed a range in estimates of recent median status, with differences largely influenced by the assumed natural mortality and the weight given to length compositions versus age compositions (Figure 10).

Natural mortality and length composition weights influenced the fits to the compositional data (Figures 11, 12, 13), as well as the trajectories of key model quantities, such as mean length and age (Figures 14, 15, 16), selectivity (Figure 17), and the standard deviation of length-at-age (Figure 18). Models with lower length-composition weight were better able to fit age data (Figures 11), at the expense of the fit to length-frequency data (Figures 12, 13). These models also estimated a smaller size at 50% selectivity (Figure 17), and a more pronounced increase in the standard deviation of length-at-age (Figure 18).

Models with higher M estimated overall smaller sizes and mean ages, whereas models with lower M estimated slightly larger sizes (Figure 14), leading to a small but consistent bias in estimated mean length (Figure 19).

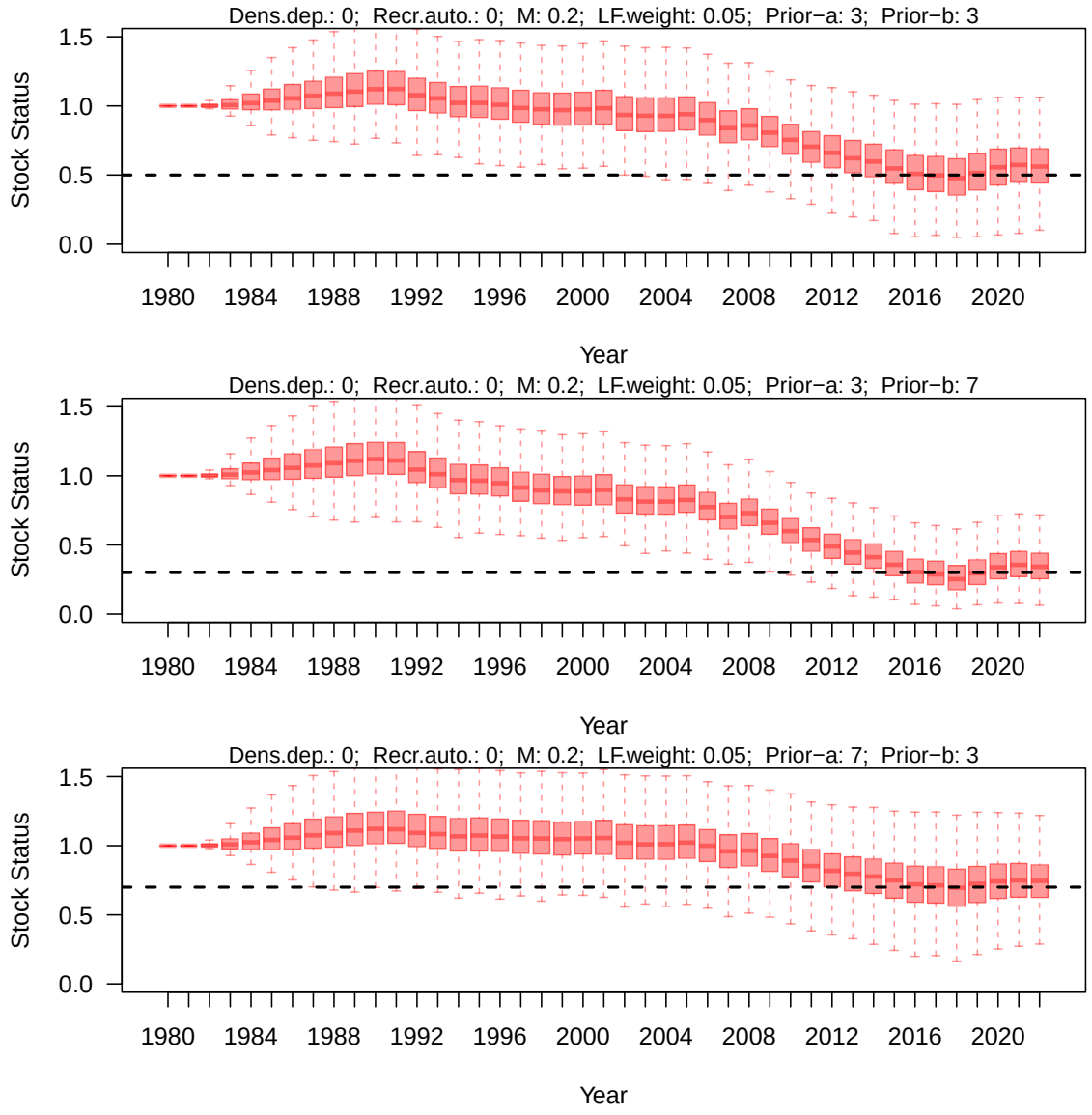

Figure 6: Prior predictive distributions of stock status after conditioning on three priors for stock status: one centred around 50% (beta(3,3); top panel), one centred on 30% (beta(3,7); middle panel) and one centred on 70% (beta(7,3); bottom panel).

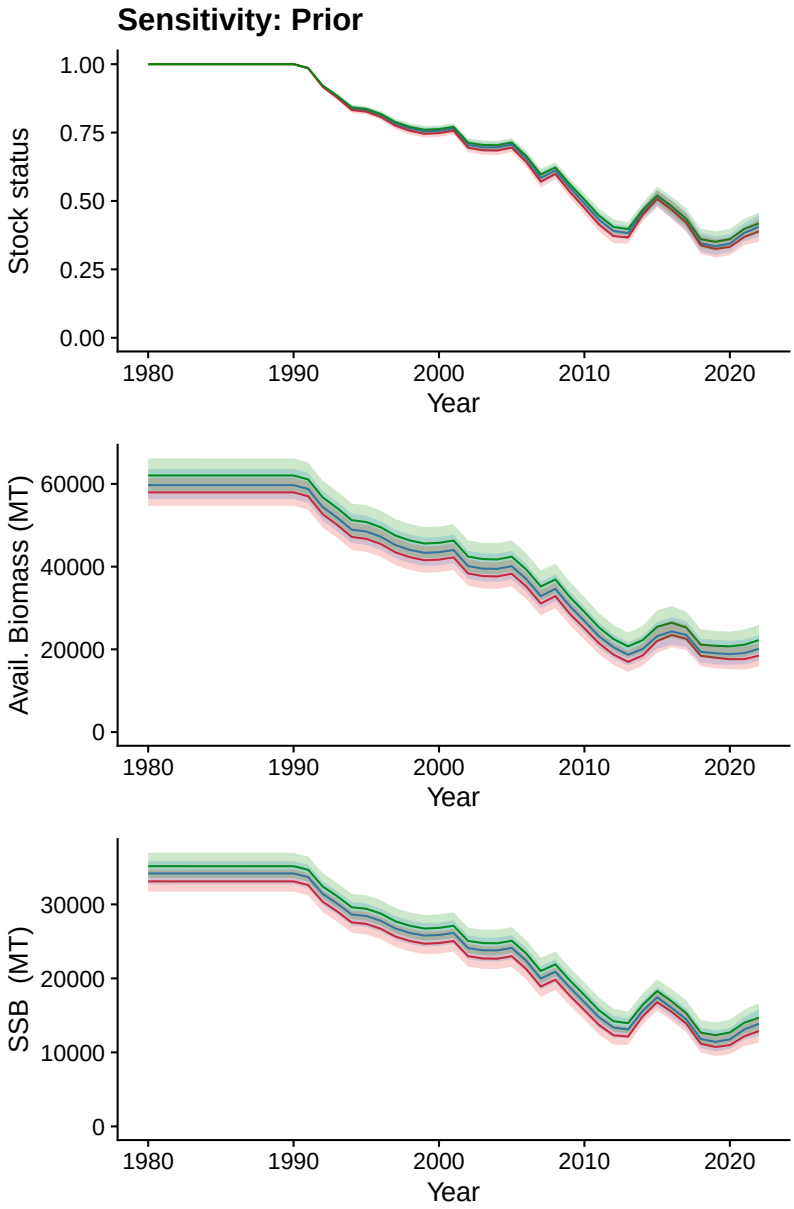

Figure 7: Estimated biomass trajectories under the model with base assumptions and the three different priors (colours; one centred around 50% prior stock status (beta(3,3); blue), one centred on 30% (beta(3,7); red) and one centred on 70% (beta(7,3); green); see Figure 6). Lines refer to simulation medians, shaded areas show 95% of simulated trajectories.

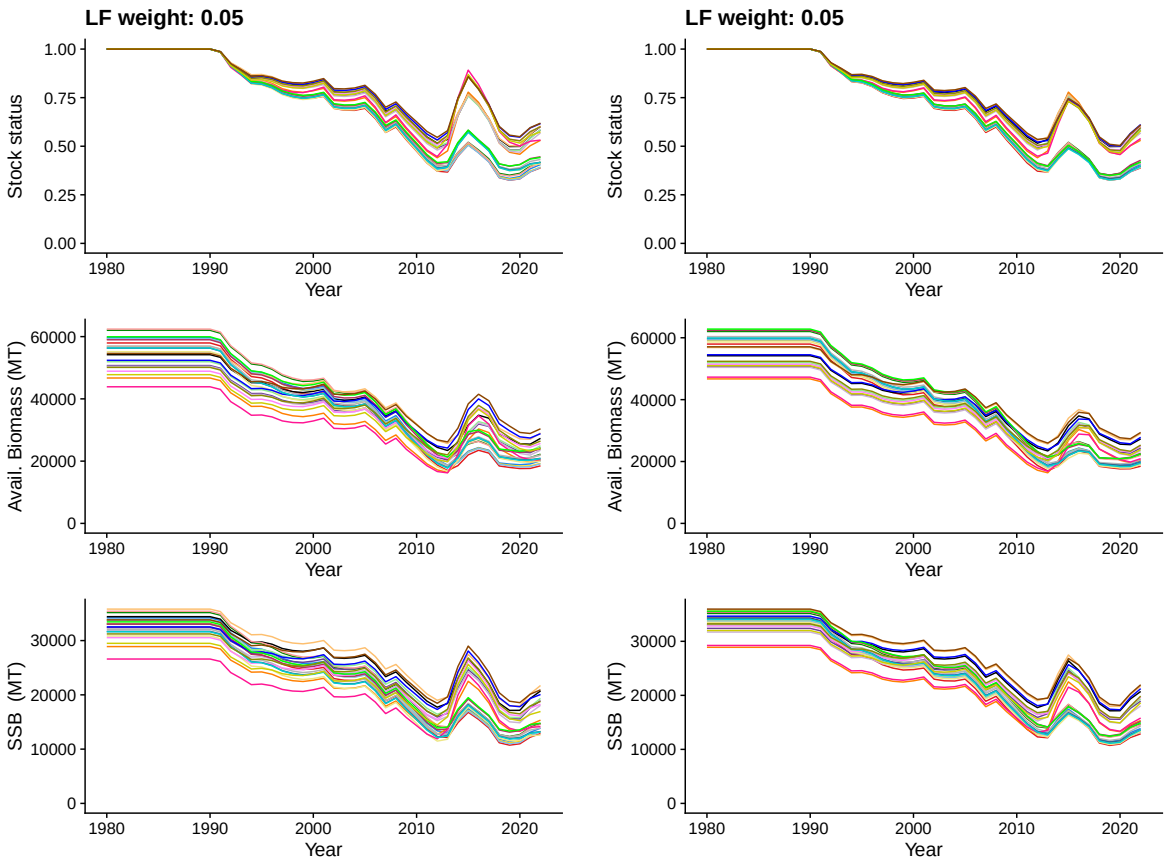

Figure 8: Estimated (posterior median) relative and absolute biomass (spawning stock and available biomass) across models for biomass (left panels) and recruitment (right panels) driven density dependence in asymptotic length, for models fitted with a length frequency (LF) weight of 0.05. Colours refer to individual model runs (alternative assumptions for other parameters) used under the setting indicated above each column.

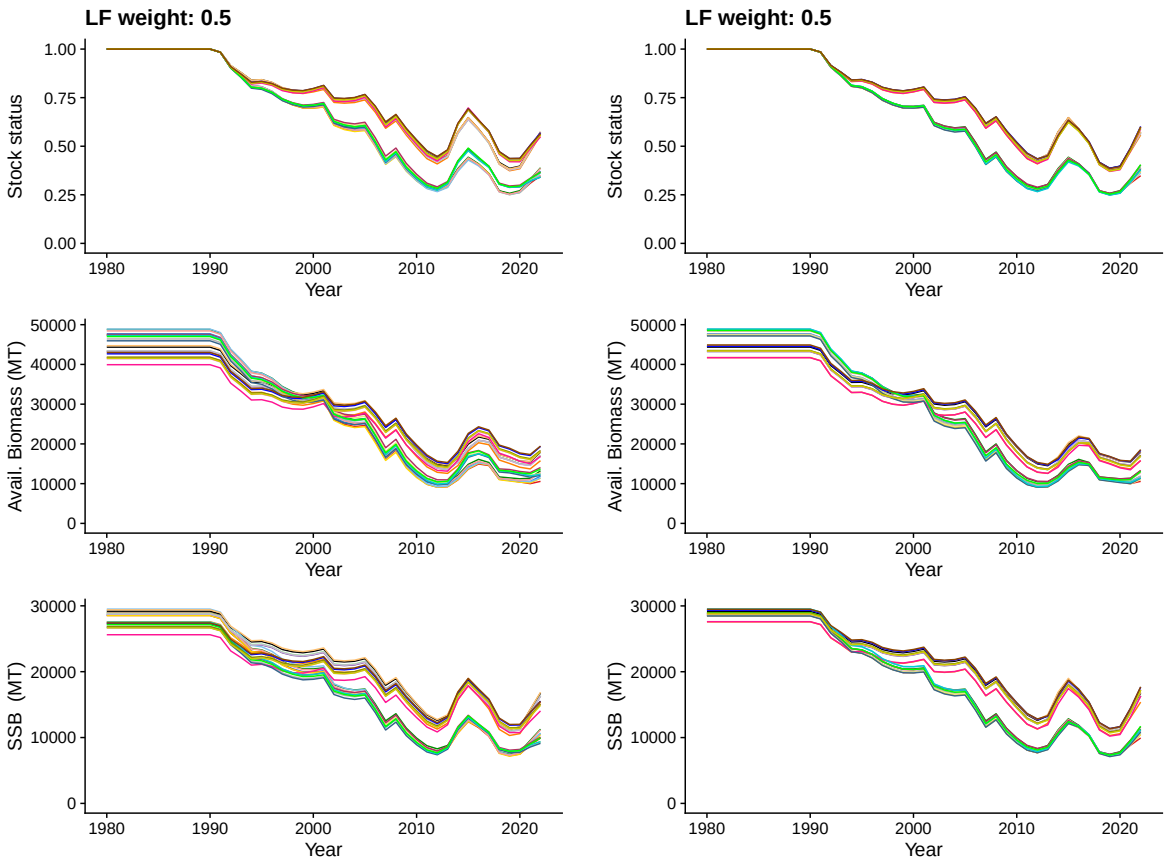

Figure 9: Estimated (posterior median) relative and absolute biomass (spawning stock and available biomass) across models for biomass (left panels) and recruitment (right panels) driven density dependence in asymptotic length, for models fitted with a length frequency (LF) weight of 0.5. Colours refer to individual model runs (alternative assumptions for other parameters) used under the setting indicated above each column.

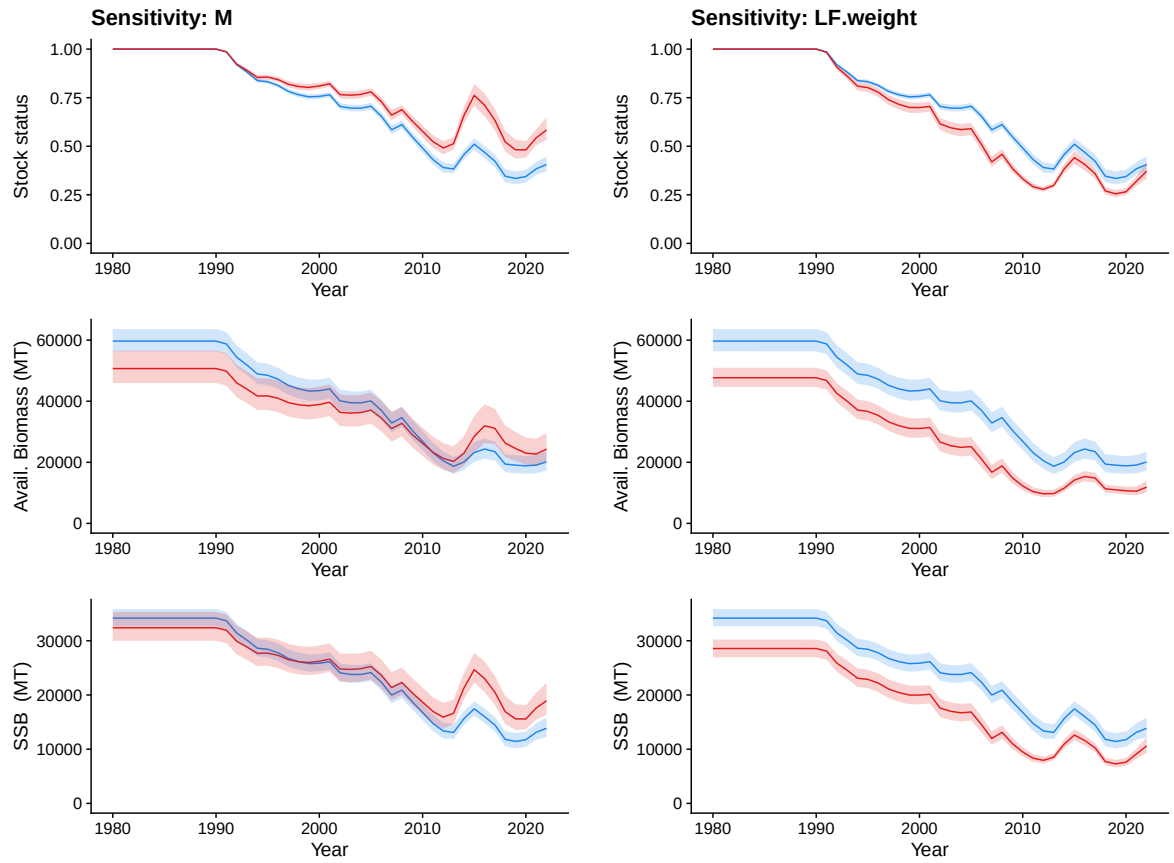

Figure 10: Estimated biomass trajectories under the base model with alternative natural mortality (*M*; left column: low M (0.2) in blue, high M (0.3) in red) and length frequency weight (LF; right column: low weight (0.05) in blue, high weight (0.5) in red). All other parameters were held at base values. Lines refer to Bayesian posterior medians, shaded areas show 95% of the posterior.

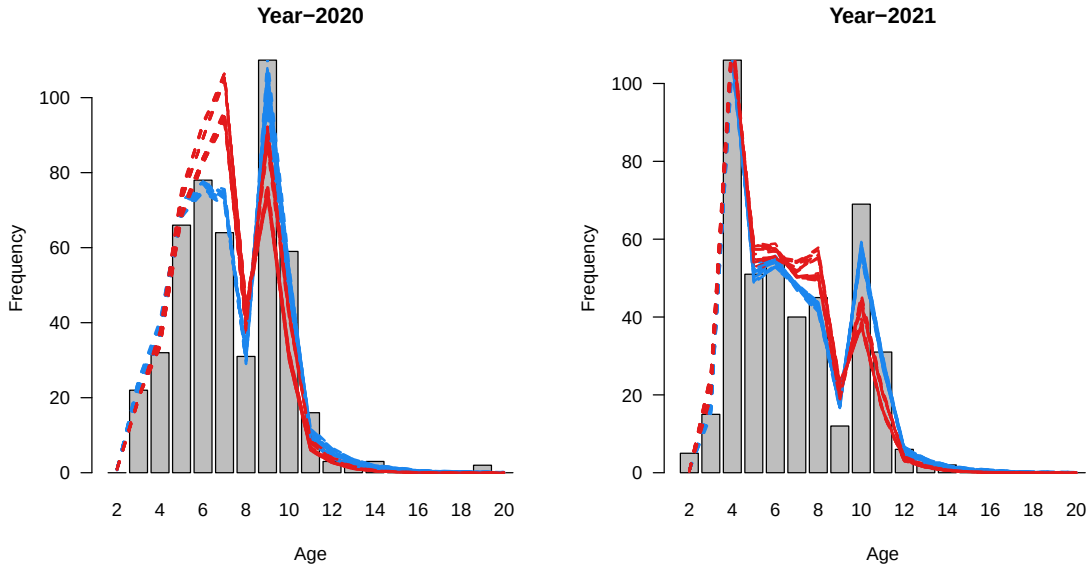

Figure 11: Fit (posterior median) to age composition data from two recent years, for models with low (blue) and high (red) weight for length frequency data.

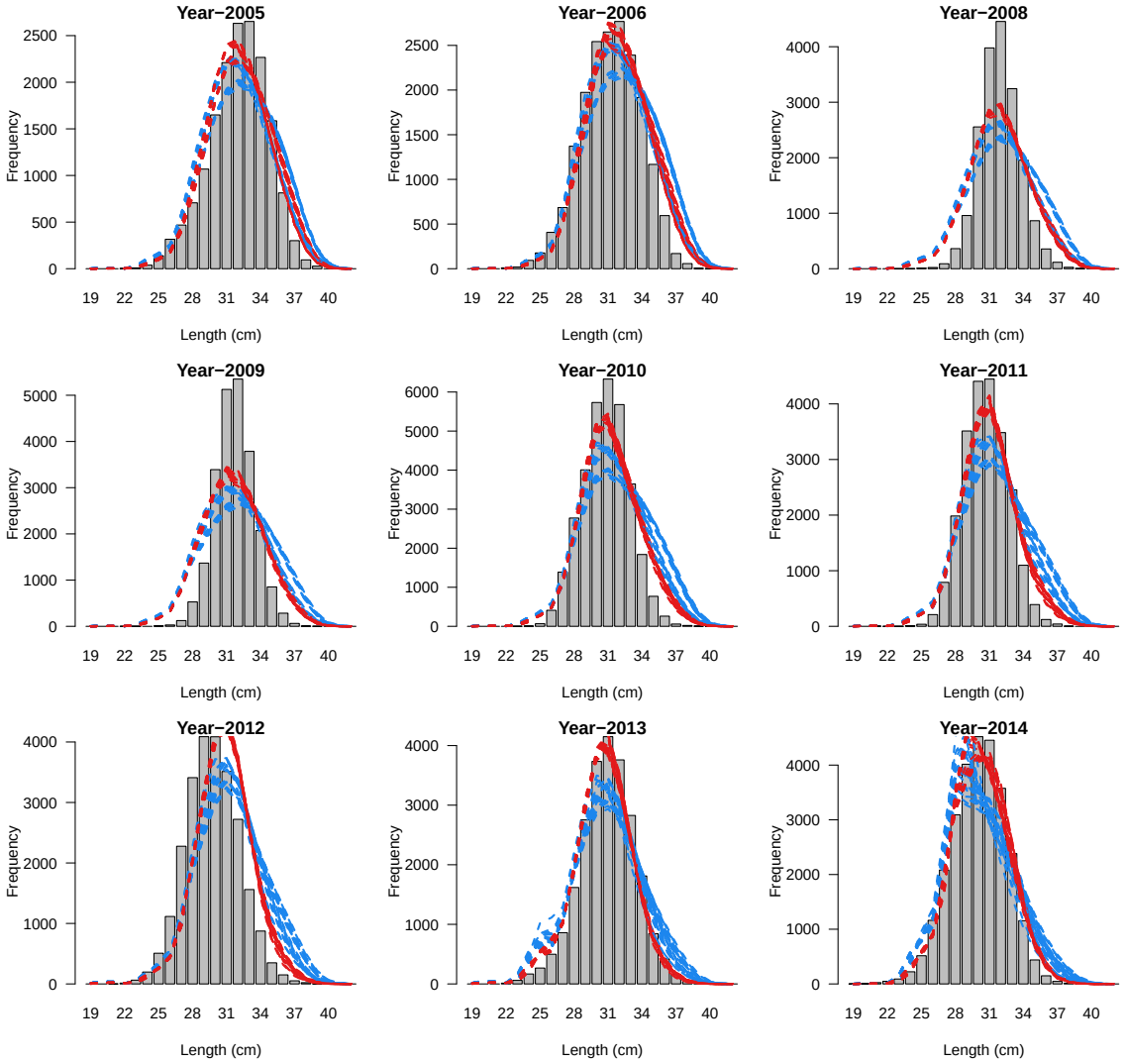

Figure 12: Fit (posterior median) to length composition data from 2005–2014, for models with low (blue) and high (red) weight for length frequency data.

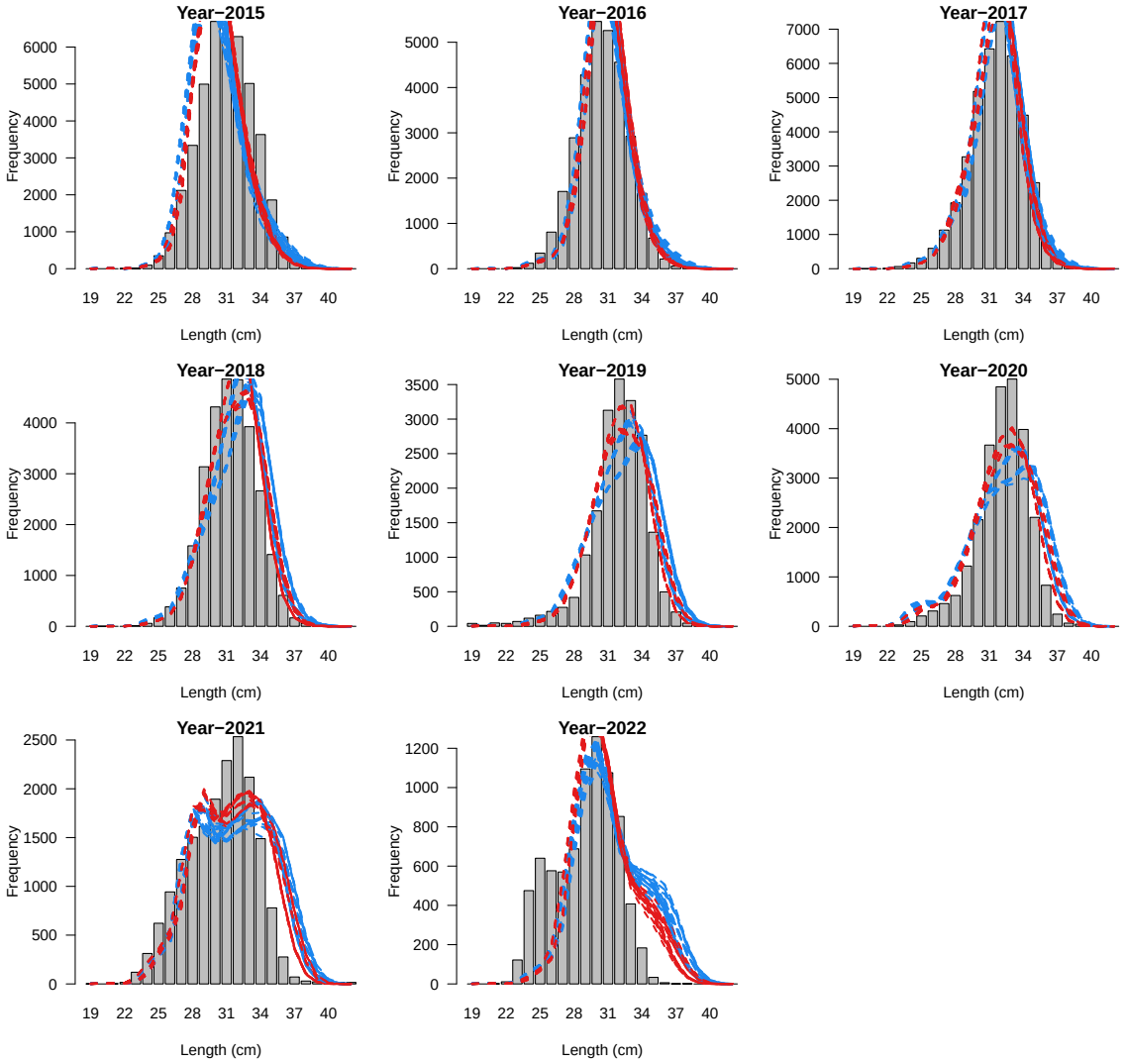

Figure 13: Fit (posterior median) to length composition data from 2015–2022, for models with low (blue) and high (red) weight for length frequency data.

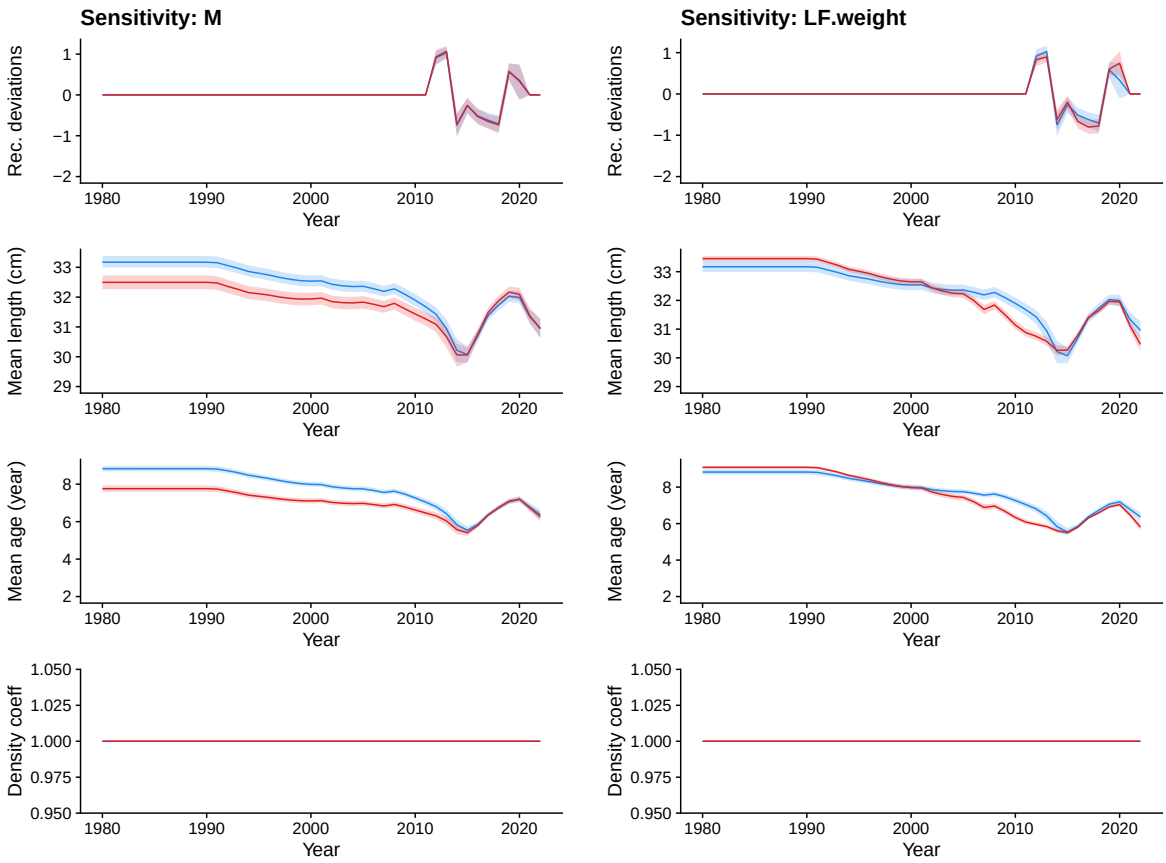

Figure 14: Estimated (posterior median) trajectories of recruitment deviations, mean length and mean age under the base model with alternative natural mortality (*M*; left column: low M (0.2) in blue, high M (0.3) in red) and length frequency weight (LF; right column: low weight (0.05) in blue, high weight (0.5) in red). All other parameters were held at base values. The density coefficient (coeff.) measures the impact of density dependence through time as a multiplier on growth parameters. Lines refer to Bayesian posterior medians, shaded areas show 95% of the posterior.

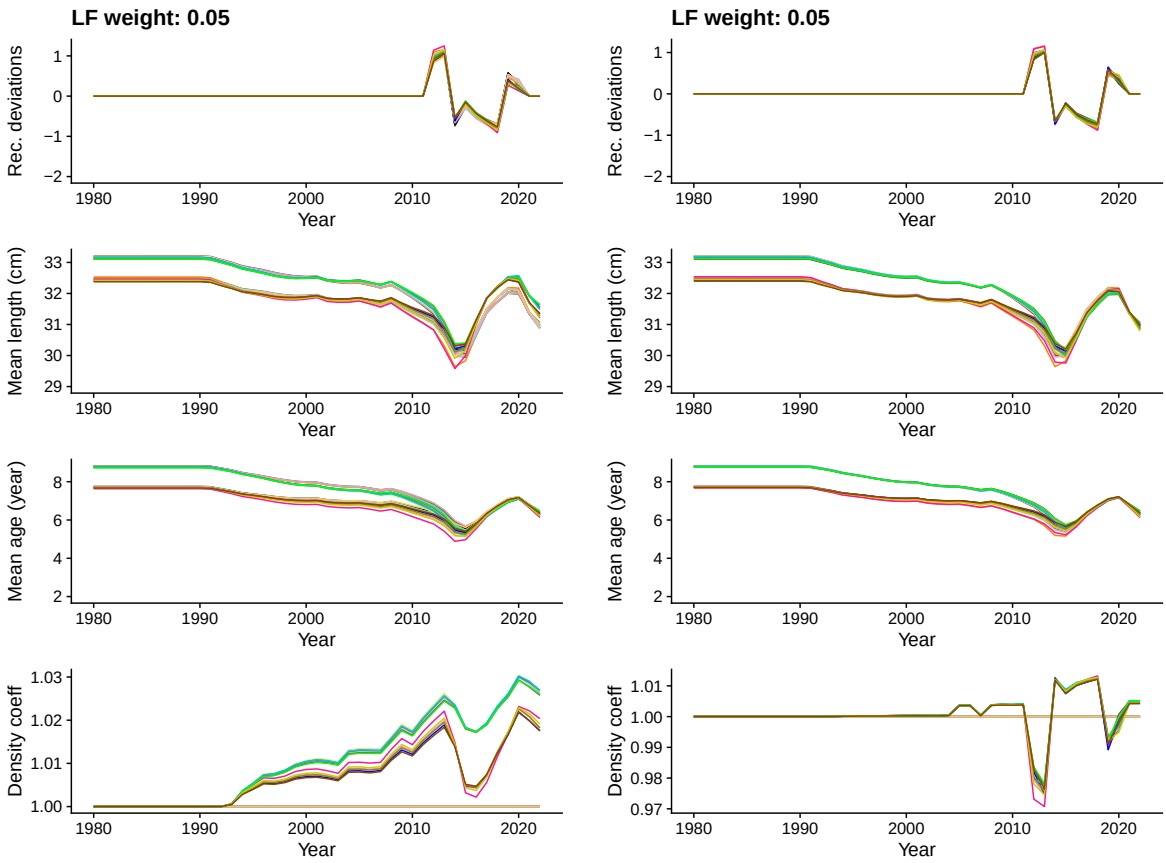

Figure 15: Estimated (posterior median) recruitment deviations, mean length and age, and density dependent change in growth parameters (asymptotic length), across models for biomass (left panels) and recruitment (right panels) driven density dependence in asymptotic length, fitted with a length frequency (LF) weight of 0.05. Colours refer to individual models runs with alternative assumptions for other parameters. The density coefficient (coeff.) measures the impact of density dependence through time as a multiplier on growth parameters.

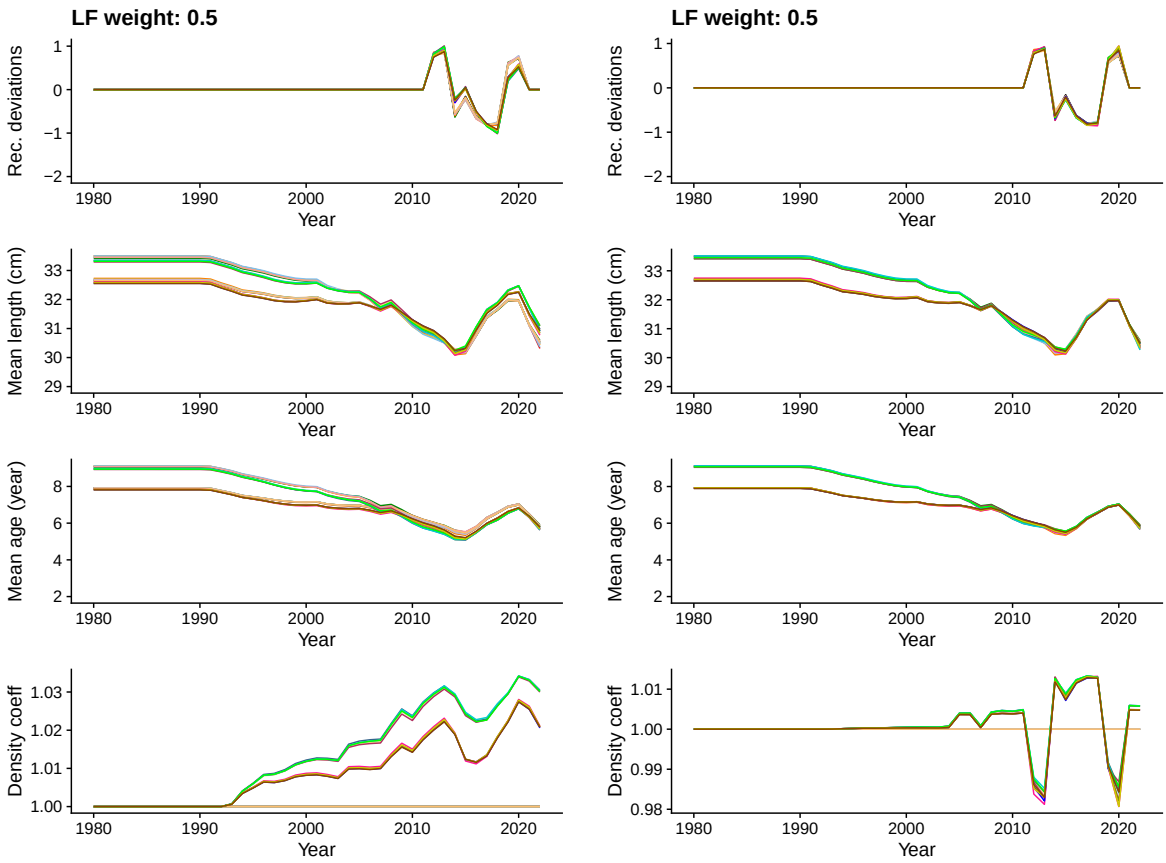

Figure 16: Estimated (posterior median) recruitment deviations, mean length and age, and density dependent change in growth parameters (asymptotic length), across models for biomass (left panels) and recruitment (right panels) driven density dependence in asymptotic length, fitted with a length frequency (LF) weight of 0.5. Colours refer to individual models runs with alternative assumptions for other parameters. The density coefficient (coeff.) measures the impact of density dependence through time as a multiplier on growth parameters.

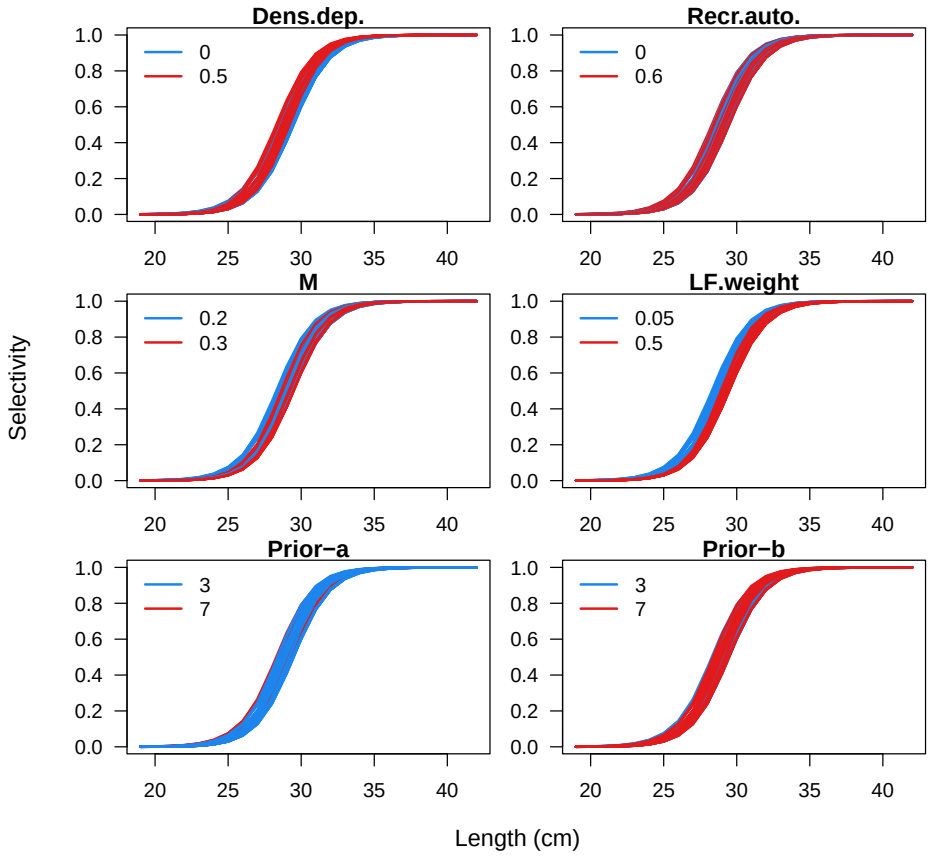

Figure 17: Estimated (posterior median) selectivity under alternative biological and model configuration assumptions. Selectivity estimates are largely determined by the length-frequency (LF) weight. Prior-a and-b refer to parameters of the beta-distribution used for prior conditioning.

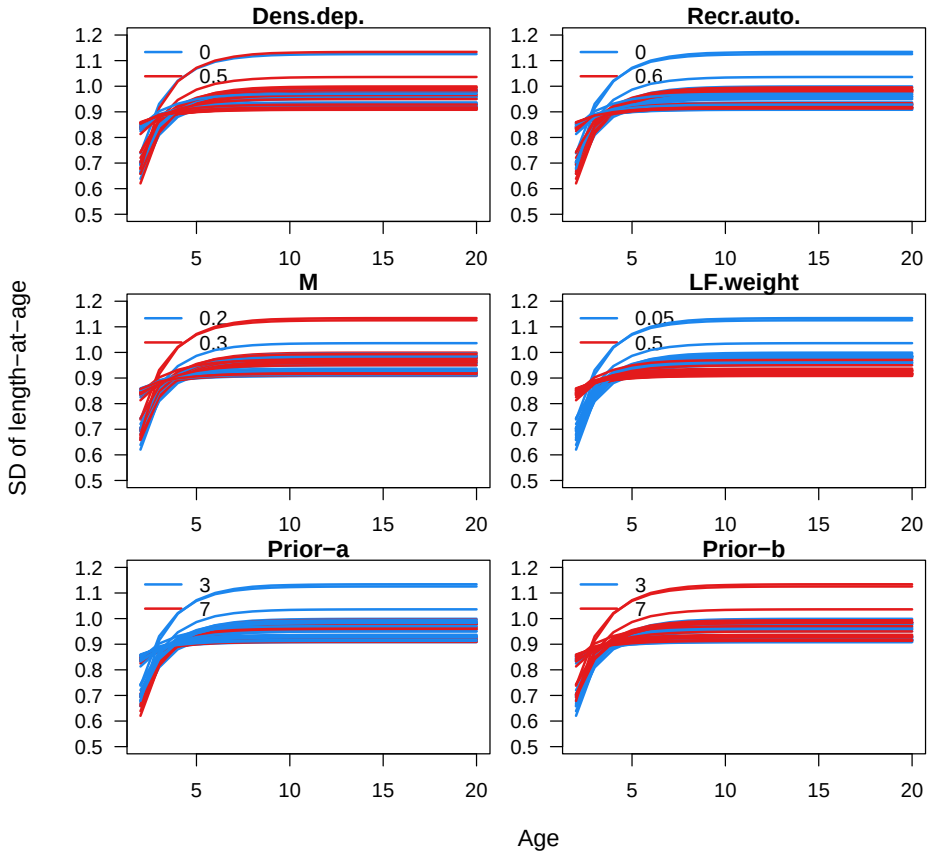

Figure 18: Estimated (posterior median) standard deviation (SD) of the length-at-age distribution by age under alternative biological and model configuration assumptions. Estimates of the SD of length-at-age are largely determined by the length-frequency (LF) weight.

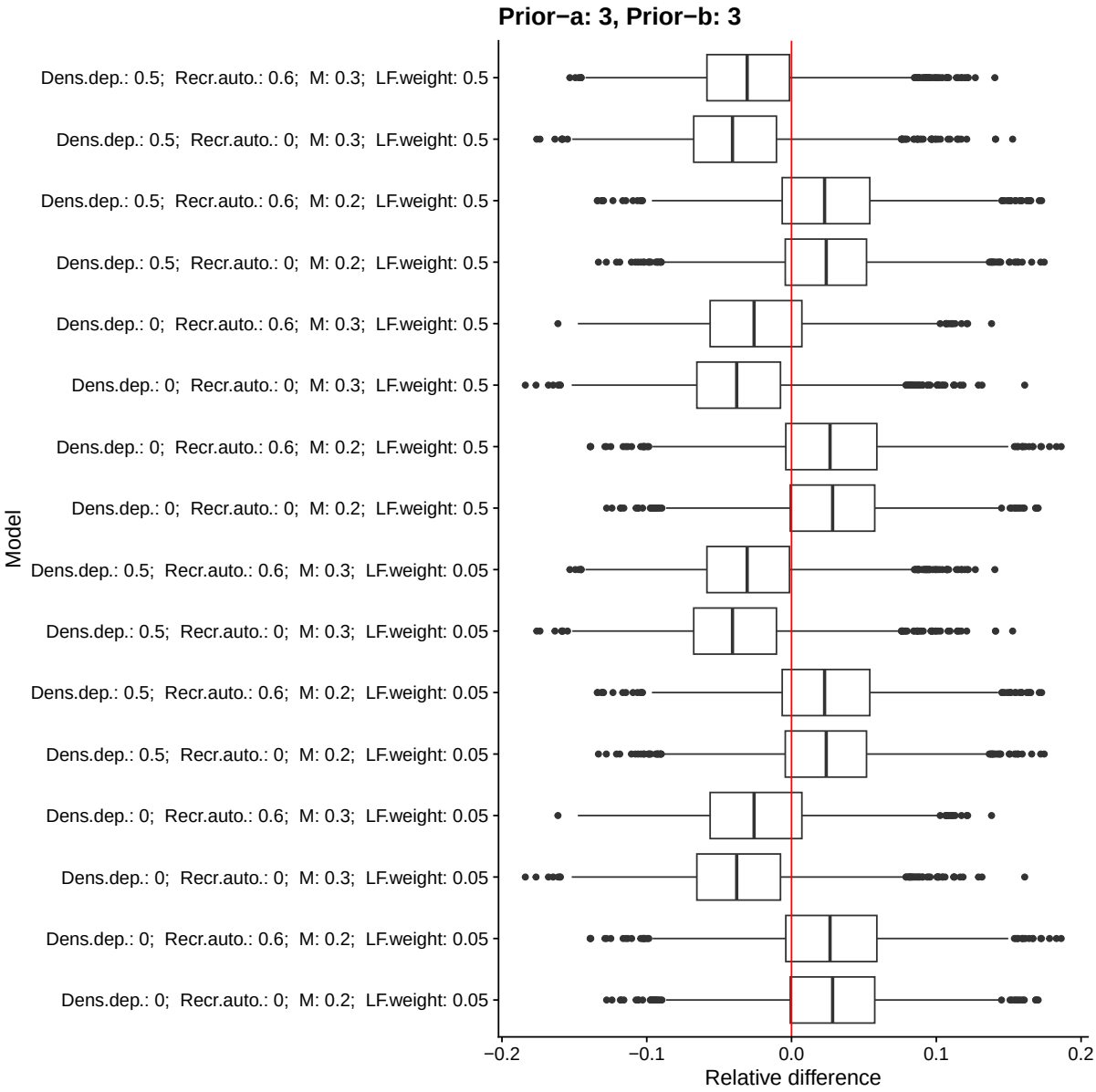

Figure 19: Relative error in mean length at age for model predictions under different model assumptions for natural mortality, length-frequency weights and recruitment autocorrelation assumptions.

3.2 Management procedure evaluation

A large number of models led to population depletion long-term, with slightly more trajectories leading to depletion at low *M* (Figures 20, 21), regardless of whether constant catch or control rules were applied. The collapse of individual simulated populations was often observed even under relatively low catch scenarios for both low and high natural mortality assumptions (i.e., catches near average long-term catches observed in the past; Figures 22, 23). The simulated populations were therefore highly unstable under all assumed fishing conditions. At stock sizes above zero, there was a clear trend in the mean of mean length with the size of the spawning stock, but also a lot of variation around this mean relationship (Figure 24), such that the range of mean lengths seen at a given stock status was wider than the decrease in expected mean size across a large range of relative biomass realisations (Figure 24).

While some model and control-rule combinations clearly had better performance than constant catch, if measured as equivalent yield at the simulation mean status (Figure 25), the overall performance was mixed. Under some circumstances, the control-rule settings (e.g., a relatively slow reaction time) led to improved performance over constant catch (Figure 26). Productivity assumptions, implicit in the scale of natural mortality, were found to be the most important factor in determining the relative performance of the length-based control rule (Figures 27, 28). For models with low *M*, other biological assumptions, such as density dependence formulations and recruitment auto-correlation were also important in determining whether length-based control rules performed as well as, or worse, than constant catch. For models with higher *M*, by contrast, control-rule parameters were most important, and the reaction rate and application intervals determined if the rule provided some benefit over constant catch. Even in that case, the average benefit was moderate (~10%) over constant catch rules.

When the set of simulations was subset to only those with control-rule parameters that appeared to provide a benefit (i.e., measured as a mean positive equivalent yield ratio at the simulated mean status; see blue values on the right hand side of Figure 28), the range of outcomes was narrowed, but the overall mean outcome was still equal to constant catch for JMN (Figure 29). Sensitivity runs with variable length-at-age for a subset of model configurations did not suggest a significant impact on relative yield at equivalent risk (Figure 30).

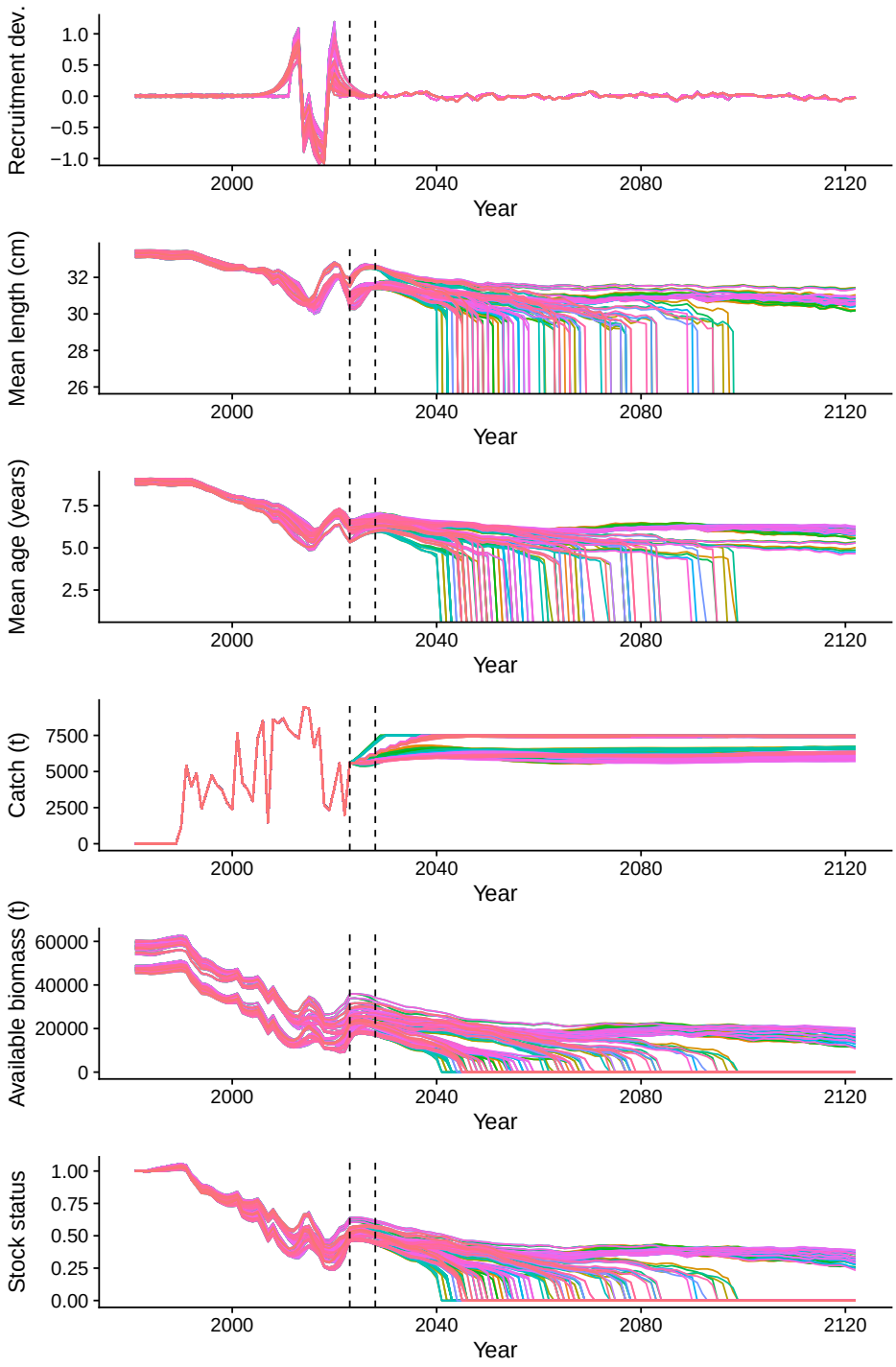

Figure 20: Median stock trajectories for all models with M = 0.3. Vertical dashed lines indicate the starting year for MPE simulations and a 5 year potential implementation horizon from the starting year.

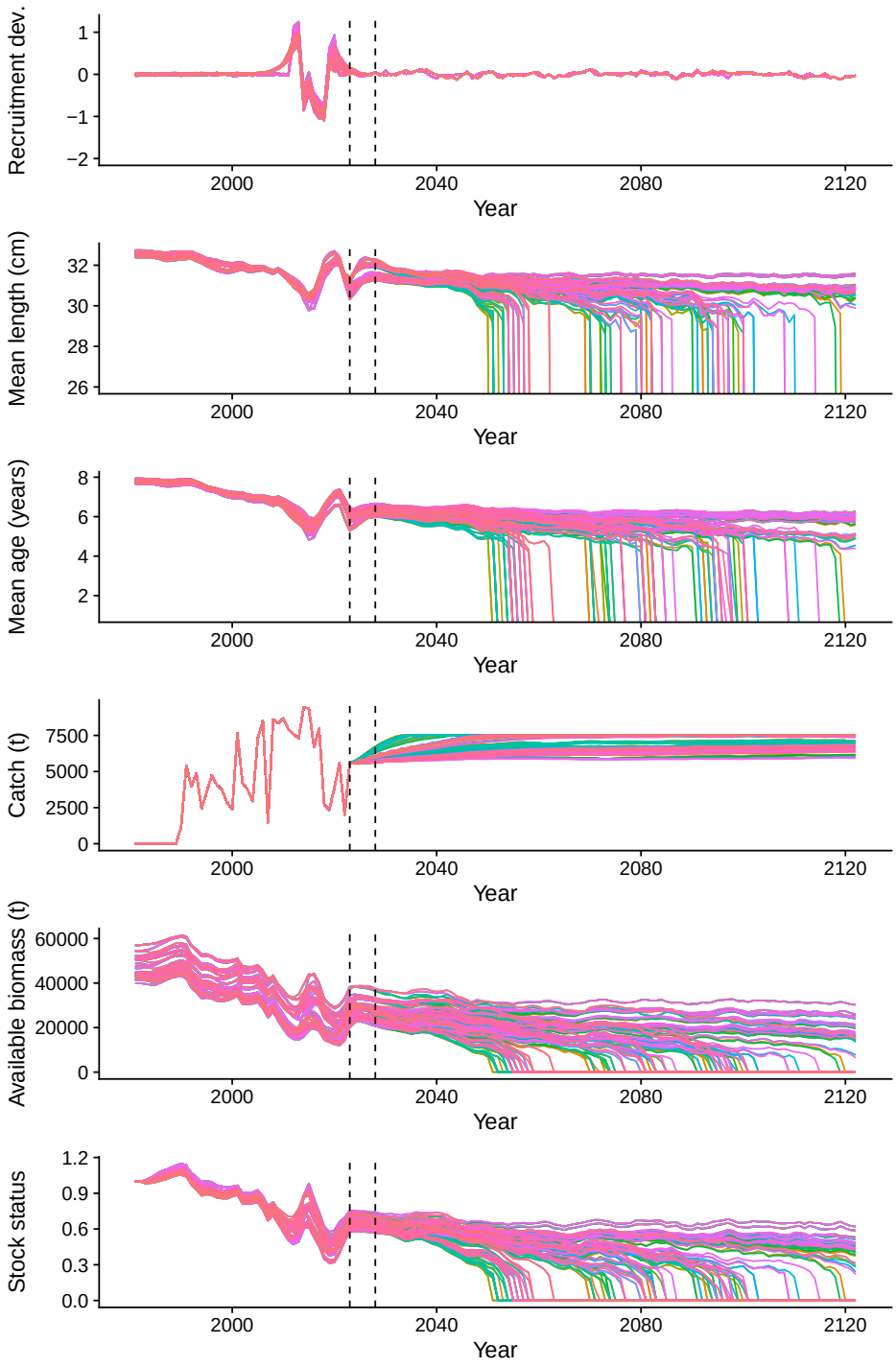

Figure 21: Median stock trajectories for all models with M = 0.2. Vertical dashed lines indicate the starting year for MPE simulations and a 5 year potential implementation horizon from the starting year.

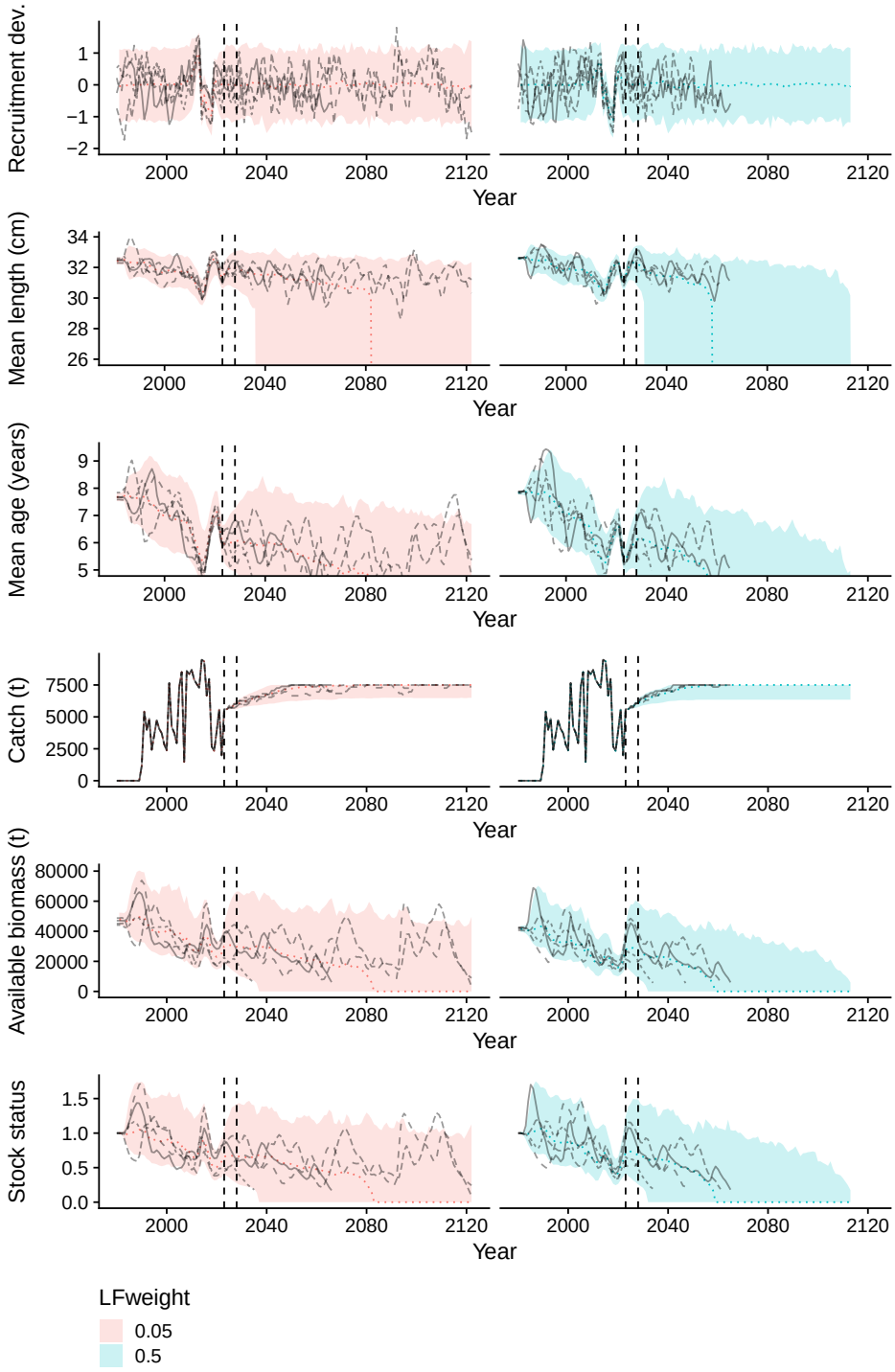

Figure 22: Illustration of median stock trajectory (solid line), 95% confidence interval (shaded area), and individual median trajectories (broken lines) for randomly sampled realisations from the simulations for a single model with M = 0.3. Vertical dashed lines indicate the starting year for MPE simulations and a 5 year potential implementation horizon from the starting year. Colours indicate models with different length-frequency weights.

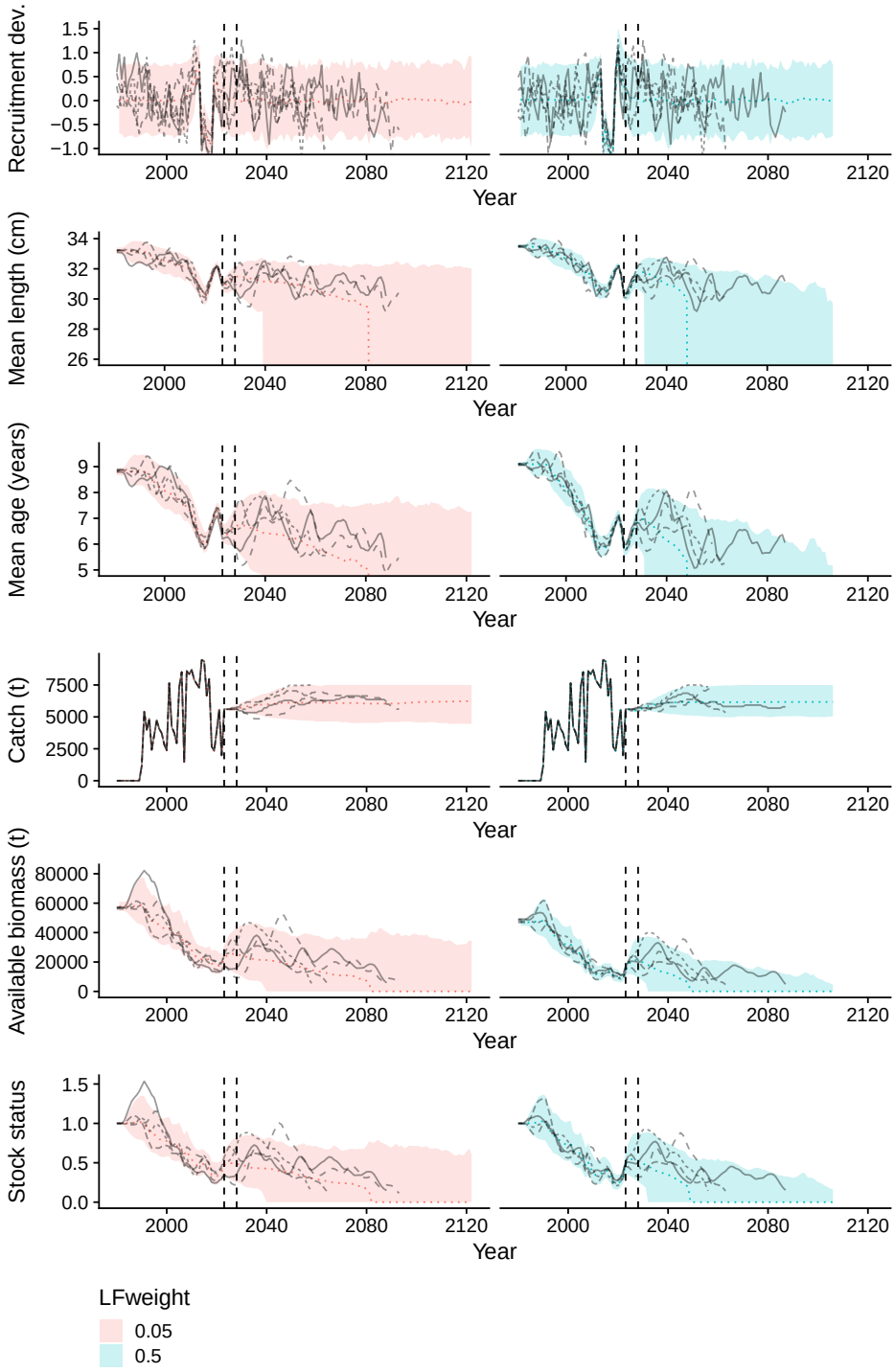

Figure 23: Illustration of median stock trajectory (solid line), 95% confidence interval (shaded area), and individual median trajectories (broken lines) for randomly sampled realisations from the simulations for a single model with M = 0.2. Vertical dashed lines indicate the starting year for MPE simulations and a 5 year potential implementation horizon from the starting year. Colours indicate models with different length-frequency weights.

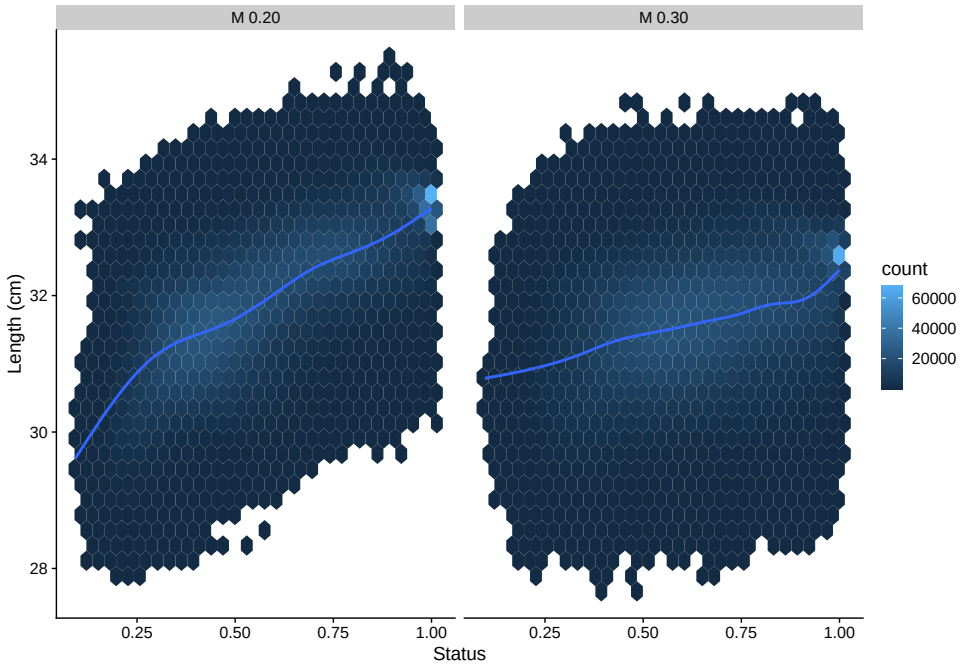

Figure 24: Distribution (hexagon-binned) samples of mean length against stock status across the range of models and harvest control-rules tested. The smoothed mean of mean-lengths is shown as the blue line.

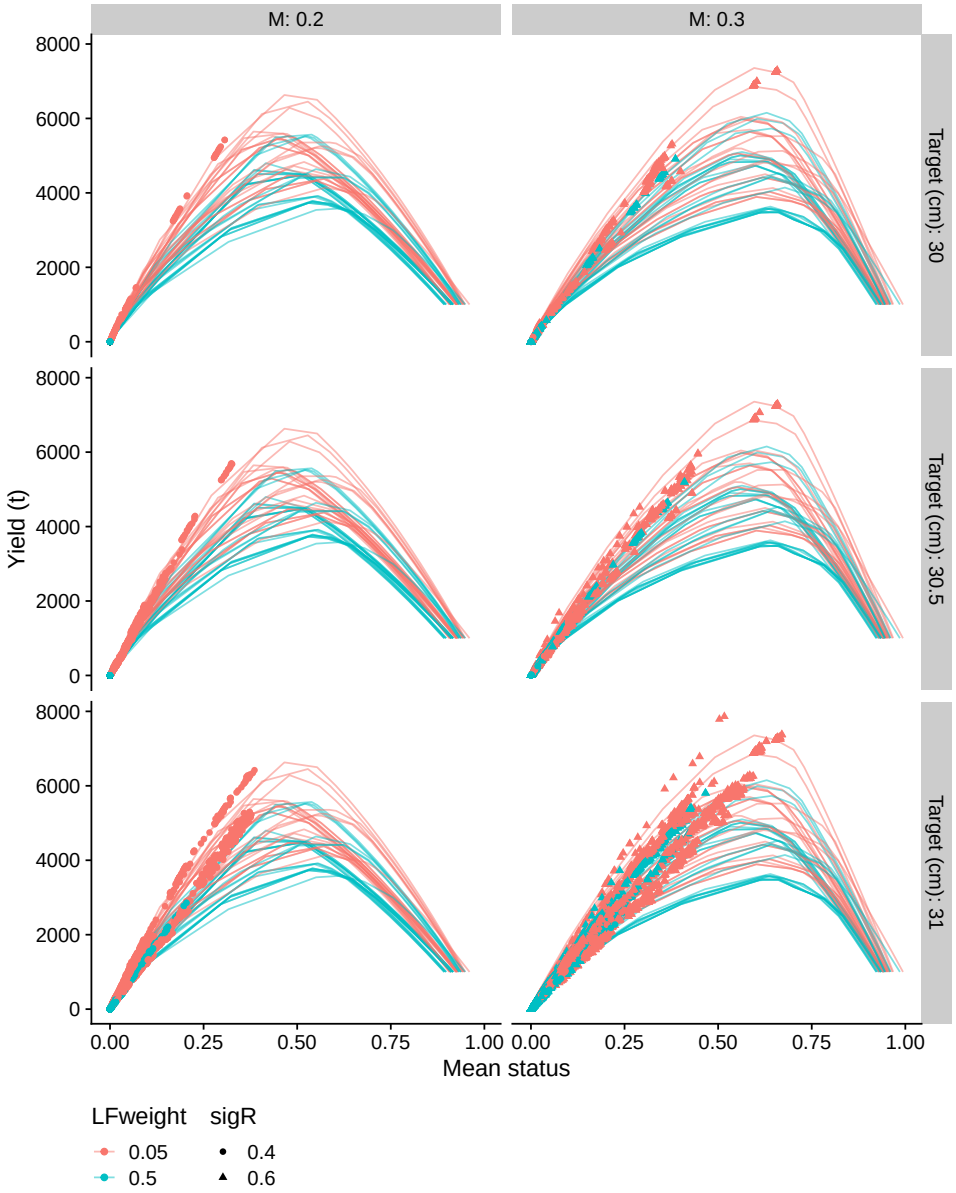

Figure 25: Long term (average) yield and associated (mean) stock status for constant catch (solid lines) and length based control rules (symbols) for the range of models considered in the management procedure evaluation, plotted by target length (rows) and natural mortality (*M*; columns).

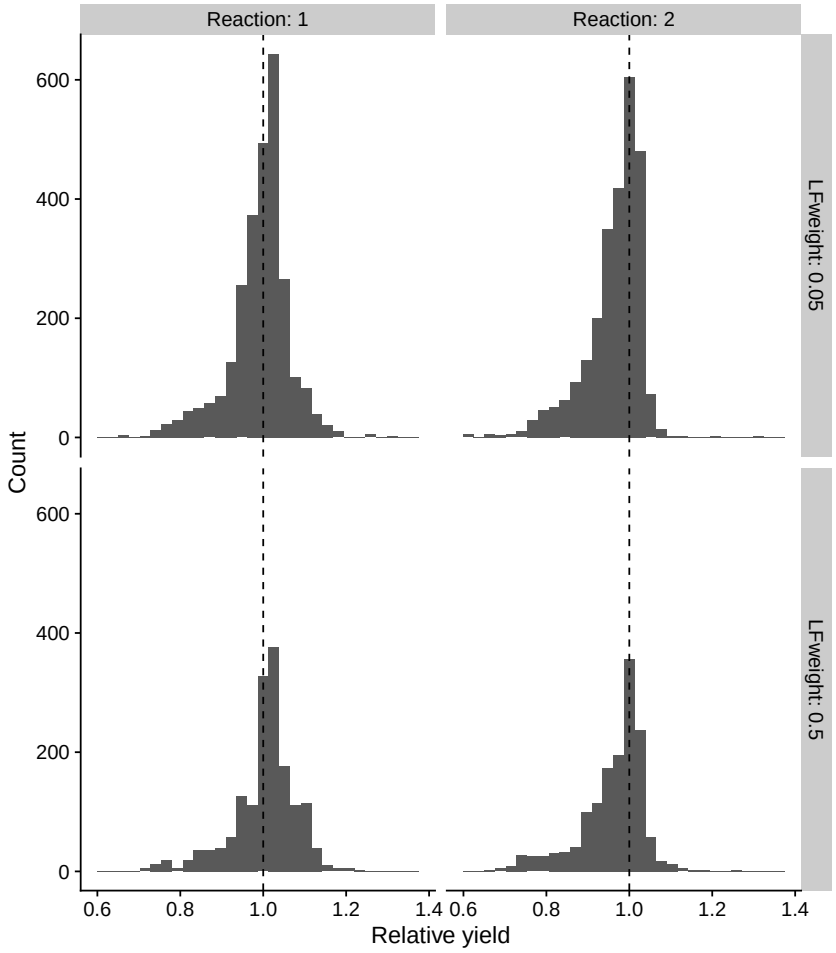

Figure 26: Average relative yield at equivalent risk across models, histograms are shown by length-frequency weight and separated into scenarios with proportional (Reaction:1) and power-scaling (Reaction:2) adjustments to catch as a function of length.

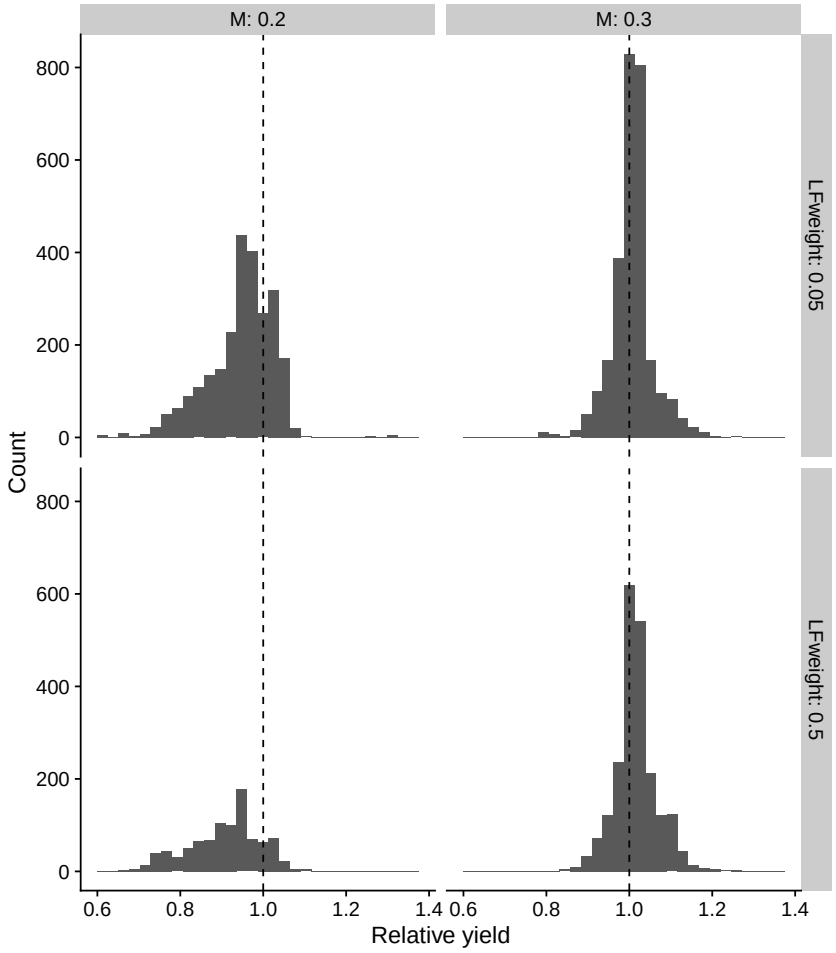

Figure 27: Average relative yield at equivalent risk across models, histograms are shown by length-frequency weight and separated into scenarios with high (M = 0.3) and low (M = 0.2) natural mortality.

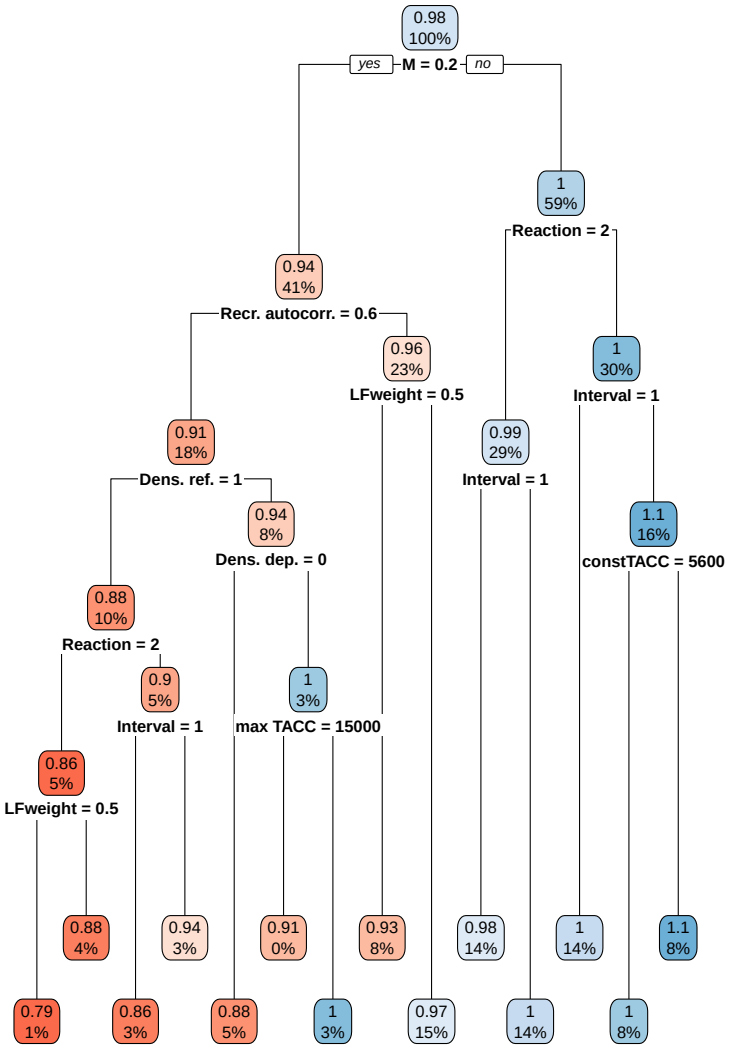

Figure 28: Regression tree of average relative yield at equivalent risk for simulations under the mean-length based harvest control rule relative to constant catch simulations. The tree partitions relative yield by factors/ covariates. Branches to the left indicate that the condition indicated at the split is true ("yes"), with branches to the left of any split leading to lower (red) relative yield than branches to the right. (*Note*, *duetosoftwarelimitations*, *thecolourscaleis***not centred on an equivalent yield (i.e., 1).)**

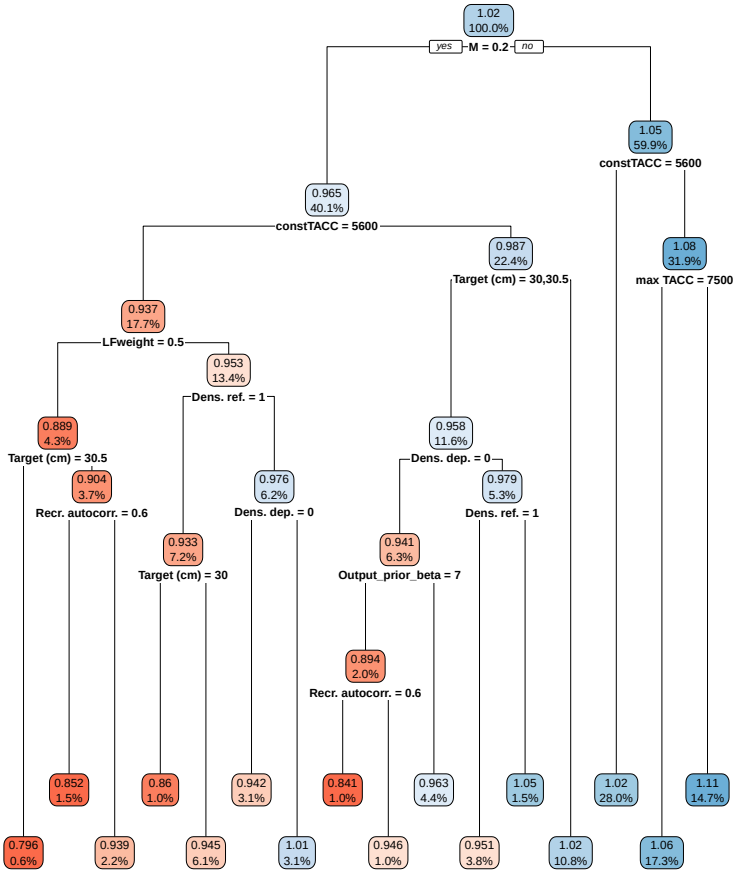

Figure 29: Regression tree of average relative yield at equivalent risk across models, subset for harvest-control rule setting that lead to positive relative performance for high *M* scenarios. Branches to the left indicate that the condition indicated at the split is true ("yes"), with branches to the left of any split leading to lower (red) relative yield than branches to the right.

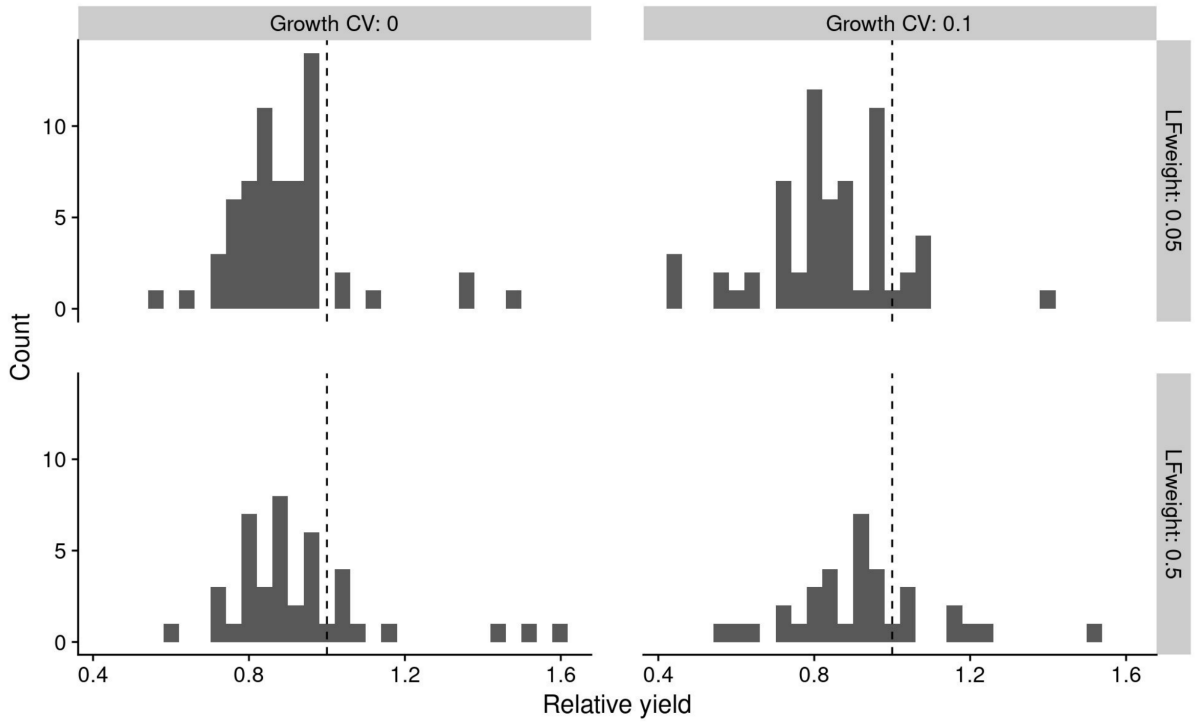

Figure 30: Average relative yield at equivalent risk across models, histograms are shown by length-frequency weight and separated into scenarios with (CV=0.1) and without (CV=0) growth variation (variable length-at-age).

4. DISCUSSION

Our evaluation of mean-length based harvest control rules for *Trachurus novaezelandiae* (JMN) in JMA 1 found that the performance of these rules, relative to constant catch, depended on the life history considered. Alrhough some rules provided additional yield at equivalent risk levels for scenarios with higher natural mortality, the same was not true for scenarios with lower natural mortality. Given that the same targets and starting catches were applied in each scenario, this implies that the rules perform worse in higher relative fishing mortality (F/Fmsy) scenarios. This may be a consequence of the high overlap in length-at-age distributions for ages that are selected by the fishery: while the age samples from the fishery contain a wide range of ages (2–19), the size frequency of the catch tends to be unimodal and so does not allow straightforward inference about fishing mortality levels. This is compounded by variability in mean length at a given depletion level: this variability is equivalent to the level of change across a wide range of depletion, implying that it may be difficult to gauge the level of depletion from mean size.

Stock structure and life-history factors have previously been highlighted as important contributing factors to the appropriateness of length-based control rules (Punt et al. 2001, Klaer et al. 2012). Key questions remain about the appropriateness of life-history parameters used in the models developed here for representing the stock of JMN fished in JMA 1. The combination of fast growth and low natural mortality led to an M/K estimate of 0.6, which, from a taxonomic perspective, puts JMN alongside grouper and surgeon fish (Prince et al. 2015, Prince et al. 2023)—species that do not tolerate high fishing mortality rates due to their slow life history. This is at least somewhat at odds with expected values for carangids (Prince et al. 2023).

Evaluating the plausibility of this M/K ratio, our selected value of K for *T. novaezelandiae* appears appropriate given the consistency in the values reported across their Australasian distribution (Horn 1991, Horn 1993, Broadhurst et al. 2018, Hartill et al. 2022), suggesting limited variability in growth rates. Estimates of natural mortality (M) appear more varied, however. Life history derived estimates (e.g., Hoenigs-M) provide a range of values between 0.16–0.49 (Prince et al. 2023), whereas catch-curve-derived estimates of M were between 0.16–0.26 when the stocks were in relatively unexploited states, using seemingly consistent otolith reading methodologies (Horn 1991, Horn 1993, Broadhurst et al. 2018). Differences in the maximum age of *T. novaezelandiae* and its asymptotic length (L_∞) are also apparent between Australian and New Zealand stocks. Neither the selectivity of fishing operations, stock structure, nor the possibility of divergent life-history strategies, are well understood across this distribution. Given that both M and K influence fishery length compositions, and potentially the appropriateness of any management target in a length-based control rule, it would appear important to resolve the apparent conflict between the life-history parameters used in the model.

Similar to uncertainties about life-history characteristics, stock structure and its interaction with the fishery selectivity, led to potentially overly conservative assumptions about current stock vulnerability. Selectivity was assumed to be logistic, and not dome-shaped, based upon comparison with length-frequency distributions of the JMA 7 midwater trawl fishery. Although this fishery takes a greater proportion of jack mackerel (JMN) in smaller size classes than the JMA 1 purse-seine fishery, the representation of larger fish within the catches of both methods is comparable (Middleton 2022). This suggests that, at least, the vertical stratification of fish sizes across 0–200 m is not an influencing factor for jack mackerel (JMN) which would provide refuge from purse seine capture. However, seasonal or inter-annual influences on fish size distributions are not accounted for by this comparison.

The incorporation of a logistic function produced an estimated length at 50% selectivity very close to the purported size at maturity, typically reported as 26–30 cm (Fisheries New Zealand 2022). It is worth noting that with no published estimates of size/age at maturity, this value contrasts to other estimates for *T. novaezelandiae*, at 20 and 22 cm fork length, for females and males respectively (Kailola et al. 1993). This overlap meant that there was essentially no refuge from fishing pressure in the model, leading to populations which easily collapse as a result of poor recruitment and continued fishing. Mean

length often increases under poor recruitment due to lower proportions of small fish in the fishery but, with the control rules evaluated, catch was not usually reduced in a timely manner to avoid a collapse in the simulated population. The assumption of full vulnerability of the stock to fishing is unlikely to be accurate. The fishery has historically operated further afield than the current Bay of Plenty fishing grounds, but it is not clear what proportion of the stock is currently vulnerable to fishing. Nevertheless, the assumption of full vulnerability was retained on the basis of taking a conservative approach.

The lack of appropriate accounting for (and therefore response to) environmental variability is a well known issue for composition-based estimators of stock size, which often make equilibrium assumptions (Chong et al. 2020). However, even composition-based methods that can deal with recruitment and non-equilibrium assumptions often struggle to provide unbiased estimates of status, and the combination of life-history and stock attributes in relation to methodological assumptions will usually drive the appropriateness of monitoring methods for data poor stocks (Punt et al. 2001, Carruthers et al. 2014). We speculate that, in the case of JMN, the limited ability to distinguish older fish from new recruits to the fishery may be limiting the utility of length-based methods to detect stock variation and drive management action. However, preliminary evaluations on the basis of mean age as opposed to mean length did not improve the performance of the composition-based control rules tested in this evaluation (Appendix C).

Our results contrast with the evaluation of control-rules that use length-based monitoring to determine catch (Klaer et al. 2012, Hordyk et al. 2015b). Using the length-based spawning potential ratio (LB-SPR; Hordyk et al. 2015a), Hordyk et al. (2015b) showed that rebuilding rules based on LB-SPR allowed rebuilding of the population to desired long-term SPR levels. Similarly, long term performance of length-based control-rules was shown to be adequate, and on par with age-based control rules, for some Australian fisheries (Klaer et al. 2012). However, there are a number of key differences between these evaluations and the one attempted here.

First, these previous evaluations translated the composition metrics into explicit fishing mortality and/or spawning potential ratio estimates that can be compared with an absolute target reference point. However, the life-history assumptions (M/K ratio for SPR, or M for mean-length-based monitoring) and operating models used strongly determine the appropriateness of the management reference point and the performance of the management procedures with such absolute reference points (Figure 4; Punt et al. (2001) and Klaer et al. (2012)). The life-history parameters and population structure and dynamics for JMN are not well enough understood to develop absolute reference points and evaluate the control rules against these (i.e., to choose a set of life-history setting and assume these are correct). This was the reasoning for our evaluation of the control-rule in a relative sense. However, it appears that the sensitivity to life-history assumptions also holds for the relative performance.

Other metrics, such as LB-SPR-based, could be tested to to evaluate if management under uncertainty about M/K would improve upon the settings here. Such an evaluation is feasible within the present framework, but would require a full MSE to be conducted, during which both the sources of error in LB-SPR (e.g., variability/bias in M/K) and uncertainty in demographic parameters and processes can be appropriately considered. In addition, given above mentioned caveats in distinguishing between young and old fish based on length in the JMN fishery, it is not clear that a LB-SPR could overcome the problems found for mean-length-based monitoring for JMN in JMA1.

5. ACKNOWLEDGEMENTS

Many thanks to Marc Griffiths and members of the Inshore Working Group for helpful discussion and suggestions; this research was co-funded by the Ministry for Primary Industries and Pelco NZ Ltd as part of the Sustainable Food and Fibre Futures programme (S3F-21147).

6. REFERENCES

Ault, J.S.; Smith, S.G.; Bohnsack, J.A.; Luo, J.; Stevens, M.H.; DiNardo, G.T.; Johnson, M.W.; Bryan, D.R. (2019). Length-based risk analysis for assessing sustainability of data-limited tropical reef fisheries. *ICES Journal of Marine Science 76*: 165–180.

Beverton, R.J.; Holt, S.J. (1957). *On the dynamics of exploited fish populations*. Chapman and Hall, London.

Broadhurst, M.K.; Kienzle, M.; Stewart, J. (2018). Natural mortality of *Trachurus novaezelandiae* and its size selection by purse seines off south-eastern Australia. *Fisheries Management and Ecology 25*: 332–338.

Carruthers, T.R.; Punt, A.E.; Walters, C.J.; MacCall, A.; McAllister, M.K.; Dick, E.J.; Cope, J. (2014). Evaluating methods for setting catch limits in data-limited fisheries. *Fisheries Research 153*: 48–68.

Chong, L.; Mildenberger, T.K.; Rudd, M.B.; Taylor, M.H.; Cope, J.M.; Branch, T.A.; Wolff, M.; Stäbler, M. (2020). Performance evaluation of data-limited, length-based stock assessment methods. *ICES Journal of Marine Science 77*: 97–108.

Cope, J.M.; Punt, A.E. (2009). Length-based reference points for data-limited situations: Applications and restrictions. *Marine and Coastal Fisheries: Dynamics, Management, and Ecosystem Science 1*: 169–186.

Deriso, R.B.; Parma, A.M. (1988). Dynamics of age and size for a stochastic population model. *Canadian Journal of Fisheries and Aquatic Sciences 45*: 1054–1068.

Fisheries New Zealand (2022). *Fisheries Assessment Plenary May 2022: Stock assessment and stock status. Volume 2: Horse mussel to red crab*. Fisheries New Zealand, Wellington, New Zealand.

Froese, R. (2004). Keep it simple: Three indicators to deal with overfishing. *Fish and fisheries 5*: 86–91.

Gabry, J.; Češnovar, R.; Johnson, A. (2023). *Cmdstanr: R interface to 'cmdstan'*. https://mc-stan.org/cmdstanr/, https://discourse.mc-stan.org.

Gelman, A.; Rubin, D.B. (1992). Inference from iterative simulation using multiple sequences. *Statistical science 7*: 457–472.

Gulland, J.A.; Rosenberg, A.A. (1992). A review of length-based approaches to assessing fish stocks. *FAO Fisheries Technical Paper 323*.

Hartill, B.; Middleton, D.A.J.; Walsh, C.; Spong, K.; Maolagáin, C.Ó. (2022). Catch-at-age sampling of *Trachurus novaezelandiae* from JMA 1 in 2019–20 and 2020–21. *New Zealand Fisheries Assessment Report 2022/37*. 16 p.

Hill-Moana, T.; Neubauer, P.; Middleton, D.; Vidal, T.; Escalle, L.; Cook, D. (2025). Towards the development of a catch per unit effort (CPUE) index for the purse seine fishery. *New Zealand Fisheries Assessment Report 2025/37*. 51 p.

Hoffman, M.; Gelman, A. (2014). The No-U-Turn sampler: adaptively setting path lengths in Hamiltonian Monte Carlo. *Journal of Machine Learning Research 15*: 1593–1623.

Hordyk, A.; Ono, K.; Valencia, S.; Loneragan, N.; Prince, J. (2015a). A novel length-based empirical estimation method of spawning potential ratio (SPR), and tests of its performance, for small-scale, data-poor fisheries. *ICES Journal of Marine Science 72*: 217–231.

Hordyk, A.R.; Loneragan, N.R.; Prince, J.D. (2015b). An evaluation of an iterative harvest strategy for data-poor fisheries using the length-based spawning potential ratio assessment methodology. *Fisheries Research 171*: 20–32.

Horn, P.L. (1993). Growth, age structure, and productivity of jack mackerels (*Trachurus* spp.) in New Zealand waters. *New Zealand Journal of Marine and Freshwater Research 27*: 145–155.

Horn, P. (1991). Assessment of jack mackerel stocks off the central west coast, New Zealand for the 1991–92 fishing year. *New Zealand Fisheries Assessment Research Document 1991/6*. 14 p.
Kailola, P.J.; Williams, M.; Stewart, P.; Reichelt, R.; McNee, A.; Grieve, C. (1993). *Australian fisheries resources*. Bureau of Resource Science; Fisheries Research; Development Corporation.
Kim, K.; Neubauer, P. (2025). Examining potential biases through prior predictive checks: Prior mis-specifications and their impact on Bayesian stock assessments. *Fisheries Research 288*: 107405.
Kim, K. (2022). State-space stock assessment models for data-moderate fisheries. Unpublished PhD thesis, Te Herenga Waka-Victoria University of Wellington. Open access.
Klaer, N.L.; Wayte, S.E.; Fay, G. (2012). An evaluation of the performance of a harvest strategy that uses an average-length-based assessment method. *Fisheries Research 134*: 42–51.
Langley, A.D.; Middleton, D.A.J.; Wilson, O.L. (2016). Species composition of the jack mackerel (genus *Trachurus*) catch from the JMA 1 purse seine fishery, 2005/06 to 2013/14. *New Zealand Fisheries Assessment Report 2016/11*. 33 p.
Middleton, D.A.J. (2022). An evaluation of species composition sampling in the JMA 7 trawl fishery. *New Zealand Fisheries Assessment Report 2022/20*. 39 p.
Parma, A.M.; Deriso, R.B. (1990). Dynamics of age and size composition in a population subject to size-selective mortality: Effects of phenotypic variability in growth. *Canadian Journal of Fisheries and Aquatic Sciences 47*: 274–289.
Parsons, D.; Bian, R. (2022). Trawl surveys of the Hauraki Gulf and Bay of Plenty in 2020 and 2021 to estimate the abundance of juvenile snapper. *New Zealand Fisheries Assessment Report 2022/10*. 134 p.
Prince, J.; Hordyk, A.; Valencia, S.R.; Loneragan, N.; Sainsbury, K. (2015). Revisiting the concept of Beverton–Holt life-history invariants with the aim of informing data-poor fisheries assessment. *ICES Journal of Marine Science 72*: 194–203.
Prince, J.D.; Wilcox, C.; Hall, N. (2023). How to estimate life history ratios to simplify data-poor fisheries assessment. *ICES Journal of Marine Science*: fsad026.
Punt, A.E.; Campbell, R.A.; Smith, A.D. (2001). Evaluating empirical indicators and reference points for fisheries management: application to the broadbill swordfish fishery off eastern Australia. *Marine and Freshwater Research 52*: 819–832.
Quinn, T.J., II; Turnbull, C.T.; Fu, C. (1998). A length-based population model for hard-to-age invertebrate populations. *In*: F. Funk, T.J. Quinn II, J. Heifetz, J.N. Ianelli, J.E. Powers, J.F. Schweigert, P.J. Sullivan; C.-I. Zhang (Eds.), Fishery Stock Assessment Models (pp. 531–556). University of Alaska Sea Grant, AK-SG-98-01 Fairbanks.
Rochet, M.-J.; Trenkel, V.M. (2003). Which community indicators can measure the impact of fishing? a review and proposals. *Canadian Journal of Fisheries and Aquatic Sciences 60*: 86–99.
Rudd, M.B.; Thorson, J.T. (2018). Accounting for variable recruitment and fishing mortality in length-based stock assessments for data-limited fisheries. *Canadian Journal of Fisheries and Aquatic Sciences 75*: 1019–1035.
Thorson, J.T.; Cope, J.M. (2017). Uniform, uninformed or misinformed?: The lingering challenge of minimally informative priors in data-limited Bayesian stock assessments. *Fisheries Research 194*: 164–172.
Vehtari, A.; Gelman, A.; Simpson, D.; Carpenter, B.; Bürkner, P.-C. (2021). Rank-normalization, folding, and localization: An improved $\hat{R}$ for assessing convergence of MCMC (with discussion). *Bayesian Analysis 16*: 667–718.

APPENDIX A: MODEL DESCRIPTION

This appendix describes the length- and age-structured population dynamics model (LASM). We extend an existing LASM which has been developed over time by Deriso & Parma (1988), Parma & Deriso (1990), Quinn et al. (1998), and Kim (2022).

We separate the model into two parts: process and observation models. We first describe the process model, where we describe how length-dependent processes are embedded into the age-structured dynamics. In the observation model, we link that process model to observations for both age and length composition data.

The LASM model we develop here does not include calculations for the age plus group because the model is structured to trace changes in the length distribution of a cohort over time. The plus group calculations for these length- and age-structured dynamics require an extra assumption to lump together different cohort-specific length distributions. One possible way to minimise the impact of the absence of the plus group calculation is to assume a sufficiently large maximum age (A), given the natural mortality rate (M) of the population used in the model. In the case of this jack mackerel study, as instructed by the inshore WG, we took $M = 0.2$ or 0.3 and $A = 20$, yielding a life time survival rate of less than 2% and 0.3% in the absence of a fishing mortality rate.

A.1 Process model

A summary of key notations used in the model is provided below (Table A-1).

Table A-1: Summary of key notations used in the model.

Notation	Description
t	Index for time.
i,j	Indices for length bins.
A	Terminal age class.
a	Index for age.
a_1	Initial age class.
c	Index for cohort.
$N_{a,t}$	Number of fish at age a at time t.
R_t	Recruitment at time t.
α, β	Beverton-Holt stock recruitment parameters.
h	Steepness parameter for Beverton-Holt stock-recruitment relationship.
R_0	Unfished equilibrium recruitment.
H_t	Harvest fraction at time t.
Y_t	Yield (catch in weight) at time t.
SSB_0	Unfished equilibrium spawning stock biomass.
L_a	Length at age a.
L_∞	von Bertalanffy parameter; asymptotic length.
κ	von Bertalanffy parameter; growth rate.
a_0	von Bertalanffy parameter; theoretical age at length 0.
ρ	Brody coefficient (i.e., $\rho = \exp(-\kappa)$).
L_i	Midpoint of length bin i.
w	Width of each length bin.
$\pi_{i\|a,t}$	Proportion of fish at age a at time t (i.e., $\sum_{i=1}^{I} \pi_{i\|a,t} = 1$).
$G_{j\|i,a+1}$	Growth transition probability (i.e., $\sum_{j=1}^{J} G_{j\|i,a+1} = 1$).
$S_{i,t}$	Length-dependent survival rate at time t.
$\bar{L}_{i,a+1}$	Mean length for length bin i after one growth increment.
σ^2_{a+1}	Variance of the distribution for length of fish at age $a+1$

Continued on next page

Table A-1: Summary of key notations used in the model. (Continued)

Notation	Description
$\sigma^2_{L,1}, \sigma^2_{L,2}$	Two length variance parameters for modelling σ^2_{a+1}.
φ	Female proportion.
ε^R_t	Autocorrelated recruitment anomaly.
σ^2_R	Variance of the recruitment deviations.
D_c	Density-dependence coefficient for cohort c.
$L_{\infty,c}$	Cohort-specific asymptotic length.
κ_c	Cohort-specific growth rate due to density dependent growth.
δ	Slope of a curve for the density dependence coefficient D_c.
Rel_t	The relative abundance or recruitment of a population compared with its unfished equilibrium state.
Mat_i	Maturity at length L_i.
v_{50}, v_{95}	Parameters for Mat_i; lengths at 50% and 95% maturity, respectively.
W_i	Weight at length L_i.
ω_1	Parameter for W_i; weight at unit length.
ω_2	Parameter for W_i; allometric scaling factor.
M	Natural mortality.
Sel_i	Selectivity at length L_i.
γ_5, γ_{95}	Parameters for the logistic selectivity curve; lengths at 5% and 95% selectivity, respectively.
$N_{a,0}$	Numbers-at-age at unfished equilibrium.
B_0	Total biomass at unfished equilibrium.
B_t	Total biomass at time t.
SSB_t	Spawning stock biomass at time t.
VB_t	Vulnerable biomass at time t.
$\mathbf{n}_t$	Vector of observed age frequency at time t.
E_t	Sample size of the observed age frequency at time t.
$\hat{\mathbf{p}}_t$	Vector of expected catch-at-age proportions at time t.
$C_{i,a,t}$	Expected catch numbers for length i and age a at time t.
$Q_{i,t}, \hat{Q}_{i,t}$	Observed and expected proportion-at-length at time t.
τ_t	Relative accuracy (sample size) of the observed length frequency collected at time t.
O_t	Sample size of the observed length frequency at time t.

A.1.1 Length- and age-structured dynamics

In this section, we describe the top-level structure of the model, which is age-dependent dynamics. Sub-models that describe each component of the top structure that has length-dependent processes are provided in the following sections.

We assume that numbers (N) at age (a) and time (t) (i.e., $N_{a,t}$) follow age-structured dynamics, where R_t is the recruitment at time t and $S_{a,t}$ is the survival rate of fish of age a at time t:

$$N_{a,t} = \begin{cases} R_t & \text{for } a = a_1 \\ N_{a-1,t-1} \cdot S_{a-1,t-1} & \text{for } a_1 + 1 \leq a < A \end{cases},$$

and the initial unfished equilibrium numbers-at-age (i.e., $N_{a,1}$) are:

$$N_{a,1} = R_0 \cdot \exp[-M \cdot (a-1)],$$

where R_0 is the unfished equilibrium recruitment, and M is the instantaneous rate of natural mortality.

To include length-dependent mortality of a population into the age-structured dynamics, we obtain the age-specific survival rate $S_{a,t}$ from the length-dependent survival rate ($S_{i,t}$, where i is the index for length bins) and the length-at-age distributions ($\pi_{i|a,t}$):

$$S_{a,t} = \sum_{i=1}^{I} \pi_{i|a,t} \cdot S_{i,t}.$$

The time-varying length-dependent survival rate, $S_{i,t}$, is

$$S_{i,t} = (1 - H_t \cdot \text{Sel}_i) \cdot \exp(-M).$$

where Sel_i is the length-dependent selectivity, and H_t is the harvest fraction at time t:

$$H_t = Y_t / VB_t,$$

where Y_t is the yield at time t, and VB_t is the vulnerable biomass at time t.

Note that if the survival rate $S_{a,t}$ is calculated based on time-invariant length-at-age distributions (e.g., $\pi_{i|a}$), then the model becomes similar to a conventional length-based age-structured model (e.g., MULTIFAN-CL).

For recruitment R_t, we assumed the Beverton-Holt (BH) stock-recruitment relationship:

$$R_t = \frac{\alpha \cdot SSB_{t-1}}{1 + \beta \cdot SSB_{t-1}} \cdot e^{\varepsilon_t^R - 0.5 \cdot \sigma_R^2},$$

where α/β defines the maximum recruitment level, $1/\beta$ defines the spawning stock biomass (SSB) which will result in 50% of the maximum recruitment, SSB_t is the spawning stock biomass at time t, and ε_t^R is the recruitment deviation due to random environmental changes.

The random recruitment deviations ε_t^R follow an AR1 process with variance σ_R^2 and correlation ρ_R:

$$\varepsilon_t^R \sim N(0, \Sigma^R), \quad \text{where } \Sigma_{t,\tilde{t}}^R = \sigma_R^2 \cdot \rho_R^{|t-\tilde{t}|}.$$

For easier interpretation, we calculate the two BH parameters, α and β, from the steepness h and the unfished equilibrium recruitment R_0:

$$\alpha = \frac{4 \cdot h \cdot R_0}{SSB_0 \cdot (1-h)}, \quad \beta = \frac{5 \cdot h - 1}{SSB_0 \cdot (1-h)}.$$

In the next section, we describe how the time-varying length-at-age distributions $\pi_{i|a,t}$ are derived from a growth model.

A.1.2 Growth model

The length of a fish can be modelled using the von Bertalanffy equation:

$$L_a = L_\infty \cdot [1 - \exp\{-\kappa \cdot (a - a_0)\}],,$$

where L_a is the length of fish at age a, L_∞ is the asymptotic length, κ is the growth rate parameter, and a_0 is the theoretical age at length 0.

In conventional length-based age-structured models (e.g., MULTIFAN-CL), this deterministic model is used to describe the mean length of fish in each age group, which is often modelled as time-invariant. However, such an age group-based approach overlooks the cumulative impacts of length-dependent processes on a population (e.g., larger fish are more susceptible to being caught than smaller fish; thus, their length distribution for the next age is more likely deviated from their current distribution).

To incorporate cumulative impacts, we considered an alternative form of the von Bertalanffy equation, which is expressed in terms of the growth increment ΔL_a (see Appendix B for the derivation):

$$\begin{aligned} L_a &= L_{a-1} + (L_\infty - L_{a-1}) \cdot (1-\rho) \\ &= L_{a-1} + \Delta L_{a-1} \end{aligned} \qquad \text{for } a_1 < a \leq A, \tag{A-1}$$

where ρ is the Brody coefficient (i.e., $\rho = \exp(-\kappa)$).

To allow stochasticity in individual growth, the model is expanded to:

$$L_{n,a} = L_{n,a-1} + \Delta L_{n,a-1} + \varepsilon_{n,a}, \qquad \text{for } a_1 < a \leq A, \tag{A-2}$$

where $\varepsilon_{n,a}$ is the random variability in growth, which is assumed to have a normal distribution with mean 0 and variance $\sigma_{L,2}^2$ (i.e., $\varepsilon_{n,a} \sim N(0, \sigma_{L,2}^2)$).

We also consider random variability for the initial age group (i.e., $a = a_1$):

$$\begin{aligned} L_{n,1} =& \mu_1 + \varepsilon_{n,1}, \\ & \text{where } \mu_1 = L_\infty \cdot [1 - \exp\{-\kappa \cdot (1 - a_0)\}], \\ & \text{and } \varepsilon_{n,1} \sim N(0, \sigma_{L,1}^2). \end{aligned} \tag{A-3}$$

Note that both (A-2) and (A-3) permit negative growth, which is not biologically reasonable for most fish species.

The following conditions are applied to ensure no decrease in length. For the first age group, we set the lower bound $L_{\min}$ which is the minimum length in the assumed length range:

$$L_{n,1} = \begin{cases} \mu_1 + \varepsilon_{n,1}, & \text{if } \mu_1 + \varepsilon_{n,1} > 0 \\ L_{\min}, & \text{otherwise} \end{cases}.$$

Similarly, for the subsequent age groups, we assumed the condition:

$$L_{n,a} = \begin{cases} L_{n,a-1} + \Delta L_{n,a-1} + \varepsilon_{n,a} & \text{if } \Delta L_{n,a-1} + \varepsilon_{n,a} \geq 0 \\ L_{n,a-1} & \text{otherwise} \end{cases}.$$

Theoretically, individual growth trajectories can be obtained by the stochastic growth equation, but with a large number of n, such an individual-based calculation requires considerable computational resources. As an alternative, we approximate the individual growth trajectories on a length bin-by-bin basis by grouping the individual lengths $L_{n,a}$ into pre-defined length bins. Thus, fish of the same age, that belong to the same length bin, are assumed to follow the same growth transition probabilities.

A.1.3 Growth transition probability

For the length bin-based approximation, we specify length bins with a width of w, where the subscripts i and j denote each length bin (i.e., $i \in \{1, 2, 3, ..., I\}, j \in \{1, 2, 3, ..., J\}$, and $I = J$). We assume that the midpoint of each length bin (denoted as either L_i or L_j) represents the length of all individuals in that same length bin. Note that for ease of explanation, we do not consider time index here, however, in the following section, we show these models with time-varying components.

For the length distribution of the initial age group (i.e., recruitment age), the discrete normal distribution is assumed:

$$\pi_{i|1} = \begin{cases} \int_{-\infty}^{L_i + w/2} f(L|\mu_1, \sigma_{L,1}^2)\, dL & \text{for } i = 1 \\ \int_{L_i - w/2}^{L_i + w/2} f(L|\mu_1, \sigma_{L,1}^2)\, dL & \text{for } 1 < i < I, \\ \int_{L_i - w/2}^{\infty} f(L|\mu_1, \sigma_{L,1}^2)\, dL & \text{for } i = I \end{cases}$$

where $f(\cdot)$ is the normal probability density function.

In the absence of any length-dependent mortality, the two-dimensional distribution of the animals in length bin i at age a, which are further distributed in length bin j at age $a + 1$, $\pi_{j,i|a+1}$ (i.e., $\sum_{j=1}^{J} \sum_{i=1}^{I} \pi_{j,i|a+1} = 1$), can be expressed as the product of the length distribution of those at age a, $\pi_{i|a}$ (i.e., $\sum_{i=1}^{I} \pi_{i|a} = 1$), and the the probability that fish of age a in length bin i grow into length bin j at age $a + 1$, $G_{j|i,a+1}$ (i.e., $\sum_{j=1}^{J} G_{j|i,a+1} = 1$):

$$\pi_{j,i|a+1} = \pi_{i|a} \cdot G_{j|i,a+1} \qquad \text{for } a_1 \leq a < A.$$

Then, by summing over the length bins, the length distribution for the next age $\pi_{j|a+1}$ is calculated:

$$\pi_{j|a+1} = \sum_{i=1}^{I} \pi_{j,i|a+1} \qquad \text{for } a_1 \leq a < A.$$

In the presence of length-dependent mortality, the subsequent length-at-age distribution, $\pi_{j|a+1}$, must vary, depending on the length-dependent survival rate ($S_i = (1 - H \cdot \text{Sel}_i) \cdot \exp(-M)$):

$$\pi_{j|a+1} = \frac{\sum_{i=1}^{I} \pi_{i|a} \cdot S_i \cdot G_{j|i,a+1}}{\sum_{j'=1}^{J} \sum_{i'=1}^{I} \pi_{i'|a} \cdot S_{i'} \cdot G_{j'|i',a+1}} \qquad \text{for } a_1 \leq a < A,$$

where the denominator is a normalisation constant.

The age-specific growth transition probability, $G_{j|i,a+1}$, was also modelled using the normal probability distribution with mean $\bar{L}_{i,a+1}$ and variance σ^2_{a+1}:

$$G_{j|i,a+1} = \begin{cases} 0 & \text{for } j < i \\ \int_0^{L_j + w/2} f(L|\bar{L}_{i,a+1}, \sigma^2_{a+1})\, dL & \text{for } j = i \\ \int_{L_j - w/2}^{L_j + w/2} f(L|\bar{L}_{i,a+1}, \sigma^2_{a+1})\, dL & \text{for } j > i \\ 1 - \int_0^{L_j - w/2} f(L|\bar{L}_{i,a+1}, \sigma^2_{a+1})\, dL & \text{for } j = I \end{cases}, \tag{A-4}$$

where $\bar{L}_{i,a+1}$ is the expected length for fish in length bin i after one growth increment and σ^2_{a+1} is the corresponding variance, which are modelled as (see Appendix B for derivation)

$$\begin{aligned} \bar{L}_{i,a+1} &= L_\infty \cdot (1 - \rho) + \rho \cdot L_i \\ \sigma^2_{a+1} &= \sigma^2_{L,2} \cdot \frac{1 - \rho^{2 \cdot a}}{1 - \rho^2} + \rho^{2 \cdot a} \cdot \sigma^2_{L,1} \end{aligned}, \tag{A-5}$$

where L_i is the midpoint of length bin i.

A.1.4 Time-varying growth transition probability

Each cohort c may have a different growth pattern because of the cohort-specific asymptotic length (i.e., $L_{\infty,c}$; see the next section for details). The three temporal indices, cohort c, time t, and age a, have the relationship:

$$c = t + 1 - a.$$

We can specify the expected growth increment of the animals in each length bin i for each cohort c as

$$\bar{L}_{i,a+1,c} = L_{\infty,c} \cdot (1 - \rho) + \rho \cdot L_i,$$

which is then used to calculate the cohort-specific growth transition probability $G_{j|i,a+1,c}$ by substituting it for $\bar{L}_{i,a+1}$ in (A-4).

If a population has time-varying survival rates (i.e., $S_{i,t}$), we have the cohort-specific, time-varying length-at-age distributions (i.e., $\pi_{i|a,t}$):

$$\begin{cases} \pi_{i|a,t} = \pi_{i|a,c} & \text{for } a = a_1 \\ \pi_{j|a+1,t+1} = \dfrac{\sum_{i=1}^{I} \pi_{i|a,t} \cdot S_{i,t} \cdot G_{j|i,a+1,c}}{\sum_{j'=1}^{J} \sum_{i'=1}^{I} \pi_{i'|a,t} \cdot S_{i',t} \cdot G_{j'|i',a+1,c}} & \text{for } a_1 + 1 \leq a < A \end{cases}$$

We assumed that the cohort-specific asymptotic length, $L_{\infty,c}$, is determined based on the density-dependence coefficient D_c:

$$L_{\infty,c} = D_c \cdot L_{\infty,0}$$

where $L_{\infty,0}$ is the asymptotic length for animals in unfished equilibrium. Additionally, we also consider the cohort-specific growth rate as follows

$$\kappa_c = D_c \cdot \kappa_0$$

where κ_0 is the growth rate in the von Bertalanffy function for animals in unfished equilibrium.

The density dependence coefficient D_c is defined with the bounded logit function with upper bound D_{upper} and lower bound D_{lower}:

$$D_c = \frac{D_{\text{upper}} - D_{\text{lower}}}{1 + \exp[-\delta \cdot (1 - \text{Rel}_t)]} + D_{\text{lower}}.$$

where δ specifies the slope of the curve, and Rel_t is the relative abundance or recruitment of a population compared with its unfished equilibrium state. For this relative quantity, we consider two different assumptions:

(i)

$$\text{Rel}_t = R_t / R_0$$

and (ii)

$$\text{Rel}_t = B_{t-1} / B_0$$

where B_t is the total biomass at time t, and B_0 is the unfished equilibrium total biomass.

A.1.5 Biological parameters

The length-dependent maturity, Mat_i, is assumed to be logistic:

$$\text{Mat}_i = \frac{1}{1 + \exp\left[-\log(19) \cdot \dfrac{L_i - v_{50}}{v_{95} - v_{50}}\right]}$$

where v_{50} and v_{95} are the lengths at 50% and 95% maturity, respectively.

The weight-at-length, W_i, is defined with the allometric relationship:

$$W_i = \omega_1 \cdot L_i^{\omega_2},$$

where ω_1 and ω_2 are the two length-weight relationship parameters.

A.1.6 Selectivity

For the length-dependent selectivity, Sel_i, the logistic curve is used:

$$\text{Sel}_i = \frac{19}{19 + \exp\left[-\log(361) \cdot \dfrac{L_i - \gamma_{95}}{\gamma_5 - \gamma_{95}}\right]}$$

where γ_5 and γ_{95} are the lengths at 5% and 95% selectivity, respectively.

A.1.7 Equilibrium quantities

Numbers-at-age at unfished equilibrium is

$$N_{a,0} = R_0 \cdot \exp[-M \cdot (a-1)], \qquad \text{for } 1 \leq a \leq A$$

Biomass quantities at unfished equilibrium are

$$B_0 = \sum_{a=1}^{A} \sum_{i=1}^{I} N_{a,0} \cdot \pi_{i|a,0} \cdot W_i$$

$$SSB_0 = \varphi \cdot \sum_{a=1}^{A} \sum_{i=1}^{I} N_{a,0} \cdot \pi_{i|a,0} \cdot W_i \cdot \text{Mat}_i$$

where B_0 is the total biomass at unfished equilibrium, and SSB_0 is the spawning stock biomass at unfished equilibrium, and φ is the female proportion.

The length-at-age of the first group at equilibrium $\pi_{i,1,0}$ is

$$\pi_{i|1,0} = \pi_{i|1}$$

Then, for the subsequent age groups,

$$\pi_{j|a+1,0} = \frac{\sum_{i=1}^{I} \pi_{i|a,0} \cdot \exp(-M) \cdot G_{j|i,a+1,0}}{\sum_{j'=1}^{J} \sum_{i'=1}^{I} \pi_{i'|a,0} \cdot \exp(-M) \cdot G_{j'|i',a+1,0}}, \qquad \text{for } a_1 \leq a < A.$$

A.1.8 Other derived quantities

The numbers of length i and age a at time t is

$$N_{i,a,t} = N_{a,t} \cdot \pi_{i|a,t}$$

Biomass quantities are derived as

$$\begin{aligned} B_t &= \sum_{a=1}^{A} \sum_{i=1}^{I} N_{i,a,t} \cdot W_i \\ \text{SSB}_t &= \varphi \cdot \sum_{a=1}^{A} \sum_{i=1}^{I} N_{i,a,t} \cdot W_i \cdot \text{Mat}_i \\ \text{VB}_t &= \sum_{a=1}^{A} \sum_{i=1}^{I} N_{i,a,t} \cdot W_i \cdot \text{Sel}_i \end{aligned}$$

where B_t is the total biomass, SSB_t is the spawning stock biomass, and VB_t is the vulnerable biomass.

The expected catch numbers of length i and age a at time t is

$$C_{i,a,t} = N_{i,a,t} \cdot H_t \cdot \text{Sel}_i$$

A.2 Observation model

We assume a multinomial distribution for the vector of age frequencies at time t (i.e., $\mathbf{n}_t$):

$$\mathbf{n}_t \sim \text{Multinomial}(E_t, \hat{\mathbf{p}}_t)$$

where E_t is the sample size of the age frequency data at time t, and $\hat{\mathbf{p}}_t$ is the vector of expected catch proportions at age

$$\hat{p}_{a,t} = \frac{\sum_i C_{i,a,t}}{\sum_i \sum_a C_{i,a,t}}$$

For the length frequency data, we use a robust normal (RN) distribution, which is used in MULTIFAN-CL. In Stan, we define its log-likelihood form as

$$\ell = -0.5 \cdot \sum_i \sum_t \cdot \log\left\{2 \cdot \pi \cdot \left[(1 - Q_{i,t}) \cdot Q_{i,t} + \frac{1}{I}\right]\right\} - I \cdot \sum_t \log(\tau_t)$$
$$+ \sum_i \sum_t \log\left\{\exp\left[\frac{-(Q_{i,t} - \hat{Q}_{i,t})^2}{2 \cdot \left((1 - Q_{i,t}) \cdot Q_{i,t} + \frac{1}{I}\right) \cdot \tau_t}\right]\right\},$$

where $Q_{i,t}$ and $\hat{Q}_{i,t}$ are the observed and expected catch proportions at length, I is the number of length bins, and τ_t represents relative accuracy of the observed length frequencies (we follow the default assumption used in MULTIFAN-CL: $\tau_t = 10/\min(1000, O_t)$, where O_t is the sample size of the length frequency data collected at time t).

The expected catch proportions at length $\hat{Q}_{i,t}$ is

$$\hat{O}_{i,t} = \frac{\sum_a C_{i,a,t}}{\sum_i \sum_a C_{i,a,t}}$$

APPENDIX B: DERIVATION OF MODEL FORMULAE

B.1 Derivation of growth

The von Bertalanffy growth model for the length of a fish at age a is

$$L_a = L_\infty \cdot [1 - \exp\{-\kappa \cdot (a - a_0)\}], \tag{B-1}$$

where L_∞ is the asymptotic length, a_0 is the theoretical age at length 0, and κ is the growth parameter.

For a fish of age $a + 1$, (B-1) can be written as

$$\begin{aligned} L_{a+1} &= L_\infty \cdot [1 - \exp\{-\kappa \cdot (a + 1 - a_0)\}] \\ &= L_\infty - L_\infty \cdot \exp\{-\kappa \cdot (a - a_0)\} \cdot \exp(-\kappa) \end{aligned}$$

We define the length increment ΔL_a as the difference between L_{a+1} and L_a:

$$\begin{aligned} \Delta L_a &= L_{a+1} - L_a \\ &= L_\infty - L_\infty \cdot \exp\{-\kappa \cdot (a - a_0)\} \cdot \exp(-\kappa) - L_\infty \cdot [1 - \exp\{-\kappa \cdot (a - a_0)\}] \\ &= L_\infty \cdot \exp\{-\kappa \cdot (a - a_0)\} \cdot \{1 - \exp(-\kappa)\} \\ &= [L_\infty \cdot \exp\{-\kappa \cdot (a - a_0)\}] \cdot \{1 - \exp(-\kappa)\} \\ &= (L_\infty - L_a) \cdot \{1 - \exp(-\kappa)\} \end{aligned}$$

Rearranging the above equation with respect to L_{a+1} with the normal error term ε_{a+1} yields

$$\begin{aligned} L_{a+1} &= L_a + \Delta L_a + \varepsilon_{a+1} \\ &= L_a + (L_\infty - L_a) \cdot \{1 - \exp(-\kappa)\} + \varepsilon_{a+1} \\ &= L_a + (L_\infty - L_a) \cdot (1 - \rho) + \varepsilon_{a+1}. \end{aligned} \tag{B-2}$$

Alternatively, for the derivation $\bar{L}_{i,a+1}$ and σ^2_{a+1} in (A-5), (B-2) can also be rearranged as

$$\begin{aligned} L_{a+1} &= L_a + \Delta L_a + \varepsilon_{a+1} \\ &= L_a + (L_\infty - L_a) \cdot (1 - \rho) + \varepsilon_{a+1} \\ &= L_\infty \cdot (1 - \rho) + L_a \cdot \rho + \varepsilon_{a+1}. \end{aligned} \tag{B-3}$$

B.2 Derivation of equation (A-5)

The expected value of (A-1) for length L_i (i.e., $\bar{L}_{i,a+1}$ in (A-5)) is

$$E[L_{i,a+1}] = \bar{L}_{i,a+1} = L_\infty \cdot (1 - \rho) + L_i \cdot \rho \tag{B-4}$$

Note that (B-3) is a geometric series:

$$
\begin{aligned}
L_{a+1} &= L_\infty \cdot \{1 - \exp(-k)\} + L_a \cdot \exp(-k) + \varepsilon_{a+1} \\
&= x + L_a \cdot \rho + \varepsilon_{a+1} \\
&= x \cdot \sum_{i=0}^{a-1} \rho^i + L_1 \cdot \rho^a + \sum_{i=0}^{a-1} \rho^i \cdot \varepsilon_{a+1-i} \\
&= x \cdot \frac{1-\rho^a}{1-\rho} + L_1 \cdot \rho^a + \varepsilon \cdot \frac{1-\rho^a}{1-\rho}
\end{aligned}
\tag{B-5}
$$

where $x = L_\infty \cdot \{1 - \exp(-k)\}$, and $\rho = \exp(-k)$

Thus, the variance of (B-3) (i.e., σ^2_{a+1} in (A-5)) is

$$
\begin{aligned}
Var(L_{a+1}) &= \sigma^2_{a+1} \\
&= Var\left(\alpha \cdot \sum_{i=0}^{a-1} \rho^i + L_1 \cdot \rho^a + \sum_{i=0}^{a-1} \rho^i \cdot \varepsilon_{a+1-i}\right) \\
&= \sigma^2_{L,1} \cdot \rho^{2\cdot a} + Var\left(\sum_{i=0}^{a-1} \rho^i \cdot \varepsilon_{a+1-i}\right) \\
&= \sigma^2_{L,1} \cdot \rho^{2\cdot a} + \sigma^2_{L,2} \cdot \frac{1-\rho^{2\cdot a}}{1-\rho^2}
\end{aligned}
\tag{B-6}
$$

B.3 Calculation of the expected average length

The expected average length for a given H (avLeng(H)) is calculated as

$$
\text{avLeng}(H) = \frac{\sum_{i=1}^{I} \sum_{a=r}^{A} C_a(H) \cdot \pi_{i|a}(H) \cdot L_i}{\sum_{i=1}^{I} \sum_{a=r}^{A} C_a(H) \cdot \pi_{i|a}(H)}
$$

where $C_a(H)$ is the catch (in numbers) at age a for a given H, $\pi_{i|a}(H)$ is the probability that fish of age a fall in length bin i, which varies depending on H because of cumulative impact of length-dependent fishing mortality, and r is the recruitment age (i.e., $r = 2$).

The catch at equilibrium for a given H is calculated as

$$
C_a = \sum_{i=1}^{I} N_{i,a}(H) \cdot H \cdot Sel_i
$$

where $N_{i,a}$ is the number of fish of a in length bin i at equilibrium for a given H.

APPENDIX C: MPE RUNS WITH AN MEAN-AGE-BASED RULE

Alternative runs were attempted with a mean-age-based control rule that mirrors the Length-Moving-Average-Range control rule. Instead of mean length the age-based rule use mean ages, with target settings of 5.5, 6, and 6.5, and all other settings as for length based rules.

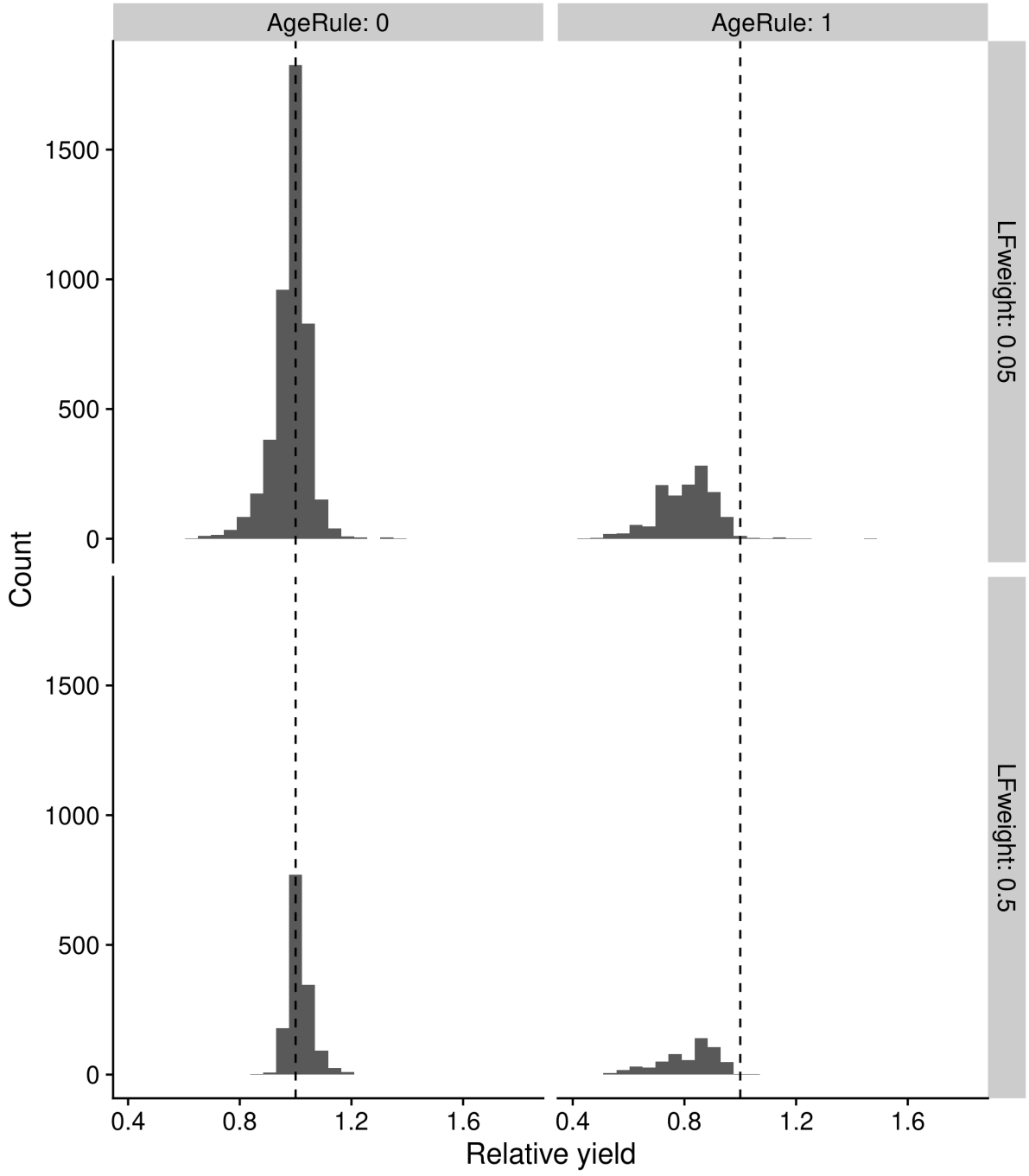

Figure C-1: Average relative yield at equivalent risk across models, histograms are shown across age (AgeRule=1) and length-based (AgeRule=0) control rules

APPENDIX D: PREVIOUS MANAGEMENT PROCEDURE EVALUATION

This appendix provides the findings from analyses undertaken in 2019 and 2021, focused on a management procedure evaluation for *T. novaezelandiae* in the JMA 1 fishery (Bentley & Middleton, unpublished data, prepared as a draft New Zealand Fisheries Assessment Report). A review of the previous analyses by the Northern Inshore Working Group raised a number of limitations with the approach taken. These limitations were addressed in the updates provided here; however, the analyses were not finalised for review or publication.

1. INTRODUCTION

New Zealand's jack mackerel (JMA) stocks comprise three species: *Trachurus declivis* (JMD), *Trachurus novaezelandiae* (JMN), and *Trachurus murphyi* (JMM). Stephenson & Robertson (1977) considered that two species of jack mackerel, *T. declivis* and *T. novaezelandiae*, were present in New Zealand waters, but the presence of *T. murphyi* was recognised in the mid-1980s (Jones 1988, Fisheries New Zealand 2018). The fishing year for jack mackerels is 1 October to 30 September and, in the remainder of this document, fishing years are referred to by the later year, i.e. the 1986–87 fishing year is referred to as 1987.

Increased availability of jack mackerels, caused by an apparent influx of *T. murphyi* in the early 1990s, resulted in an increase in the Total Allowable Commercial Catch (TACC) in JMA 1 from the 5970 t set in 1987, to 8000 t in 1994 and 10 000 t in 1995, where it has remained. An abundance index for JMA 1 is not available at this time. Aerial sightings data, from spotter plane pilots working in the purse seine fishery, were analysed but it was concluded that the inter-annual variation was too great for these data to provide a reliable index (Fisheries New Zealand 2018).

In JMA 1 (Figure 1), the jack mackerel catch is largely taken by the target purse seine fishery. Routine species sampling of the catch from the fishery has been conducted since 1995, and the resulting species-specific catch estimates showed that JMA 1 purse seine catches of *T. novaezelandiae* increased from about 2000 t to 5000 t during the 1990s to about 8300 t in 2008–-2014 (Langley et al. 2016). An approach for ensuring that catches of *T. novaezelandiae* are managed within sustainable limits is therefore of particular interest.

This document summarises work on developing and evaluating management procedures for the JMA 1 fishery for *T. novaezelandiae*.

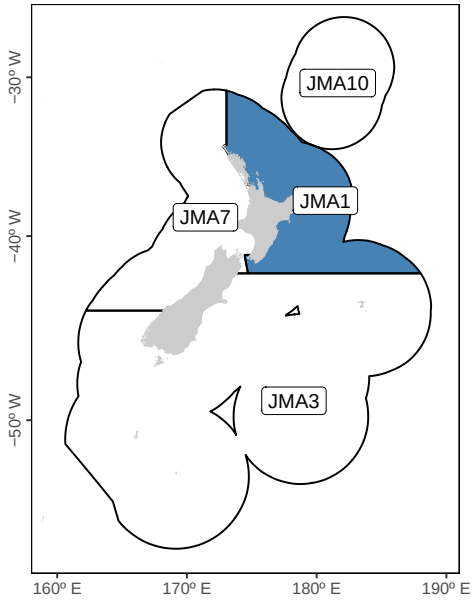

Figure 1: Jack mackerel quota management areas with JMA 1 highlighted.

A management procedure is an algorithm which defines how data on a fishery should be used to adjust management controls, in this case a catch limit for JMN (which represents part of the TACC for the JMA species group). We developed a simulation model of the JMA 1 fishery for *T. novaezelandiae* and used it to evaluate alternative management procedures (MPs) on the basis of a suite of performance statistics.

Management procedures are often based on the use of a relative abundance index such as standardised Catch per Unit Effort (CPUE). In the absence of a relative abundance index for *T. novaezelandiae* in JMA 1, we have considered the use of size composition data collected as part of the routine catch sampling programme, relying on the fact that 'quite good estimates of total mortality can be obtained from length data' (Gulland 1969).

2. METHODS

Each part of the methodology described below is a customised configuration of generalised components in the Fisheries Simulation Library (FSL), an open-source library of C++ components for doing fisheries simulation with a particular emphasis on MPE, that is available at https://github.com/trident-systems/fsl.

2.1 Simulation model structure

Existing information on the productivity of *T. novaezelandiae*, in particular growth and natural mortality (Horn 1991), allows the parameterisation of a population model for use as an operating model in the Management Procedure Evaluation process (see, for example, De Oliveira et al. 2009, Figure 3).

The operating model used here is based on the general age-structured fisheries model in FSL, configured with a single sex, ages 0–25, 50 length bins and a single fishery. The model was adapted for the JMA 1 situation by adding interannual variability in the inflection point of the selectivity-at-age curve. This adaption was made to account for the fact that jack mackerel schools may contain fish of a similar size and age, and that purse seine fishing targeting of individual schools may therefore result in additional variation in the realised selectivity. Variation in selectivity at age could also arise as a result of inter-annual variation in growth.

Reference and prior distributions for parameters used for the population and harvesting sub-models are provided in Table 1 and Table 2. The selectivity at age is a flexible double-normal formulation with a potential plateau (illustrated, for the reference values, in Figure 2). In addition, we used the catch history derived by Langley et al. (2016) for *T. novaezelandiae* in JMA 1 (Figure 3). From 1990–2021, catches of JMN in JMA 1 totalled 169 704 t.

Table 1: Parameters of the fish population sub-model with reference values and priors. U = Uniform, F = Fixed, LN = Lognormal, NCv = Normal parameterised with a CV.

Parameter	Description	Reference value	Prior	Source
s0	Equilibrium unfished spawning biomass	75000.00	U(50000,400000)	
h	Stock-recruit steepness	0.90	U(0.7,0.99)	
v	Recruitment variability	0.60	F(0.6)	
m	Natural mortality	0.18	LN(0.18,0.036)	Horn (1991) with 20% CV
k	Growth coefficient	0.30	NCv(0.3,0.05)	Horn (1991) with 5% CV
linf	Asymptotic length	36.00	NCv(36,0.05)	Horn (1991) with 5% CV
t0	t-zero	-0.65	NCv(-0.65,0.05)	Horn (1991) with 5% CV
lcv	Coefficient of variation of length at age	0.10	F(0.1)	
a	Intercept of length-weight relation	0.00	NCv(2.8e-5,0.05)	Horn (1991) with 5% CV
b	Exponent of length-weight relation	2.84	NCv(2.84,0.05)	Horn (1991) with 5% CV
mi	Inflection point of maturity-at-age ogive	3.50	U(3,4)	
ms	Steepness of maturity-at-age ogive	1.00	U(0.1,2)	

Table 2: Parameters of the harvesting sub-model: symbols, priors etc. U = Uniform, F = Fixed, LN = Lognormal, NCv = Normal parameterised with a CV.

Parameter	Description	Reference value	Prior
si	Inflection point of the selectivity-at-age	8.00	U(5,15)
sd	Width of the selectivity 'plateau'	0.00	U(0,5)
sl	Steepness of the left side of selectivity curve	1.00	U(1,5)
sr	Steepness of the right side of selectivity curve	100.00	U(1,100)
sc	Interannual changes in inflection point ('si')	0.50	U(0,3.0)
li	Imprecision of length observations (lognormal c.v. on proportion at length)	0.03	U(0.01,0.4)

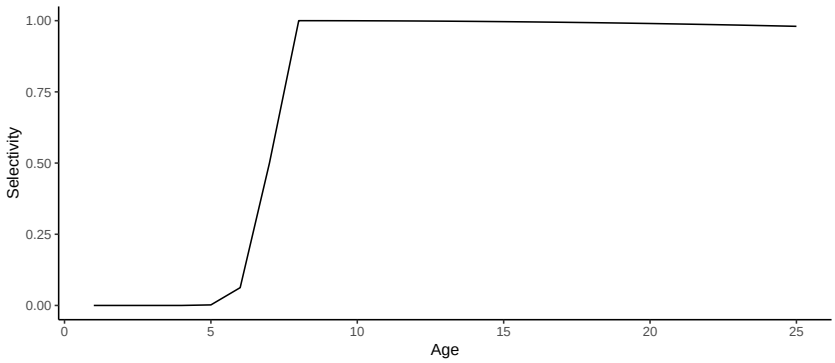

Figure 2: Selectivity at age for the reference values in Table 2, and no annual shift applied.

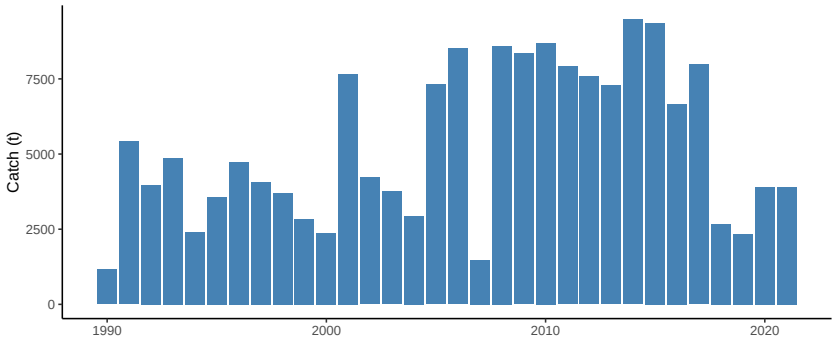

Figure 3: Catch history for *T. novaezelandiae* in JMA 1 used in the simulation model.

2.2 Simulation model conditioning

The model was conditioned to obtain a set of model parameter values that were broadly consistent with the observed data and the catch history. Parameter values were drawn at random from each parameter's prior and the fishery was then simulated from 1980 to 2017. Several constraints were defined based on the observed age and length frequency data and assumptions regarding the maximum harvest rate and lowest level of depletion (Table 3). Only parameters sets for simulations where the simulated data met these constraints were retained, yielding a set of feasible stock trajectories (Bentley & Langley 2012).

Several constraints were derived from observed age (Figure 4) and length (Figure 5) data (Taylor et al. 2012, Langley et al. 2016). The constraints related to length ("Mean length", "MRAD"" and "Mean Length Diff") are all based on the length of the catch in the years 2005–2017. Similarly, the constraints related to age are based on the simulated age of the catch (i.e. after fishery selectivity is taken into account) in the years 2006–2009 only (when age data is available).

Table 3: Constraints used to condition the JMA 1 simulation model.

Name	Description
Status>10%	Stock must remain above 10% B0
Harvest rate	Harvest rate must remain below 0.7
Mean length	Mean length must remain within 2cm of observed trend in the years 2005 to 2017
Length MRAD	Mean of the relative absolute difference in proportions at length must be between 0.016 and 0.026
Mean length diff	Change in mean length from previous year must be greater than 0.05cm and less than 1.3cm
Mean age	Mean age must be between 6 and 10 years from 2006 to 2009
Status(2010-2017)<100%	Stock must be less than 100% B0 in the years 2010 to 2017

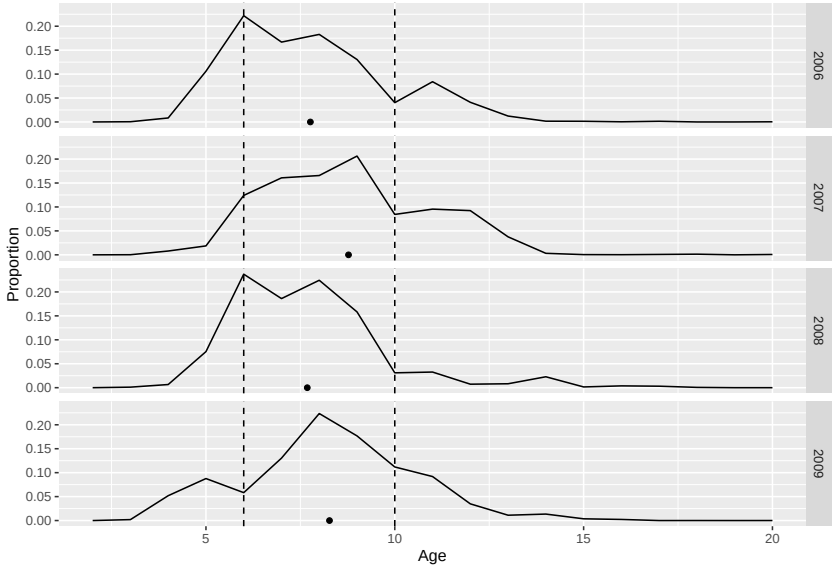

Figure 4: Catch age frequency distributions for JMA 1. The dot shows the mean age in each year. Data are derived from Taylor et al. (2012). Sampling spanned the fishing year boundary (see Taylor et al. 2012, Appendix B) and data are therefore aggregated here by calendar year. The dashed lines illustrate the constraint applied (Table 3).

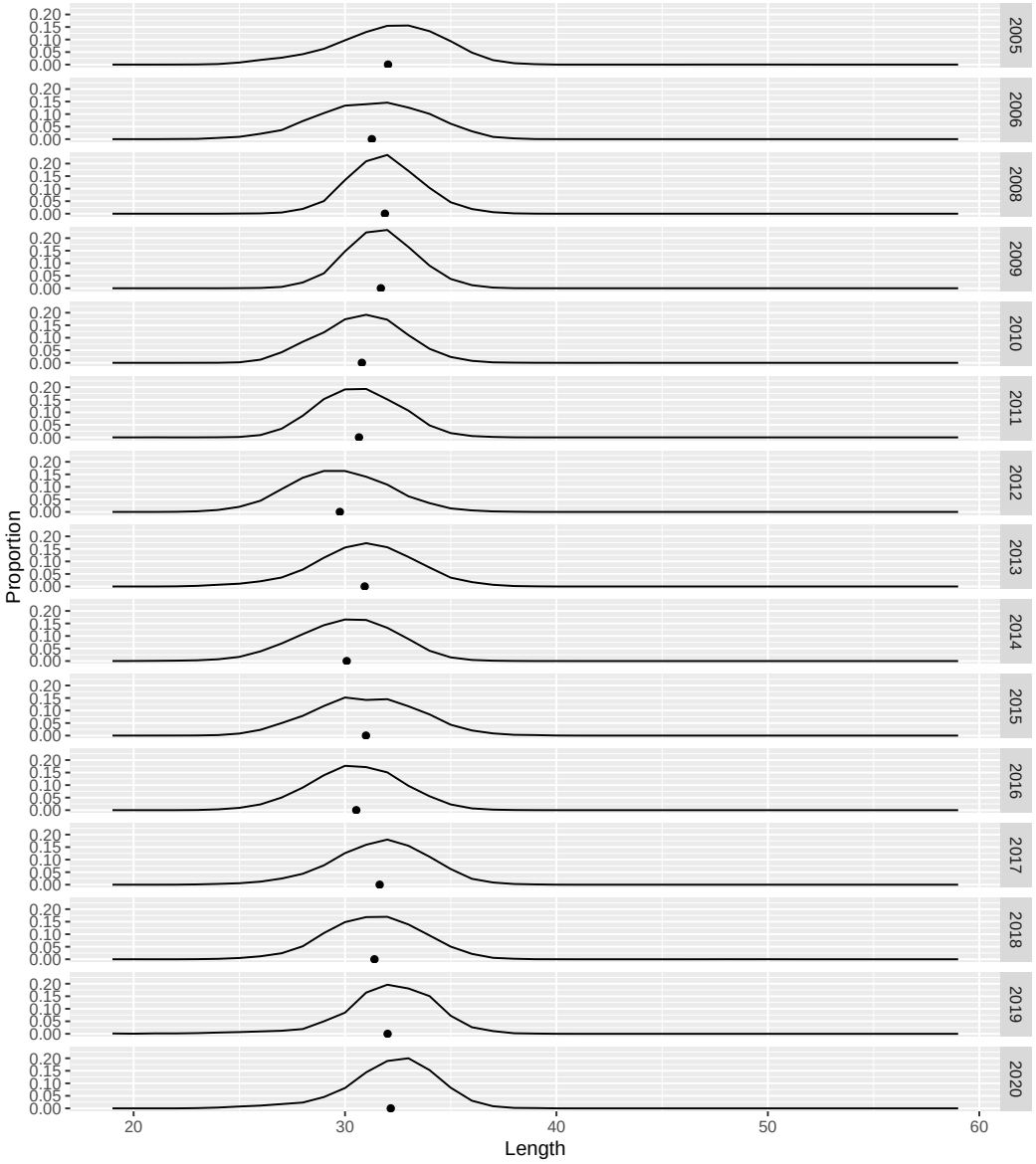

Figure 5: Catch length frequency distributions for JMA 1. The dot shows the mean length in each year. Data are from Langley et al. (2016), updated to the 2016 fishing year. The constraint applied from these data is shown in (Figure 10).

2.3 Management procedure

We developed a class of management procedures for the JMN component of JMA 1 that alters the catch limit in response to changes in the mean length of the catch. The rationale of the Length-Moving-Average-Range (LMAR) management procedure is to maintain the mean length, as a proxy for exploitation rates, within a range. All else being equal, when exploitation rates are higher, mean length will be smaller (Gulland & Rosenberg 1992). If the mean length falls below the lower bound of the range then the catch limit is cut by a fixed percentage. Conversely, if mean length rises above the upper bound of the range, indicating lower exploitation rates, the catch limit is increased by the same percentage.

More precisely, LMAR uses some measure, L_y, of the central tendency of the length distribution of the catch in each year. For simplicity, and because the length distribution of the JMA 1 catch is relatively symmetric (Figure 5), we have used the the mean length of the catch (alternatives would include the median and geometric mean). To mitigate the effects of potential observation or process error on variation in the mean length, the measure is smoothed using an exponential moving average,

$$\tilde{L_y} = rL_y + (1-r)\tilde{L_{y-1}}$$

where r is the *Responsiveness* control parameter. A higher value for r will result in $\tilde{L_y}$ being more responsive to changes in mean length in the last year. When $r = 1$, there is no smoothing.

In each year, $\tilde{L_t}$ is compared to a range defined by the two control parameters *Target*, t, and *Buffer*, b. If the value is outside of the range defined by those parameters then there is a increase or decrease in the catch limit whose magnitude is determined by (i) how far the mean length is below or above target, (ii) the *Reaction* parameter, a. When $\tilde{L_y} > t + b$ or $\tilde{L_y} < t - b$ then the catch limit is multiplied by $(\tilde{L_y}/t)^a$. For example, if $t = 30\ cm$, $b = 1\ cm$ and $a = 1$, and if $\tilde{L_y} = 28$ (i.e. 93% of target) then the existing catch limit will be reduced to $(28/30)^1 = 93\%$ of its current value. However, if $a = 3$ then it would be reduced to $(28/30)^3 = 81\%$.

2.4 Performance statistics

Several performance statistics were used to evaluate alternative parameterisations of the LMAR management procedure (Table 4). These include performance statistics for yield, stock status, sustainability and variability in catches. The Safety1 and Safety2 indicators are relevant to assessing whether or not a particular management procedure meets the requirements of the Harvest Strategy Standard (HSS). The HSS (Ministry of Fisheries 2008) specifies that management procedures should be designed to ensure that:

- the probability of achieving the MSY-compatible target or better is at least 50%;
- the probability of breaching the soft limit does not exceed 10%; and
- the probability of breaching the hard limit does not exceed 2%.

Alternatively, the requirements relating to the hard and soft limit can be collapsed to a requirement that there is no more than a 5% probability of breaching the soft limit (see Ministry of Fisheries 2008, para. 27).

T. novaezelandiae has characteristics of both low and medium productivity stocks (Ministry of Fisheries 2011), implying a default target of 35% to 40% B0. The Safety1 performance statistic relates to the default soft limit of 20% B0, and Safety2 to the default hard limit of 10% B0 (Ministry of Fisheries 2008).

Table 4: Performance statistics used to compare alternative management procedures.

Statistic	Description
Yield	Mean annual yield
Status	Mean stock status (%B0)
Safety1	Probability that stock status remains above 20% B0
Safety2	Probability that stock status remains above 10% B0
Variability1	Mean absolute relative change in TACC

3. RESULTS

3.1 Model conditioning

A total of 303 689 simulation trials were performed to generate a sample of 1000 parameter sets that were not removed by any of the contraints (Figure 6). The mean length constraint is the most influential, responsible for rejecting 186 566 parameter sets, followed by the Mean length difference and Mean age constraints.

Figure 7 shows the prior and posterior distributions for each parameter. The majority of the parameters show little movement from the prior. An important exception is the pristine biomass where values less than approximately 75 000 t are essentially ruled out and, while large values are possible, the greatest posterior density is in the range 100 000 t to 150 000 t. Larger values of si, the inflection point of the selectivity-at-age, and also of sc, the interannual variation in si, are also not favoured.

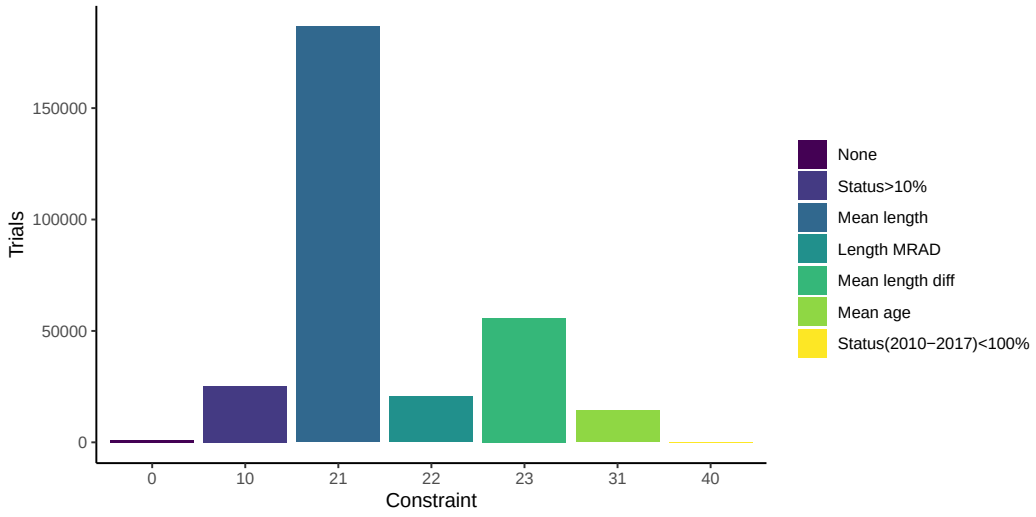

Figure 6: Frequency of parameter set trials which were rejected by each constraint.

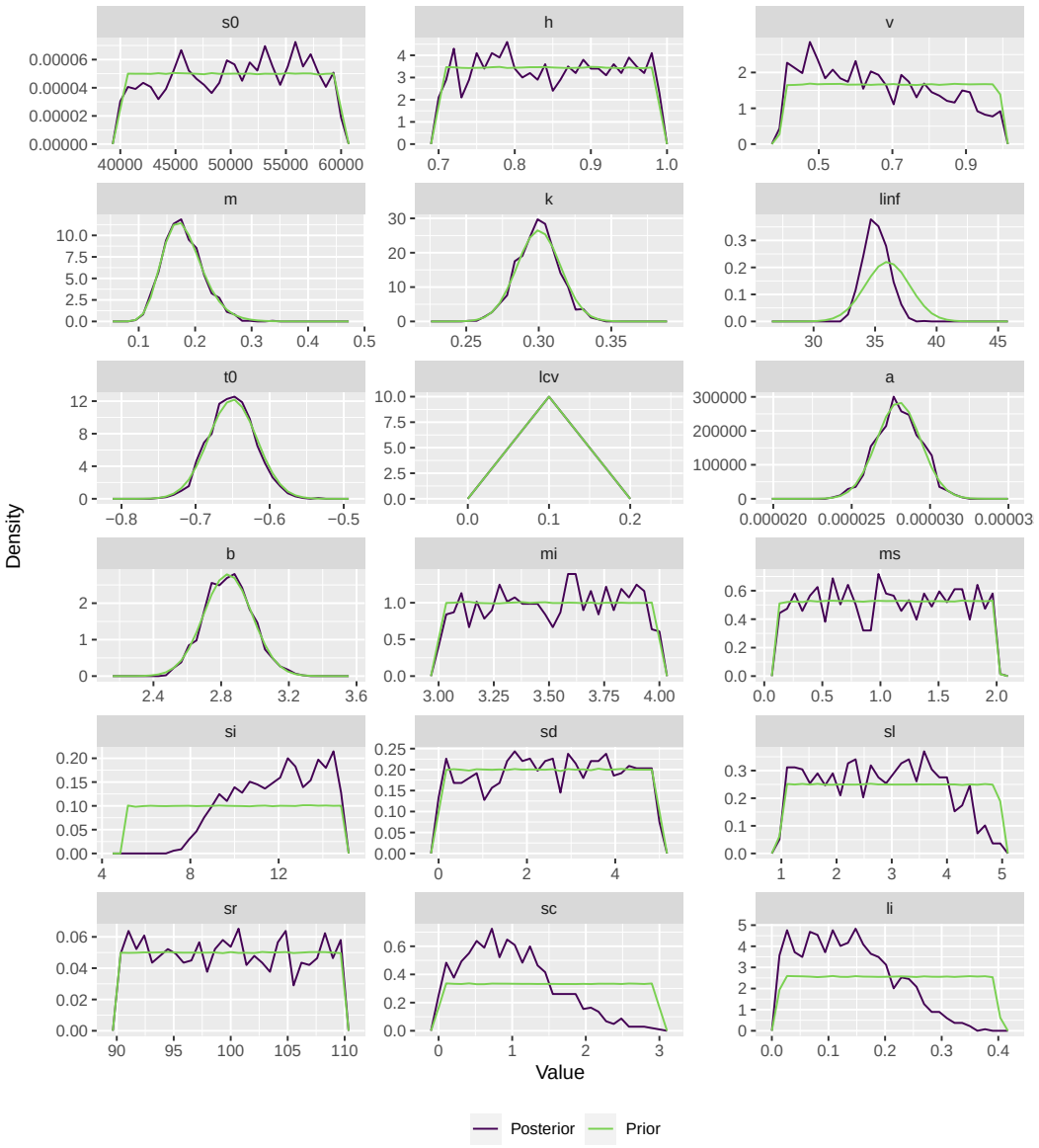

Figure 7: Prior and posterior distributions for each model parameter.

3.2 Operating model characteristics

Example trajectories, using a random selection of 100 realisations accepted during conditioning, are illustrated for stock status (%B0; Figure 8) and harvest rate (Figure 9), together with some of the variables involved in the constraints: mean length (Figure 10), the mean of the relative absolute difference in proportions (MRAD; Figure 11) and the interannual absolute difference in mean length (Figure 12).

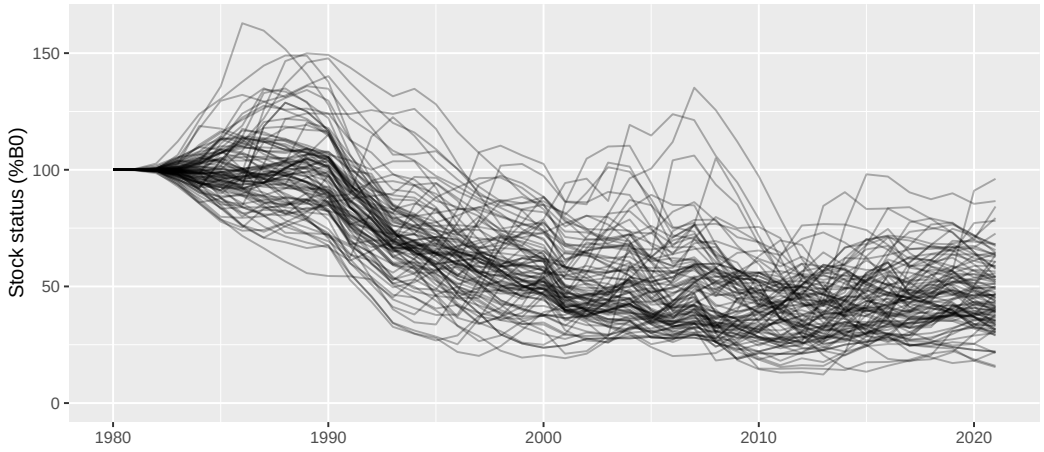

Figure 8: Stock status trajectories for simulations accepted during conditioning.

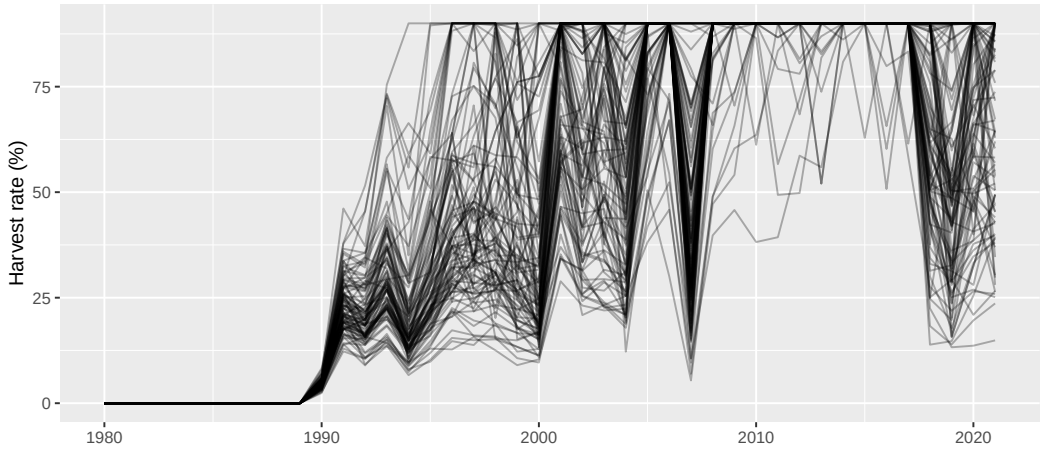

Figure 9: Harvest rate trajectories for simulations accepted during conditioning.

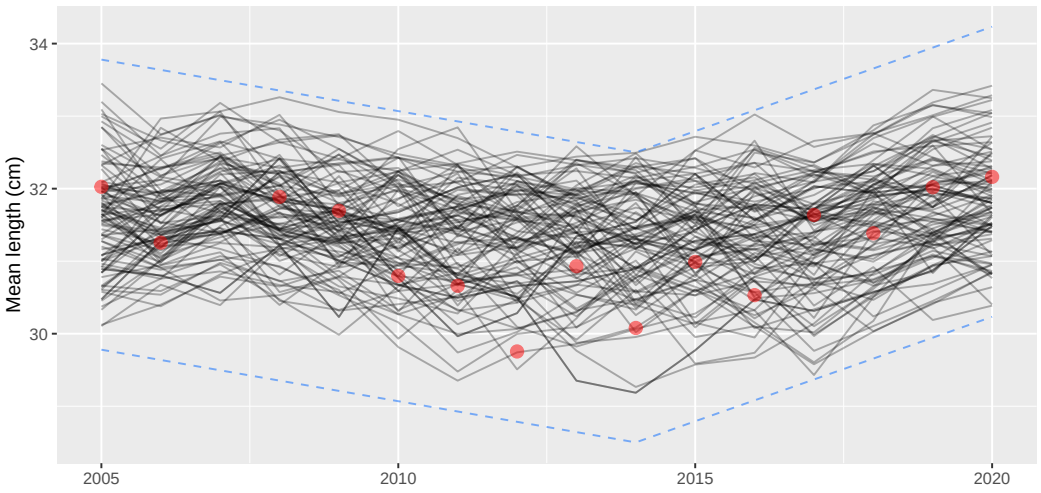

Figure 10: Mean length trajectories for simulations accepted during conditioning. Red dots show observed mean lengths by year, while the dashed lines illustrate the constraint.

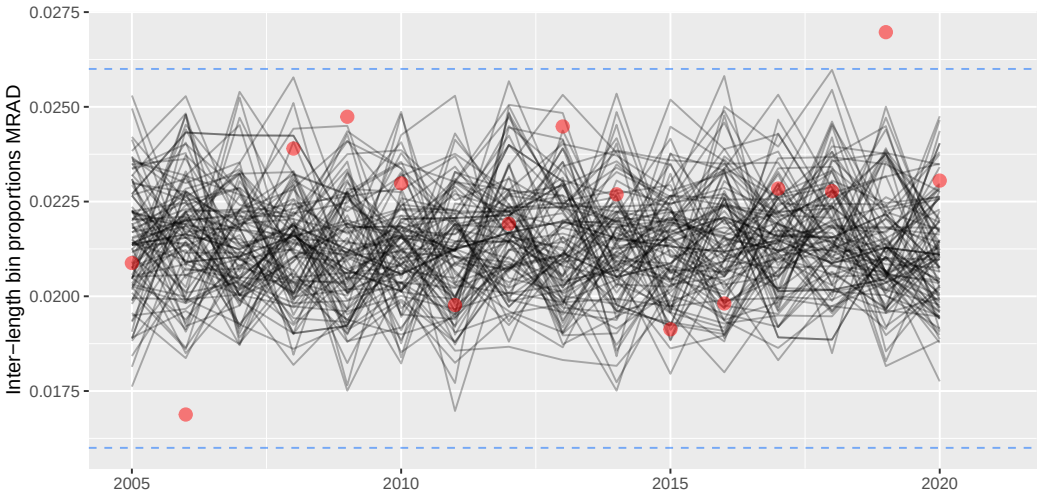

Figure 11: Inter-length bin proportions MRAD trajectories for simulations accepted during conditioning. Red dots show observed mean lengths by year, while the dashed lines illustrate the constraint.

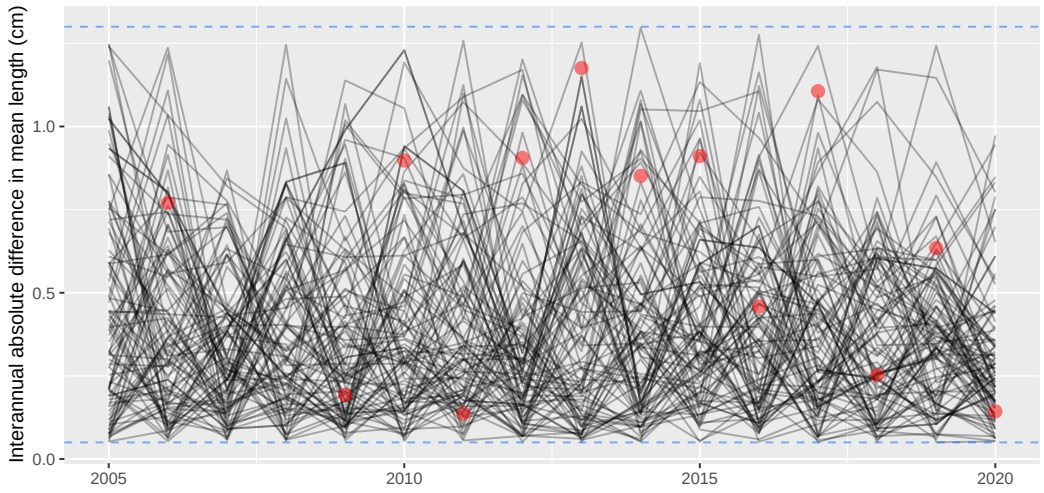

Figure 12: Interannual absolute difference in mean length trajectories for simulations accepted during conditioning. Red dots show observed mean lengths by year, while the dashed lines illustrate the constraint.

3.3 Management procedure evaluations

We begin by illustrating the behaviour of the LMAR class of management procedure and how each of its control parameters affect this behaviour. This is done by using a reference set of control parameters and then varying each in turn (Table 5). Neither the reference set or alternatives are 'special', they simply provide some useful contrasts. For each of the control parameters we show simulated trajectories for a single replicate simulation. In each case, a replicate simulation was chosen which illustrates the effect of the control parameter. As such, the replicate chosen, and thus the consequent simulation trajectories may differ among each of the following figures.

For all evaluations, the full catch limit available under the management procedure was assumed to be taken each year from 2018 onwards.

Table 5: Reference and alternative values for control parameters of the LMAR management procedure.

Parameter	Value	Alternatives
Responsiveness, r	1	
Target, t, (cm)	30	28, 32
Buffer, b, (cm)	2	1, 3
Reaction, a	1	2, 3
Wait (yrs)	3	1, 5
Maximum TACC (t)	15000	

3.3.1 Target

The Target control parameter specifies the centre of the range of 'acceptable' mean length values. All else being equal, the higher the Target, the lower the catch and the higher the spawning biomass (Figure 13).

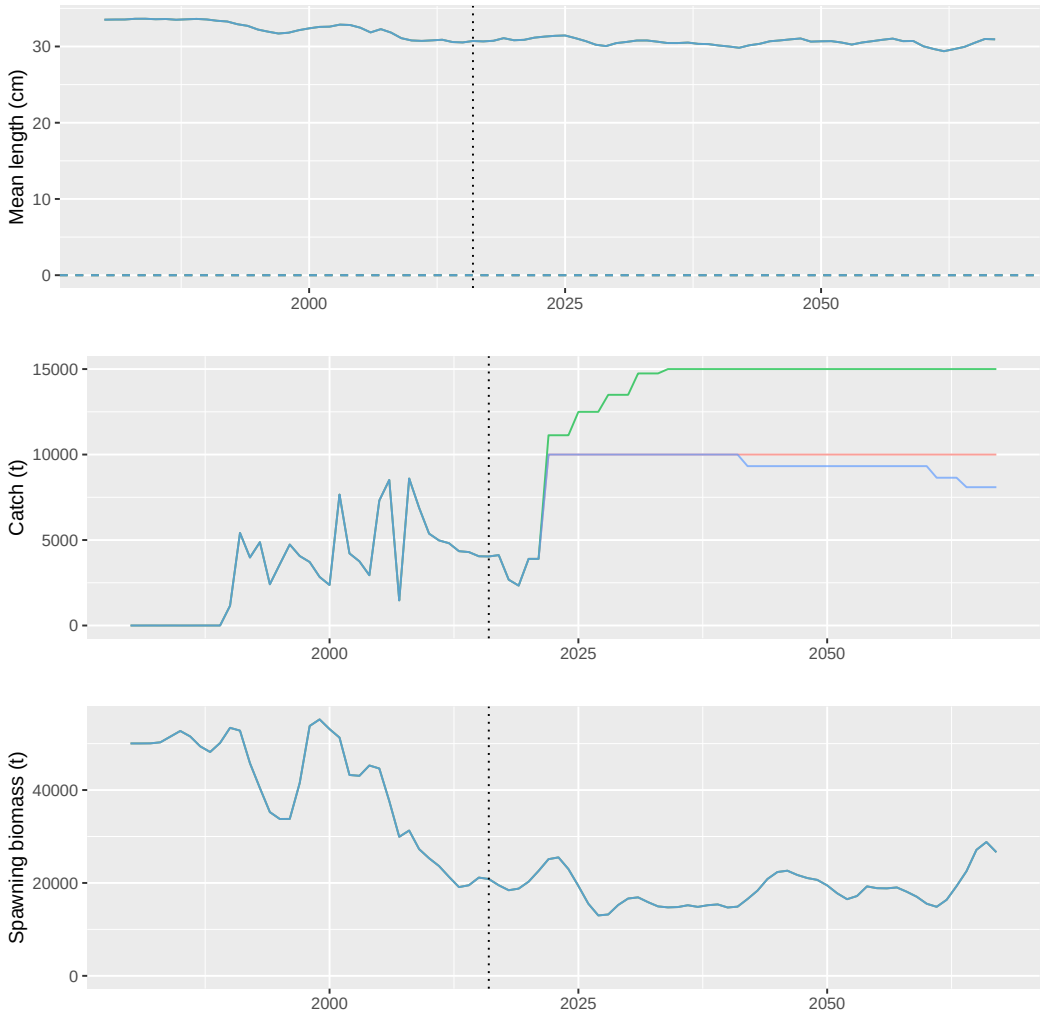

Figure 13: Illustration of the effect of the Target control parameter: blue 32cm, red 30cm, green 28cm.

3.3.2 Buffer

The Buffer control parameter specifies the width of the range of 'acceptable' mean length values. All else being equal, when the Buffer is lower, and thus the range is narrower, there will be more frequent changes in catch limit (Figure 14).

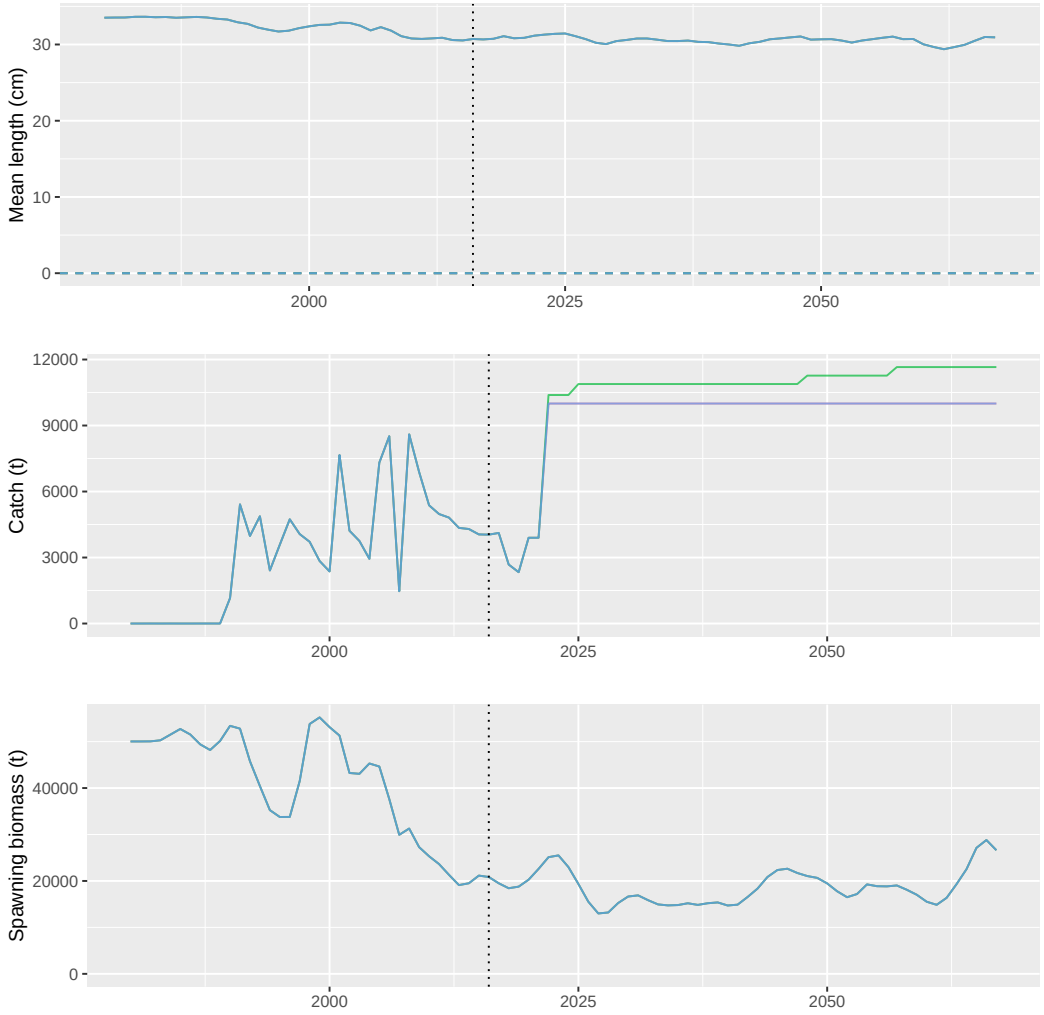

Figure 14: Illustration of the effect of the Buffer control parameter: blue 3cm, red 2cm, green 1cm.

3.3.3 Reaction

The Reaction control parameter determines the degree of catch limit change when the mean length falls outside of the range. Note that, for the illustration shown, in 2024 the mean length falls below the lower bound of the range and triggers a reduction in catch limit (Figure 15). This reduction is greatest when Reaction is 3 and causes the mean length to recover fastest.

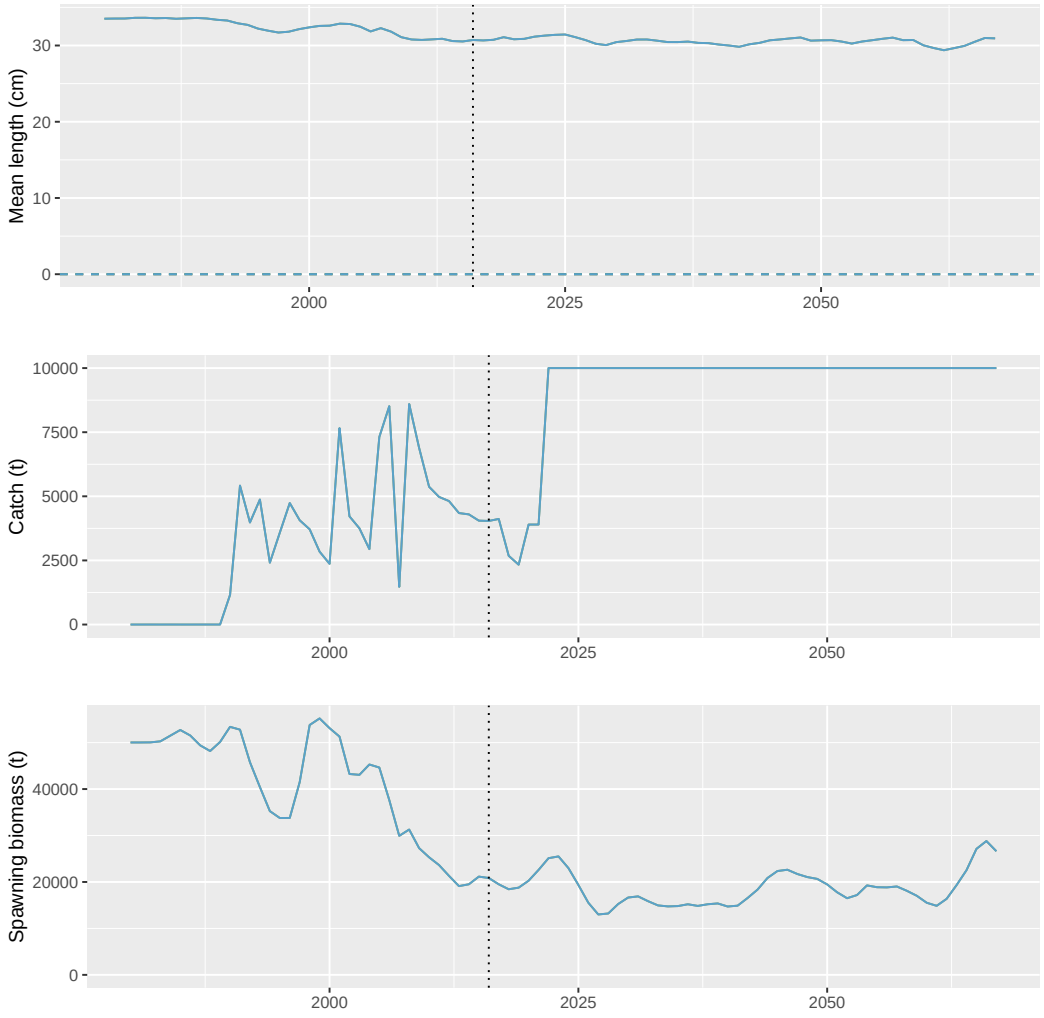

Figure 15: Illustration of the effect of the Reaction control parameter: blue 3, red 2, green 1.

3.3.4 Wait

The Wait control parameter is the minimum time between successive changes in catch limit (Figure 16).

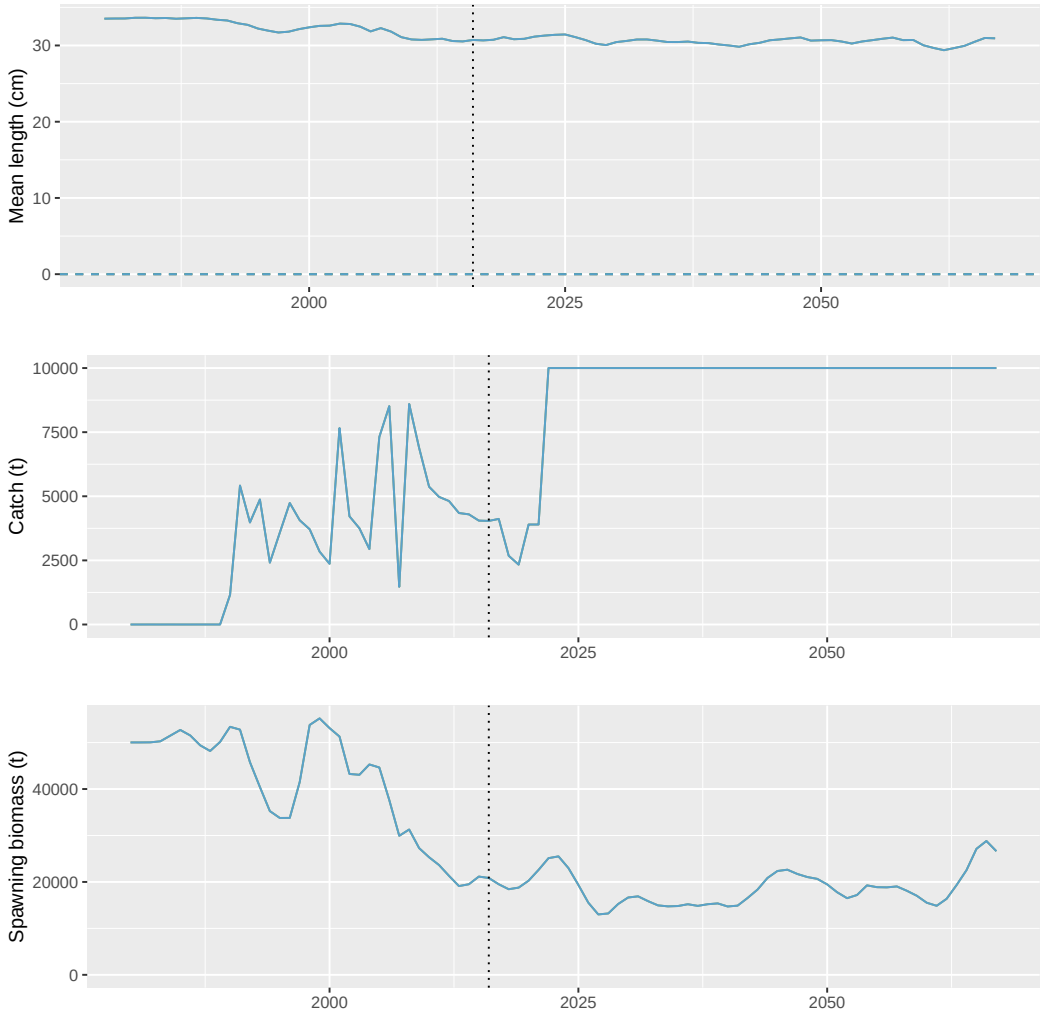

Figure 16: Illustration of the effect of the Wait control parameter: blue 5yrs, red 3yrs, green 1yr.

3.4 MP performance

Exploratory ANOVAs (analysis of variance) were carried out to examine which control parameters have the greatest effect on the key performance statistics: Yield, Status and Safety1. These suggested that Target and Reaction were the most important control parameters. Trade-offs were examined between Yield and Status (Figure 17), Safety1 (Figure 18) and Safety2 (Figure 19) for LMAR management procedures with different Target and Reaction settings. For reference, constant catch limits were also included in these plots for limits ranging from 5000 t to 15 000 t at 500 t intervals.

For all MPs examined, mean stock status is greater than 40% B0. However, only a subset of the procedures evaluated meet the requirements of the Harvest Strategy Standard with respect to risk of falling below the soft (Figure 18) and hard (Figure 19) limits. The value of a management procedure that adjusts harvest limits in response to mean length (as a proxy for exploitation rate) is evident as these procedures provide greater mean Yield for a given level of Safety.

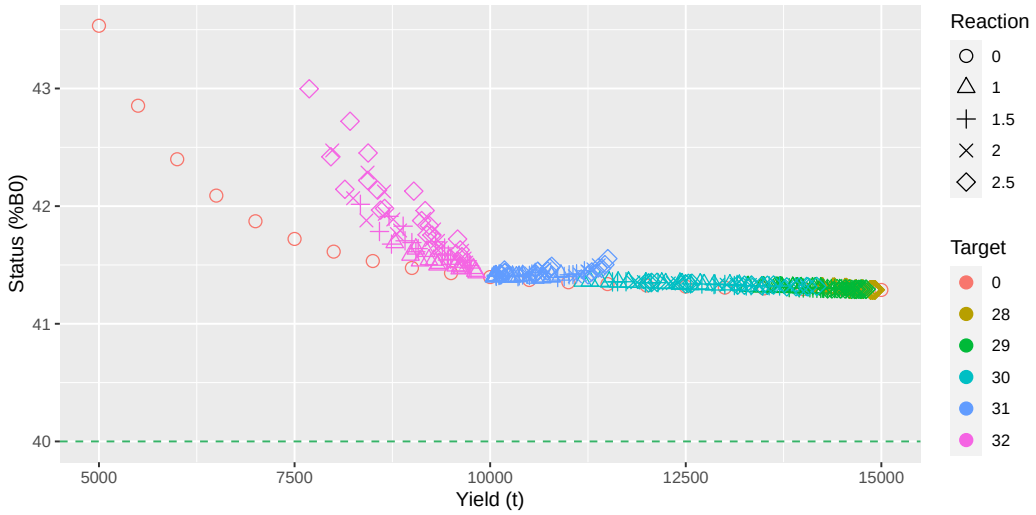

Figure 17: Tradeoff between Yield and Status. Each point represents the mean performance of a management procedure over all replicate simulations. Colours and shapes are used to represent alternative values of MP control parameters. The red circles (denoted as MP parameters of 0) indicate evaluations with a constant catch limit, constant catch evaluations were included for limits between 5000 t and 15 000 t at 500 t intervals. The dashed line shows a reference point of 40% B0 which is the upper end of the range of possible default targets.

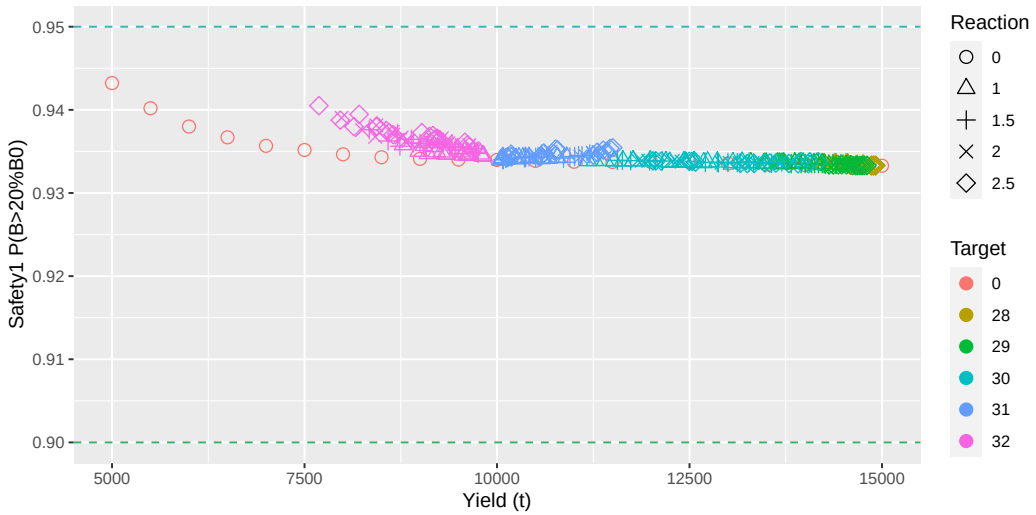

Figure 18: Tradeoff plot between Yield and Safety1. The red circles (denoted as MP parameters of 0) indicate evaluations with a constant catch limit, constant catch evaluations were included for limits between 5000 t and 15 000 t at 500 t intervals. The dashed lines correspond with a 5% and 10% probability of falling below the default HSS soft limit of 20% B0.

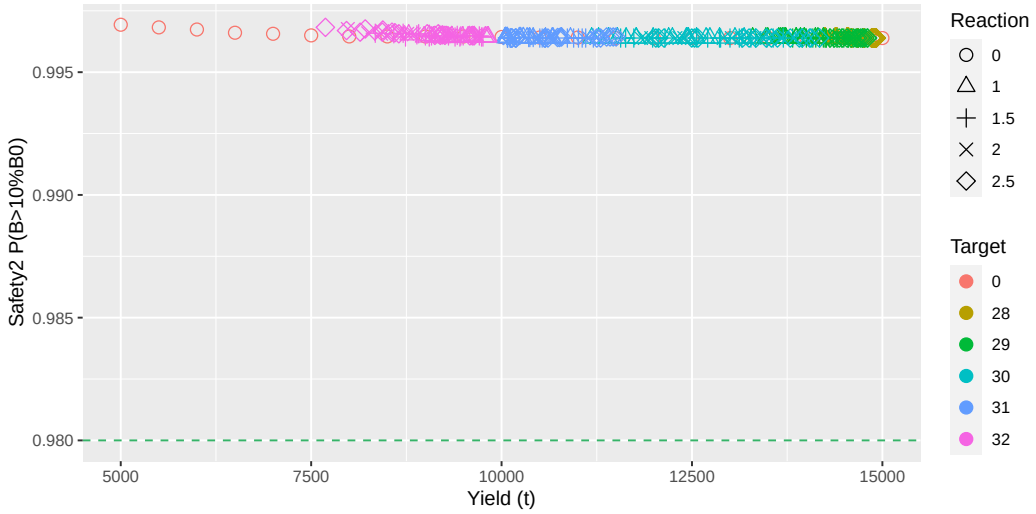

Figure 19: Tradeoff plot between Yield and Safety2. The red circles (denoted as MP parameters of 0) indicate evaluations with a constant catch limit, constant catch evaluations were included for limits between 5000 t and 15 000 t at 500 t intervals. The dashed line corresponds to a 2% probability of falling below the default HSS hard limit of 10% B0.

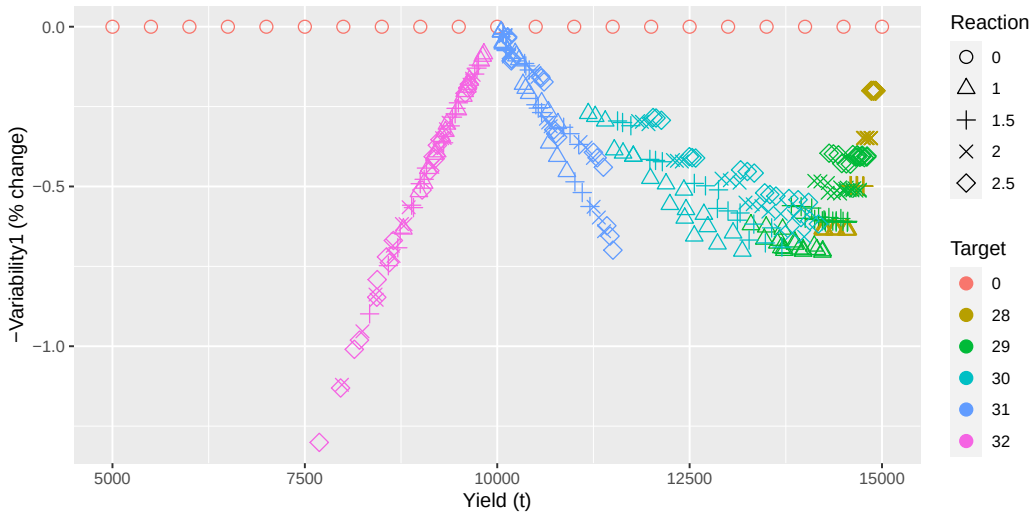

Figure 20: Tradeoff plot between Yield and Variability1. The red circles (denoted as MP parameters of 0) indicate evaluations with a constant catch limit, constant catch evaluations were included for limits between 5000 t and 15 000 t at 500 t intervals.

4. DISCUSSION

Management of the JMA 1 fishery faces some particular challenges. The QMS stock is a complex of three species, one of which, *T. murphyi*, may be part of a single, extensive trans-Pacific stock (Fisheries New Zealand 2018). There has been no success in deriving a relative abundance index from aerial sightings data. Even if aerial sightings were useful, use of spotter planes by the purse seine fishery has reduced with increasing use of sonar. Use of standardised catch per unit effort information to monitor abundance is problematic due to the fact that the purse seine method sets on schools and the associated searching effort is not captured in current data systems.

A pilot survey for jack mackerel on the west coast of the North Island using acoustic methods was undertaken in 2012 (O'Driscoll et al. 2013). This suggested that it was feasible to survey jack mackerel using acoustics, but that it would be very difficult to do any kind of aggregation-based acoustic survey because no concentrations of fish were identified. While schools of jack mackerel are clearly present on the east coast at some times of year, these are also close to the surface at times which impacts on the ability to carry out acoustic surveying.

Development of an abundance index for jack mackerel on the east coast would clearly be a long term proposition. In the meantime, however, it is desirable to have a quantitative basis for setting catch limits. The existing time series of length-frequency data shows some trends which are potentially related to changes in exploitation rate of the population of *T. novaezelandiae*, the key jack mackerel species in catches over the last decade. Using these data, and other information on the productivity of the species, it has been possible to parameterise a population model and condition this on the available data. This model provides a basis for evaluating management procedures.

We have identified parameterisations of a Length-Moving-Average-Range (LMAR) management procedure which, conditional on the operating model, meets the performance targets of the Harvest Strategy Standard. This MP uses information on mean size collected from routine catch sampling and therefore provides the opportunity to adopt a particular management procedure for immediate fisheries management needs. If *T. novaezelandiae* remains the key species taken in the JMA 1 purse seine fishery, then a catch limit for that species may be provide a suitable surrogate for setting the TACC for the wider JMA 1 species complex. However, if other species of jack mackerel become more significant parts of the catch then a more sophisticated approach, for example including evaluation of length-based MPs for other jack mackerel species, may be required. In either case, it is advisable that, if a management procedure is adopted as part of a management plan, then that plan also includes a focus on continuous improvement in the information available for fisheries management in the future. The approach applied here to select a MP could also be applied to assist in the evaluation of alternative data collection regimes (Bentley & Stokes 2009).

The requirements of the Harvest Strategy Standard constrain the particular LMAR parameterisations that could be adopted as part of a management plan to those that are evaluated to have no more than a 5% probability of breaching the soft limit (e.g., Figure 18). Having met the HSS requirements, fisheries managers and stakeholders have the opportunity to consider other performance measures, including average yield and likely variability in catch limits (e.g., Figure 20), in choosing the particular procedure to adopt.

5. ACKNOWLEDGEMENTS

Adam Langley compiled the length and age distributions used in model conditioning. This work was contracted by Fisheries Inshore New Zealand with funding from JMA 1 quota owners, in particular Sanford Limited and Pelco NZ Limited.

6. REFERENCES

Bentley, N.; Langley, A.D. (2012). Feasible stock trajectories: a flexible and efficient sequential estimator for use in fisheries management procedures. *Canadian Journal of Fisheries and Aquatic Sciences 69*: 161–177.

Bentley, N.; Stokes, T.K. (2009). Moving fisheries from data-poor to data-sufficient: evaluating the costs of management versus the benefits of management. *Marine and Coastal Fisheries: Dynamics, Management, and Ecosystem Science 1*: 378–390.

De Oliveira, J.A.A.; Kell, L.T.; Punt, A.E.; Roel, B.A.; Butterworth, D.S. (2009). Managing without best predictions: the management strategy evaluation framework. *Advances in Fisheries Science: 50 years on from Beverton and Holt*: 104–134.

Fisheries New Zealand (2018). Fisheries Assessment Plenary, May 2018: stock assessments and stock status. Compiled by the Fisheries Science and Information Group, Fisheries New Zealand, Wellington, New Zealand. 1 660 p.

Gulland, J.A. (1969). Manual of methods for fish stock assessment. Part 1. Fish population analysis. Food and Agriculture Organisation of the United Nations, Rome.

Gulland, J.A.; Rosenberg, A.A. (1992). A review of length-based approaches to assessing fish stocks. *FAO Fisheries Technical Paper 323*.

Horn, P.L. (1991). Assessment of jack mackerel stocks off the central west coast, New Zealand, for the 1990–91 fishing year. *New Zealand Fisheries Assessment Research Document 1991/6*. 14 p.

Jones, J.B. (1988). Jack mackerels. *New Zealand Fisheries Assessment Research Document 88/19*. 20 p.

Langley, A.D.; Middleton, D.A.J.; Wilson, O.L. (2016). Species composition of the jack mackerel (genus *Trachurus*) catch from the JMA 1 purse seine fishery, 2005/06 to 2013/14. *New Zealand Fisheries Assessment Report 2016/11*. 33 p.

Ministry of Fisheries (2008). Harvest Strategy Standard for New Zealand Fisheries. Ministry of Fisheries, Wellington, New Zealand.

Ministry of Fisheries (2011). Operational Guidelines for New Zealand's Harvest Strategy Standard, Revision 1. Ministry of Fisheries, Wellington, New Zealand.

O'Driscoll, R.L.; Oeffner, J.; Ross, O.; Dunford, A.J.; McMillan, P.J. (2013). Pilot acoustic survey for jack mackerel on the west coast New Zealand (JMA7). *New Zealand Fisheries Assessment Report 2013/1*. 53 p.

Stephenson, A.B.; Robertson, D.A. (1977). The New Zealand species of *Trachurus* (Pisces: Carangidae). *Journal of the Royal Society of New Zealand 7 (2)*: 243–253.

Taylor, P.R.; Horn, P.L.; Maolagáin, C.Ó. (2012). Commercial catch sampling for species proportion, sex, length, and age of jack mackerels in JMA 1 in the 2006–07, 2007–08 and 2008–09 fishing years. *New Zealand Fisheries Assessment Report 2012/48*. 36 p.